Follow your nose: the computational role of olfaction in spatial memory and navigation

Scott Charles Sterrett

A dissertation
submitted in partial fulfillment of the
requirements for the degree of

Doctor of Philosophy

University of Washington
2024

Reading Committee:

Adrienne Fairhall, Chair

David Henry Gire, Chair

Sam Golden

Program Authorized to Offer Degree:

Neuroscience

University of Washington

Abstract

Follow your nose: the computational role of olfaction in spatial memory and navigation

Scott Charles Sterrett

Co-Chairs of the Supervisory Committee:
Adrienne Fairhall
Neurobiology and Biophysics

David Gire
Psychology

Olfactory stimuli permit perception of distant objects and odors are intimately connected to memories. The brain must integrate olfactory stimuli with the time and place that they were experienced, but the brain lacks receptors for time or place. How does the olfactory system link odors to spatial memory in order to adaptively navigate complex environments? We find that the mouse olfactory system is modulated by multiple aspects of the animal's environment as early as the olfactory bulb, the first synapse in the olfactory system. The spiking activity of olfactory bulb neurons encodes the sniffing behavior at both a subsecond, intersniff timescales as well as longer timescale breathing rhythms. Additionally, we find that olfactory bulb neurons represent an animal’s allocentric location. Through task-trained recurrent neural network simulations, we hypothesize that this olfactory-spatial interaction depends on the behavioral demands of a simulated searcher to adaptively support localization. These findings provide novel insights into the nature of olfactory perception in awake behaving animals that motivate a more integrative approach to the study of olfactory physiology.

Table of Contents

to my parents, who taught me to
watch and wonder

Acknowledgements

> "The starting-point of critical elaboration is the consciousness of what one really is, and is 'knowing thyself' as a product of the historical processes to date, which has deposited in you an infinity of traces, without leaving an inventory. Therefore it is imperative at the outset to compile such an inventory."
> Antonio Gramsci, *Prison Notebooks* (1929)

> “To do science is to be a social actor engaged, whether one likes it or not, in political activity. The denial of the interpenetration of the scientific and the social is itself a political act, giving support to social structures that hide behind scientific objectivity to perpetuate dependency, exploitation, racism, elitism and colonialism.”
> Richard Lewontin and Richard Levins, *Dialectical Biologist* (1985)

First and foremost, I want to acknowledge my parents, whose thoughtfulness sparked all of this: in summer nights watching the bats fly overhead and the stars emerge, noting each spring peeper frog's return, an endless zoo of pets, and reverse engineering every piece of electronics we could salvage from the curb on trash nights. I am also grateful for the early influences of high school teachers Mr. Shiner, Mrs. Selinger, Mrs. Yacamelli

My undergraduate professors at Johns Hopkins provided foundations in mathematics, physics, and biology. I am especially grateful to Drs. Eileen Haase, Mike Beer, Sri Sarma, Nitish Thakor, Gene Fridman, Reza Shadmehr. The swimming pool provided a different kind of education, for which I’d like to thank Coach Kennedy, Evan Holder, and Patrick Flynn.

I learned many early lessons on research from Drs. Xiaoqin Wang, Lingyun Zhang, and Michael Osmanski, and life lessons from Hong Lan.

Starting at University of Washington during the COVID-19 pandemic was made easier by the support of Kyle Shea, John Tuthill, and the rest of the Graduate Program in Neuroscience. Through the doldrums of zoom, thank you to Jess Jones, Anna Li, Leila Elabbady, and the 2020 cohort. I’m grateful to Rich Pang, Kevin Chen, Marga Peixeira for friendships across conferences. The Computational Neuroscience Center community has provided essential community support: Eric Shea-Brown, Ellen Lesser, Patrick Zhang, PoChen Kuo, Srinidhi Naidu, David Bell, Divyansch Gupta, Yusi Chen, and many others. It has been a perk of the new zoom proliferation to have shared a collaboration with the University of Oregon: Matt Smear, Reese Findley, Morgan Brown, Amanda Welch, James Murray, and many others. The campus is a vessel for so much more than science: Jenn, Vassiki, Calvin and others at Science for the People; Levin, Tahiyat, Soohyung, Jai and the thousands of members of UAW4121; Nikhil, Zho, Victor, Anna, Daniel and Resist US-Led War; and the Plaza cafe FNS workers.

This work is the fruit of the collective efforts of co-advisors Drs. Adrienne Fairhall and David Gire. Adrienne's buoyant optimism and keen sense for interesting questions has carried me through many difficult periods and on to insights. David's curiosity about animal behavior and physiology has revealed many delightful areas of animal cognition and allowed me to explore my own contributions to the field.

Lastly, I thank Cera Hassinan for her steadfast support, without which this would not be possible, and our late cat Xena, who showed me when to play and when to nap.

Chapter 1: Introduction

Animal behavior is incredibly resilient and adaptive in order to maintain essential functions in the face of conditions which change across a multitude of timescales. As a child, watching and wondering about the bats that would emerge from the nature preserve at dusk on summer nights raised a lot of questions. Bats use self-generated auditory calls and their echoes to actively sense the world around them, called echolocation. This way of perceiving and moving through the world was and remains impossible for me to subjectively comprehend. Their subsecond clicks, their acrobatic flight paths to capture prey, the regularity of their evening visits, and the seasonality of their foraging exemplify the many timescales of behavior in a single organism (Kohles et al., 2024; Schnitzler et al., 2003; Simmons et al., 1979). Looking at longer timescales, we can marvel at how mammals evolved flight behaviors (Tsagkogeorga et al., 2013), the way human society exhausted millennia of guano deposits for British fertilizer in a few short decades in the 18th century (Clark & Foster, 2009), and how bats' physiology as a natural reservoir for viruses spreads diseases in a globally interconnected world (Dobson, 2005). Bats are just one example amongst many in the animal kingdom of the range of timescales - from evolutionary, to ecological, to organismal - that biologists must consider in all species (Miller et al., 2022).

On the organismal level, the nervous system plays a foundational role in adaptive control of behavior. At all times, the brain is processing, controlling, and storing the flow of experiences both within and outside the body. This functionality comes at a cost, with the brain consuming 20% of the body's energy. However, this efficiency far outpaces the energy required by modern robotics and artificial intelligence systems, which remain incapable of matching the flexibility that can be found throughout the animal kingdom (Crawford, 2024). By studying the brain's unique ability to adaptively and efficiently support behavior, we can gain insights that improve our understanding of cognition in health and disease.

1.1 Neuroscience needs behavior

> "It begins to be difficult, and even in some cases impossible, to say where ethology stops and neurophysiology begins." Niko Tinbergen *On Aims and Methods of Ethology* 1963

Tinbergen's observation of the fuzzy boundaries between fields speaks to the multi-scale nature of explanations in biology and the interdisciplinary training required of its investigators. This is obvious when studying the debates around which fields should be invited to the first meeting of the Society for Neuroscience in 1971, including cognitive science, artificial intelligence, neurophysiology, genetics, psychology, and linguistics. (Fields, 2018; Society for Neuroscience, 2019). The first meeting covered a

variety of model organisms ranging from invertebrates like orb web spiders, crayfish, and octopus, to vertebrates like electric fish, raccoons, and pigeons. This diversity of model organisms reflected the field's disparate and comparative studies of the principles of nervous systems. As the field developed, technological advances would lead to a tension between holistic approaches that consider the variety of behaviors of diverse organisms and increasingly reductionist tools and approaches in a small set of model organisms.

Figure 1: Neuroscience old and new. (a) Santiago Ramon y Cajal's diagram of the early olfactory system from 1894 (b) cover image for the 1969 Survey of Research Facilities and Manpower in Brain Sciences in the U.S, which coincided with the founding of the Society for Neuroscience . Reproduced from: (Ramón y Cajal, 1894; Society for Neuroscience, 2019))

In the subsequent five decades, the field of neuroscience has made incredible progress, predominantly by a reductionist approach to the brain. Reductionism is the approach of searching out simple units of a system and attempting to isolate that part from other interacting parts and timescales. Cajal and Golgi learned much about basic neuroanatomy from new staining techniques along with anatomists like Brodmann. (Hegel warned "Limbs and organs become mere parts, only when they pass under the hands of an anatomist, whose occupation be it remembered, is not with the living body but with the corpse." (Hegel, 1816)). Hubel and Weisel described the early visual system's "receptive fields" or the visual patterns that drove activity, by presenting simple stimuli to anesthetized cats. As our understanding of the brain grows, it has become increasingly clear that many cognitive behaviors emerge from interactions between multiple brain regions and the body. This realization highlights the limitations of the reductionist approach and motivates a complimentary, holistic approach.

Systems neuroscience is an attempt to integrate this detailed knowledge of molecular and cellular neuroscience with an appreciation for their interactions across circuits, regions, and behaviors. One example is the discovery of the auditory localization circuit in the midbrain of owls, a champion model organism for auditory-guided prey capture,

by Mark Konishi and colleagues. This work integrated behavioral studies with electrophysiology and circuit models to elegantly describe how the midbrain maps auditory inputs to construct a map of the auditory world and localize sources within that map. This work required an appreciation for the behavioral function of neural circuits, diligent experimental work, and theoretical modeling in order to arrive at an understanding of the neural circuit at multiple levels. This is one of many examples, including place and grid cells for spatial mapping, animal communication, and social behaviors, which were made possible by an approach to neuroscience which integrates across multiple disciplines.

In the last decade, technological advances have dramatically changed neuroscience, with many new methods resulting from the BRAIN Initiative (*BRAIN 2025: A Scientific Vision*, n.d.; Ngai, 2022). We can now record from orders of magnitude more neurons, across days and months. We can reconstruct an atlas of all the cell types and their connections across whole brains. We can track the precise posture of behaving animals across days, weeks, or even lifetimes. We can stimulate or silence precise sets of neurons with millisecond precision. Gene editing tools can be used across an array of model organisms (CRISPR). These technological advances offer an unprecedented opportunity to revisit longstanding questions with a new perspective.

How can we look back at the existing literature and combine new approaches to answer open questions? This thesis is part of a growing community of researchers seeking to integrate advanced methods with more complex, ecological behaviors - an approach typically called naturalistic systems neuroscience (Datta et al., 2019; Dennis et al., 2020; Gomez-Marin et al., 2014; Kennedy, 2022; Krakauer et al., 2017; Pereira et al., 2020). Future insights will likely come from integrating understandings across multiple levels to move us toward a more complete understanding of the behaving brain.

Why study awake, behaving brains?

Tinbergen's four questions for biology

Niko Tinbergen described four complementary questions for biology that offer a pluralistic understanding of animal behavior which remains a useful framework today (Bateson & Laland, 2013; Tinbergen, 1963):

1. Function (or adaption): Why is the animal performing the behavior?
2. Evolution (or phylogeny): How did the behavior evolve?
3. Causation (or mechanism): What causes the behavior to be performed?
4. Development (or ontogeny): How has the behavior developed during the lifetime of the individual?

Naturalistic systems neuroscience focuses on function and mechanism questions, but with an appreciation for the evolutionary and developmental processes that motivate experiments which more closely resemble an organism's natural environment and behaviors (Dennis et al., 2020; Ding et al., 2024). This approach argues that the brain has evolved to solve complex problems and that studying it under highly constrained conditions may miss important aspects of its function (Anderson, 1972). While Tinbergen's four questions provide a framework for the broader field of biology, David Marr's three levels, situated within the function and mechanism questions, are the most prominent framework used to describe the multiple levels of analysis in computational neuroscience: computational, algorithmic and representational, and implementational (Marr, 1982). The continued relevance of Marr's framework has been debated, but remains a popular schema to describe the different levels of explanation across fields in computational neuroscience (Bechtel & Shagrir, 2015; Fairhall, 2014; Lengyel, 2024; Pillow, 2024a, 2024b). Together, these frameworks allow us to investigate both the 'why' and 'how' of neural systems.

Neural activity during anesthesia is drastically different from that during wakefulness. In olfaction, the sense of smell, the important role of the animal's state has been noted since the earliest electrophysiological study of the olfactory system :

> "In very deep anaesthesia when the bulb is quiet, a moderate olfactory stimulus sets up a discharge of impulses in the mitral axons at each inspiration and there are no impulses between. In less deep anaesthesia the olfactory discharges appear against a background of continuous irregular activity and as the anaesthesia lightens the continuous activity becomes more and more prominent until it may be no longer possible to detect any change due to the stimulus" (Adrian, 1950)

Feedback activity relating to motor efference, context-dependence, arousal, learning, and much more is absent during anesthesia. With awake behaving preparations, one can study the brain during learning and decision making processes. In olfaction, the breathing cycle is a powerful regulator of spiking activity (Ackels et al., 2021; Adrian, 1950; Chaput et al., 1992; Kay & Laurent, 1999; Macrides & Chorover, 1972; Onoda & Mori, 1980). Additionally, aspects like internal states and learned associations can modulate olfactory neural circuits (Reinert & Fukunaga, 2022; Rinberg & Gelperin, 2006).

Motivated by the importance of studying brains in complex, ecological-inspired tasks, olfactory navigation provides one exemplary behavior for understanding the olfactory system's role in perception, decision making, and motivated behavior (Miller et al., 2022).

1.2 Olfactory navigation

> "The nose permits the perception of distant sources in the present environment and even of the places where animals have been in the past." - James J. Gibson *The Senses Considered as Perceptual Systems* (1966)

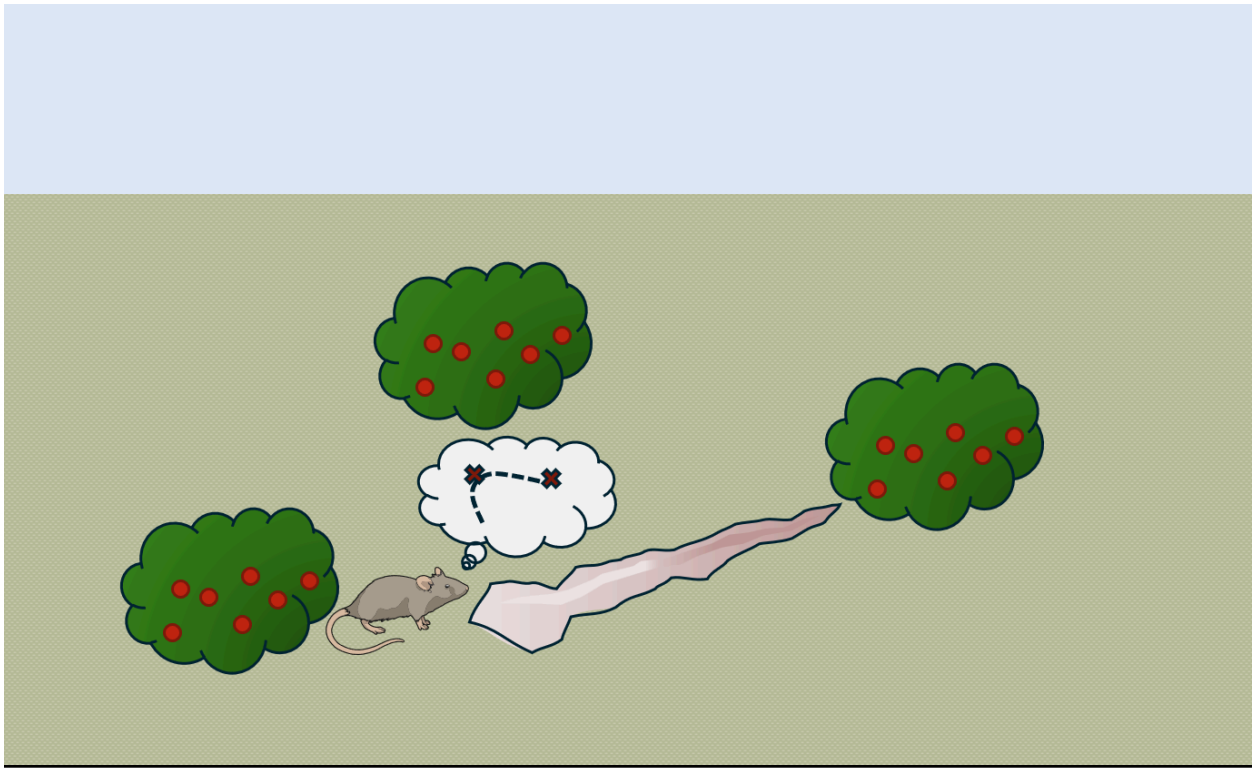

Figure 2: A schematic overview of central questions of the thesis.

<u>The active nature of olfaction</u>

Olfaction, like all senses, is tightly connected to memory and action. Olfaction is a necessarily active sense. Chemicals in the air are brought into the nose by nasal respiration. This air is mixed in the turbinates, small ridges within the nasal cavity, and odorants are absorbed into the olfactory mucosa as air passes through to the lungs. In many terrestrial mammals, olfactory perception requires active respiration; if an odor is presented to the olfactory epithelium without concurrent mechanical stimulation, it is not

perceived (Bocca et al., 1965; Proetz, 1953; Sobel et al., 2001). Active sampling structures the content of olfactory perception, often in ways that provide useful information to the animal. This active framework motivates studying the olfactory system in awake, behaving animals.

Diagnostic and directional olfaction

Chemosensation was the first sensory system to evolve and has therefore found diverse forms throughout the animal kingdom. It guides animals toward food and mates and away from predators. Two principal functions of olfaction are diagnostic and directional. Diagnostic olfaction is the process of identifying, classifying, or assigning valence to perceived odorants. Directional olfaction is the process of localizing the direction, distance, or spatial location of perceived odorants. These two functions are akin to the “what where” distinctions in vision. We will focus on directional olfaction for the remainder of the introduction, but many excellent reviews of diagnostic olfaction exist (Ache & Young, 2005; Secundo et al., 2014). We will use the computational, algorithmic, and implementational levels to structure the review.

Comparative computations

Olfaction drives complex navigational behaviors across the animal kingdom: worms, flies, rodents, lobsters, birds, polar bears, humans and many more have all been subjects in studies of olfactory navigation (Murthy, 2024; Reddy et al., 2022).

Ants track pheromone trails using both antennae (Draft et al., 2018). Lobsters and locusts flick their antennae to sample odor cues (Koehl et al., 2001; Mellon Jr., 1997; Murlis et al., 2003). Elephants use their large trunks to sniff and can discriminate amongst individual scents and understand their spatial relationships. Humans are capable of following odor trails, and likely use stereo cues to track sources (Bao et al., 2019; Jacobs et al., 2015; Porter et al., 2007). Salmon will learn the smell of their spawning pools and return, hundreds of miles and months later, to that same spawning pool in subsequent seasons (Webster & Weissburg, 2009).

This diverse phylogeny lends itself to comparative studies of behavioral strategies, anatomy, and more (Baker et al., 2018). Olfaction is not the only sense used for any of these tasks. Visual, gustatory, and auditory cues are typically used in concert for daily tasks. However, there are cases where olfaction is essential, for example at long distances, in low-light conditions, or in water.

Why rodents? Rodents have a highly developed sense of smell making them a champion model system for this topic . Mice primarily use olfactory cues when localizing food sources (Howard et al., 1968). Olfaction is so central to their experience that inducing anosmia is a common way to induce depression. Rodents are obligate nasal

breathers, so their noses are constantly sampling ambient odors, even in the absence of intentional sniffing.

Algorithms.

There are multiple sources of information present in odor plumes which could be used to associate odor inputs with spatial information (Crimaldi and Koseff, 2001; Boie et al 2018; Demir et al, 2020; Rigolli et al 2022). Navigation can also be multisensory, with visual and wind cues in particular being used in conjunction with odor cues to guide strategies like cast and surge (Kennedy and Marsh, 1974; Balkovsky and Shraiman, 2002; van Breugel et al, 2014; Alvarez-Salvado et al, 2018; Ouyang et al 2024). Each model captures some aspects of animal behavior but making comparisons across models demonstrates that no model captures all aspects of behavior (Pang et al, 2018). Reinforcement learning models have captured various aspects of search behaviors: cast-surge, head-casting, alternation (Rando et al, 2024; Rigolli et al, 2022; Reddy et al, 2021; Loisy and Eloy, 2022; Singh et al, 2023). What many sensorimotor algorithms cannot capture is that when rodents gain knowledge about the spatial distribution of sources, they often switch from sensory-guided strategies to spatial-memory guided strategies (Gire et al, 2016; Jackson et al, 2020). Often models ignore the embodied respiratory dynamics, which could be key for more biologically realistic models (Severino et al 2024).

Cognitive maps are an influential theory for how the brain organizes relationships between spaces, both physical and abstract (Tolman, 1948). These maps are likely used in navigation, learning, and memory across the animal kingdom (Gallistel, 1990). Olfaction in particular has a close functional, anatomical, and evolutionary relationship with hippocampus and entorhinal cortex (Barwich, 2023; Jacobs, 2012, 2023; Jacobs & Schenk, 2003).

Time, like space, is another fundamental aspect of representation learning (Eichenbaum, 2014). There are generally two mechanisms to encode time in the nervous system: oscillations and slow population drift. Oscillations can be used to linearly integrate short time events, for example theta oscillations (Buzsáki, 2019) or inhalations (Kepecs et al., 2006; Wachowiak, 2011). Slow population drift has noisy estimates in local time but could be better used to estimate longer intervals with slower evolving dynamics (Karmarkar & Buonomano, 2007; Schoonover et al., 2021).

Dynamical systems theories of cognition describe the emergent, time-varying neural processes with many useful analytical tools. Walter Freeman established many fundamental aspects of a dynamical systems view of the nervous system through studies of the olfactory system. Primarily using EEG methods in rabbits, he established that responses to odors was not a simple, linear system, but highly dependent on

context, action, and behavioral state. He used the emerging perspectives of dynamical systems theory to describe the chaotic dynamics of the observed neural signals and propose how they may be well suited for adaptation and learning. (Freeman, 1978; Kay et al., 1996; Sussillo, 2014)

Mechanism

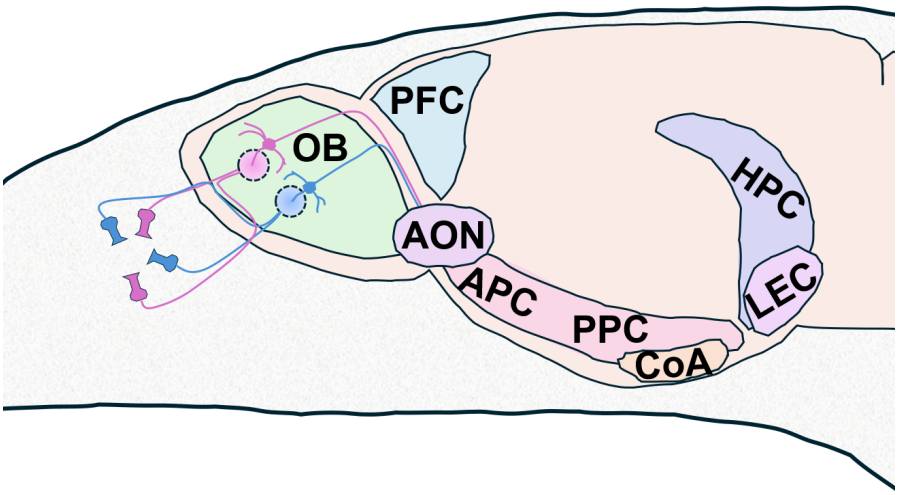

Figure 3: Anatomy of an integrated olfactory system. The anatomical logic of the early olfactory system separates olfactory sensory neurons to specific localized bundles of synapses called glomeruli in the olfactory bulb. There, mitral and tufted cells are the primary outputs, with granule cells providing lateral inhibition as well as relaying centrifugal feedback. Olfactory bulb is reciprocally connected to a variety of regions. Piriform cortex, hippocampus, and entorhinal cortex together form the three-layered “allocortex” with bidirectional communication. OB: Olfactory bulb; AON - Anterior Olfactory Nucleus; APC/PPC - Anterior/Posterior piriform cortex; CoA - Cortical amygdala; HPC - Hippocampus; LEC - Lateral entorhinal cortex; PFC - Prefrontal cortex.

Volatile chemical compounds bind to odorant receptors on olfactory sensory neurons in the olfactory epithelium of the nose. These OSNs project to glomeruli, collections of synapses in the olfactory bulb, which are segregated by receptor type. Local circuitry in the olfactory bulb, like inhibitory granule cells, receive feedforward sensory signals as well as centrifugal feedback to modulate activity in the OB. Mitral and Tufted cells (MC, TCs) are the primary projection neurons from the olfactory bulb, which target a variety of targets, primarily Anterior Olfactory Nucleus (AON), anterior and posterior piriform cortex (A/PPC), cortical amygdala, and lateral entorhinal cortex (LEC).

Olfactory Sensory Neurons

Much of the progress in molecular neuroscience was hindered by the elusive nature of olfactory stimuli. Unlike visual or auditory cues, until the 1990s, we knew very little about how basic signal transduction occurred. That changed when Richard Axel and Linda Buck discovered the family of olfactory receptor genes and introduced the possibility of modern molecular tools to the field of olfaction (Axel, 2005; L. Buck & Axel, 1991; L. B. Buck, 2005).

Olfactory Bulb

Starting with Lord Adrian in 1950 who discovered theta oscillations in the olfactory bulb of hedgehogs. The olfactory bulb is a driving force for respiratory oscillations. In humans, nasal respiration, but *not* oral respiration is implicated in memory tasks. Olfaction is the only sense that when humans were asked to imagine a sensation, it evoked the act of sniffing. The olfactory information enters the brain through chemoreceptors of olfactory sensory neurons (OSNs) in the olfactory epithelium. These project principally to the olfactory bulb through a structured one receptor to one glomeruli relationship.

Allocortex

Extensive anatomical and physiological work has characterized the close relationship between olfactory bulb, piriform cortex, hippocampus, and entorhinal cortex.

The hippocampus has long been known to be central for navigation and memory. Lucia Jacobs has drawn out the evolutionary connections between the OB and HPC which suggest a close functional relationship. Spatially distributed olfactory cues are capable of driving spatial fields in HPC in rats and gridlike representations in human EC. The respiratory rhythm of OB is seen in HPC and HPC theta appears in the OB of head-fixed mice.

There are myriad anatomical connections from the OB -> HPC. Lateral EC (LEC) is the most direct route and respiratory coupling in OB has been seen in LEC. The PC also offers a route and has been shown to couple with the respiratory rhythm under anesthesia. The PC also has direct connections with the EC (Reinert & Fukunaga, 2022).

1.3 Modeling

> “The purpose of building a model should never be to attempt to replicate the fullness of biological complexity, but to provide a simplified version that reveals general principles.” - Eve Marder (2015)
>
> *"The Analytical Engine has no pretensions to originate anything. It can do whatever we know how to order it to perform"* Ada Lovelace (1843)

What is the role of modeling in neuroscience? While perspectives on this question fill textbooks, in general modeling aspires to move the field from experimental findings to general principles (Mel, 2000). These principles will undoubtedly be restricted to a specific set of spatiotemporal scales, as a ‘grand unified theory’ of biology is likely impossible (Marshall et al., 2024). However, it is important to work towards the construction of models to make sense of the increasingly large and complex data that experimental techniques are generating.

Modeling neural data can be simply described as fitting parameters of a model to the data and investigating the results. With the increasing size and complexity of neural datasets, the phrase “big data” and “data-driven” neuroscience have become popular buzzwords. However, no model can ever be free of assumptions; constructing a statistical model requires formulating hypotheses about the data generating process. Thus, careful consideration and model comparison remain essential skills for statistical analysis of neural data (Kass et al., 2016).

Descriptive models are a class of models that fit free parameters to maximize some measure of likelihood of the observed data under the model. Normative models are those that describe how one *should* perform some objective and what neural data might look like under that behavior. These two classes of models can be thought of in a top-down (normative) and bottom-up (descriptive) dichotomy, which can provide complementary approaches to hone in on mechanistic descriptions of data (Linderman & Gershman, 2017).

Prediction vs understanding

Computational neuroscience is a big field comprising many different perspectives and goals. In the era of big data and big compute, machine learning approaches have become increasingly popular in neuroscience. A succinct framing of this perspective is Sutton’s bitter lesson, which states that in most cases using large scale compute and data for a problem will almost always beat intuitions provided by expert analysis (Sutton, 2019). This has held true in some respects, for example Atari and AlphaGO (documentary cite), large language models, speech prosthesis (Chang lab). However, the goal of many neuroscientists is not expert gameplay or next token prediction. Many of us seek to find relatively concise and understandable models of cognition. Prediction and understanding are often, but not necessarily, in tension with each other (Chirimuuta, 2021).

Task-trained neural networks

Artificial neural networks have a long history in cognitive and computational sciences (Lindsay, 2021). In the last decade, they have powered numerous advances in the field of artificial intelligence and systems neuroscience (Fetz, 1994; Nobel Committee for Physics, 2024; Yamins & DiCarlo, 2016). While many applications exist for ANNs, this thesis focuses on their use as expressive, yet interpretable models of cognitive phenomena (He et al., 2024; van Rooij et al., 2024). Importantly, the networks I have developed and studied in this thesis will not break any machine learning benchmarks or leaderboards - that is not the goal of this work. Instead, we hope that by training ANNs to solve simulated tasks, we can learn useful abstractions about representations and algorithms that might improve our understanding of how biological systems solve a related task.

What types of abstractions of neural circuits do ANNs make? While some may make one-to-one comparisons between ANN units and neurons, many view the level of population dynamics and algorithms as an appropriate level of comparison (Lindsay, 2024). In fact, it has been shown that the highly nonlinear transformations of an individual neuron can be approximated by a neural network (Beniaguev et al., 2021; Gidon et al., 2020). ANNs provide hypotheses for how the population activity of neurons might represent and transform information efficiently to support adaptive behaviors. For example, attractor structures have a long theoretical history as useful dynamical structures for memory (Freeman, 1978; Hopfield, 1999), and there is growing evidence that neural systems use attractors for computation (Inagaki et al., 2019; Vinograd et al., 2024).

1.4 Overview of thesis

Key questions

How does the olfactory system influence the construction and updating of internal models of space, or cognitive maps? How do these cognitive maps influence the representation and interpretation of incoming olfactory information?

Summary of Chapters

In chapter 2, we present an exploratory analysis of the structure of olfactory bulb spiking activity under freely behaving, task- and stimulus-free conditions. We find that the olfactory bulb encodes sniffing behaviors as well as the mouse’s allocentric place. This work motivates follow up experiments to test the role these representations play in active spatial-olfactory behaviors like odor source localization, spatial-associative learning, and navigation.

In chapter 3, we take a normative approach to ask what types of neural dynamics might be useful for spatial-olfactory memories, flexible navigation, and foraging. We find that networks use odor cues during exploration but not in subsequent memory-guided exploitation episodes. This is reflected in the neural dynamics, which are separated into an exploration subspace and an exploitation subspace to support adaptive behaviors. These findings demonstrate the strength of simulations for exploring task designs and suggesting hypotheses for how neural systems may perform flexible behavior.

In chapter 4, we review recent advances in computational behavioral analysis along with excerpts demonstrating the diversity of situations we've usd them, including mouse olfactory navigation, zebrafish optomotor responses, and *C. elegans* locomotor development. These highlight the strengths of new computational approaches for naturalistic behavioral experiments and the need for behavioral methods which are as detailed as our physiological tools.

In chapter 5, we close with some conclusions about the findings and some speculation about where future research in naturalistic systems neuroscience is heading.

Contributions

Systems neuroscience papers are becoming increasingly collaborative, with experimental and computational contributions. This makes traditional author lists increasingly limited in communicating the nuanced contributions of all authors. Recently, journals and individual authors have used contribution matrices to communicate the many roles each author has played in a paper (*Researchers Are Embracing Visual Tools to Give Fair Credit for Work on Papers*, 2021). We will use this method for each chapter, but present a summary of contributions for each chapter below.

	Chapter 2	Chapter 3	Chapter 4		
	Olfactory bulb tracks breathing and place. Sterrett*, Findley*, et al	Recurrent neural networks balance sensory- and memory-guided policies for spatial foraging. Sterrett et al.	Dynamics of odor source localization. Tariq, Sterrett, et al *Plos One*	Attentional Switching in Zebrafish (3rd author)	Development of dimensionality. Hassinan*, Sterrett*, et al *Plos Comp Bio*
Contributor Role					
Conceptualization	x	x	x		x
Data Curation		x			
Formal Analysis	x	x	x	x	x
Funding Acquisition					
Investigation		x			x
Methodology	x	x	x	x	x
Project Administration		x			
Resources					
Software	x	x	x	x	x
Supervision	x				x
Validation	x	x			x
Visualization	x	x	x	x	x
Writing – Original Draft	x	x			x
Writing – Review & Editing	x	x	x	x	x

References

Ache, B. W., & Young, J. M. (2005). Olfaction: Diverse species, conserved principles. *Neuron*, *48*(3), 417–430. https://doi.org/10.1016/j.neuron.2005.10.022

Ackels, T., Erskine, A., Dasgupta, D., Marin, A. C., Warner, T. P. A., Tootoonian, S., Fukunaga, I., Harris, J. J., & Schaefer, A. T. (2021). Fast odour dynamics are encoded in the olfactory system and guide behaviour. *Nature*, 1–6. https://doi.org/10.1038/s41586-021-03514-2

Adrian, E. D. (1950). The electrical activity of the mammalian olfactory bulb. *Electroencephalography and Clinical Neurophysiology*, *2*(1–4), 377–388. https://doi.org/10.1016/0013-4694(50)90075-7

Anderson, P. W. (1972). More Is Different. *Science*, *177*(4047), 393–396. https://doi.org/10.1126/science.177.4047.393

Axel, R. (2005). Scents and Sensibility: A Molecular Logic of Olfactory Perception (Nobel Lecture). *Angewandte Chemie International Edition*, *44*(38), 6110–6127. https://doi.org/10.1002/anie.200501726

Baker, K. L., Dickinson, M., Findley, T. M., Gire, D. H., Louis, M., Suver, M. P., Verhagen, J. V., Nagel, K. I., & Smear, M. C. (2018). Algorithms for Olfactory Search across Species. *Journal of Neuroscience*, *38*(44), 9383–9389. https://doi.org/10.1523/JNEUROSCI.1668-18.2018

Bao, X., Gjorgieva, E., Shanahan, L. K., Howard, J. D., Kahnt, T., & Gottfried, J. A. (2019).

Grid-like Neural Representations Support Olfactory Navigation of a Two-Dimensional Odor Space. *Neuron*, *102*(5), 1066-1075.e5. https://doi.org/10.1016/j.neuron.2019.03.034

Barwich, A.-S. (2023). If Proust had whiskers: Recalling locations with smells. *Learning & Behavior*, *51*(2), 121–122. https://doi.org/10.3758/s13420-022-00549-x

Bateson, P., & Laland, K. N. (2013). Tinbergen's four questions: An appreciation and an update. *Trends in Ecology & Evolution*, *28*(12), 712–718. https://doi.org/10.1016/j.tree.2013.09.013

Bechtel, W., & Shagrir, O. (2015). The Non-Redundant Contributions of Marr's Three Levels of Analysis for Explaining Information-Processing Mechanisms. *Topics in Cognitive Science*, *7*(2), 312–322. https://doi.org/10.1111/tops.12141

Beniaguev, D., Segev, I., & London, M. (2021). Single cortical neurons as deep artificial neural networks. *Neuron*, *109*(17), 2727-2739.e3. https://doi.org/10.1016/j.neuron.2021.07.002

Bocca, E., Antonelli, A. R., & Mosciaro, O. (1965). Mechanical Co-Factors in Olfactory Stimulation. *Acta Oto-Laryngologica*, *59*(2–6), 243–247. https://doi.org/10.3109/00016486509124558

BRAIN 2025: A Scientific Vision. (n.d.). 146.

Buck, L., & Axel, R. (1991). A novel multigene family may encode odorant receptors: A molecular basis for odor recognition. *Cell*, *65*(1), 175–187. https://doi.org/10.1016/0092-8674(91)90418-x

Buck, L. B. (2005). Unraveling the Sense of Smell (Nobel Lecture). *Angewandte Chemie International Edition*, *44*(38), 6128–6140. https://doi.org/10.1002/anie.200501120

Buzsáki, G. (2019). *The Brain from Inside Out*. Oxford University Press. https://doi.org/10.1093/oso/9780190905385.001.0001

Chaput, M. A., Buonviso, N., & Berthommier, F. (1992). Temporal Patterns in Spontaneous and Odour-evoked Mitral Cell Discharges Recorded in Anaesthetized Freely Breathing Animals. *European Journal of Neuroscience*, *4*(9), 813–822. https://doi.org/10.1111/j.1460-9568.1992.tb00191.x

Chirimuuta, M. (2021). Prediction versus understanding in computationally enhanced neuroscience. *Synthese*, *199*(1–2), 767–790. https://doi.org/10.1007/s11229-020-02713-0

Clark, B., & Foster, J. B. (2009). Ecological Imperialism and the Global Metabolic Rift: Unequal Exchange and the Guano/Nitrates Trade. *International Journal of Comparative Sociology*, *50*(3–4), 311–334. https://doi.org/10.1177/0020715209105144

Crawford, K. (2024). Generative AI's environmental costs are soaring—And mostly secret. *Nature*, *626*(8000), 693–693. https://doi.org/10.1038/d41586-024-00478-x

Datta, S. R., Anderson, D. J., Branson, K., Perona, P., & Leifer, A. (2019). Computational Neuroethology: A Call to Action. *Neuron*, *104*(1), 11–24. https://doi.org/10.1016/j.neuron.2019.09.038

Dennis, E. J., El Hady, A., Michaiel, A., Clemens, A., Gowan Tervo, D. R., Voigts, J., & Datta, S. R. (2020). Systems Neuroscience of Natural Behaviors in Rodents. *The Journal of Neuroscience*, JN-SY-1877-20. https://doi.org/10.1523/JNEUROSCI.1877-20.2020

Ding, S. S., Fox, J. L., Gordus, A., Joshi, A., Liao, J. C., & Scholz, M. (2024). Fantastic beasts and how to study them: Rethinking experimental animal behavior. *Journal of*

Experimental Biology, *227*(4), jeb247003. https://doi.org/10.1242/jeb.247003
Dobson, A. P. (2005). What Links Bats to Emerging Infectious Diseases? *Science*, *310*(5748), 628–629. https://doi.org/10.1126/science.1120872
Draft, R. W., McGill, M. R., Kapoor, V., & Murthy, V. N. (2018). Carpenter ants use diverse antennae sampling strategies to track odor trails. *Journal of Experimental Biology*, *221*(22), jeb185124. https://doi.org/10.1242/jeb.185124
Eichenbaum, H. (2014). Time cells in the hippocampus: A new dimension for mapping memories. *Nature Reviews Neuroscience*, *15*(11), 732–744. https://doi.org/10.1038/nrn3827
Fairhall, A. (2014). The receptive field is dead. Long live the receptive field? *Current Opinion in Neurobiology*, *25*, ix–xii. https://doi.org/10.1016/j.conb.2014.02.001
Fetz, E. E. (1994). Are movement parameters recognizably coded in the activity of single neurons? In P. Cordo & S. Harnad (Eds.), *Movement Control* (1st ed., pp. 77–88). Cambridge University Press. https://doi.org/10.1017/CBO9780511529788.008
Fields, R. D. (2018). The First Annual Meeting of the Society for Neuroscience, 1971: Reflections Approaching the 50th Anniversary of the Society's Formation. *Journal of Neuroscience*, *38*(44), 9311–9317. https://doi.org/10.1523/JNEUROSCI.3598-17.2018
Freeman, W. J. (1978). Spatial properties of an EEG event in the olfactory bulb and cortex. *Electroencephalography and Clinical Neurophysiology*, *44*(5), 586–605. https://doi.org/10.1016/0013-4694(78)90126-8
Gallistel, C. R. (1990). *The organization of learning* (pp. viii, 648). The MIT Press.
Gidon, A., Zolnik, T. A., Fidzinski, P., Bolduan, F., Papoutsi, A., Poirazi, P., Holtkamp, M., Vida, I., & Larkum, M. E. (2020). Dendritic action potentials and computation in human layer 2/3 cortical neurons. *Science*, *367*(6473), 83–87. https://doi.org/10.1126/science.aax6239
Gomez-Marin, A., Paton, J. J., Kampff, A. R., Costa, R. M., & Mainen, Z. F. (2014). Big behavioral data: Psychology, ethology and the foundations of neuroscience. *Nature Neuroscience*, *17*(11), 1455–1462. https://doi.org/10.1038/nn.3812
He, Z., Achterberg, J., Collins, K., Nejad, K., Akarca, D., Yang, Y., Gurnee, W., Sucholutsky, I., Tang, Y., Ianov, R., Ogden, G., Li, C., Sandbrink, K., Casper, S., Ivanova, A., & Lindsay, G. W. (2024). *Multilevel Interpretability Of Artificial Neural Networks: Leveraging Framework And Methods From Neuroscience* (arXiv:2408.12664). arXiv. http://arxiv.org/abs/2408.12664
Hegel, G. (1816). *Science of Logic*. https://www.marxists.org/reference/archive/hegel/works/hl/hlconten.htm
Hopfield, J. J. (1999). Odor space and olfactory processing: Collective algorithms and neural implementation. *Proceedings of the National Academy of Sciences*, *96*(22), 12506–12511. https://doi.org/10.1073/pnas.96.22.12506
Howard, W. E., Marsh, R. E., & Cole, R. E. (1968). Food detection by deer mice using olfactory rather than visual cues. *Animal Behaviour*, *16*(1), 13–17. https://doi.org/10.1016/0003-3472(68)90100-0
Inagaki, H. K., Fontolan, L., Romani, S., & Svoboda, K. (2019). Discrete attractor dynamics underlies persistent activity in the frontal cortex. *Nature*, *566*(7743), 212–217. https://doi.org/10.1038/s41586-019-0919-7

Jacobs, L. F. (2012). From chemotaxis to the cognitive map: The function of olfaction. *Proceedings of the National Academy of Sciences*, *109*(Supplement 1), 10693–10700. https://doi.org/10.1073/pnas.1201880109

Jacobs, L. F. (2023). The PROUST hypothesis: The embodiment of olfactory cognition. *Animal Cognition*, *26*(1), 59–72. https://doi.org/10.1007/s10071-022-01734-1

Jacobs, L. F., Arter, J., Cook, A., & Sulloway, F. J. (2015). Olfactory Orientation and Navigation in Humans. *PLOS ONE*, *10*(6), e0129387. https://doi.org/10.1371/journal.pone.0129387

Jacobs, L. F., & Schenk, F. (2003). Unpacking the cognitive map: The parallel map theory of hippocampal function. *Psychological Review*, *110*(2), 285–315. https://doi.org/10.1037/0033-295X.110.2.285

Karmarkar, U. R., & Buonomano, D. V. (2007). Timing in the absence of clocks: Encoding time in neural network states. *Neuron*, *53*(3), 427–438. https://doi.org/10.1016/j.neuron.2007.01.006

Kass, R. E., Caffo, B. S., Davidian, M., Meng, X.-L., Yu, B., & Reid, N. (2016). Ten Simple Rules for Effective Statistical Practice. *PLOS Computational Biology*, *12*(6), e1004961. https://doi.org/10.1371/journal.pcbi.1004961

Kay, L. M., Lancaster, L. R., & Freeman, W. J. (1996). Reafference and attractors in the olfactory system during odor recognition. *International Journal of Neural Systems*, *7*(4), 489–495. https://doi.org/10.1142/s0129065796000476

Kay, L. M., & Laurent, G. (1999). Odor- and context-dependent modulation of mitral cell activity in behaving rats. *Nature Neuroscience*, *2*(11), Article 11. https://doi.org/10.1038/14801

Kennedy, A. (2022). The what, how, and why of naturalistic behavior. *Current Opinion in Neurobiology*, *74*, 102549. https://doi.org/10.1016/j.conb.2022.102549

Kepecs, A., Uchida, N., & Mainen, Z. F. (2006). The Sniff as a Unit of Olfactory Processing. *Chemical Senses*, *31*(2), 167–179. https://doi.org/10.1093/chemse/bjj016

Koehl, M. A. R., Koseff, J. R., Crimaldi, J. P., McCay, M. G., Cooper, T., Wiley, M. B., & Moore, P. A. (2001). Lobster Sniffing: Antennule Design and Hydrodynamic Filtering of Information in an Odor Plume. *Science*, *294*(5548), 1948–1951. https://doi.org/10.1126/science.1063724

Kohles, J. E., Page, R. A., Wikelski, M., & Dechmann, D. K. N. (2024). Seasonal shifts in insect ephemerality drive bat foraging effort. *Current Biology*, *34*(14), 3241-3248.e3. https://doi.org/10.1016/j.cub.2024.05.074

Krakauer, J. W., Ghazanfar, A. A., Gomez-Marin, A., MacIver, M. A., & Poeppel, D. (2017). Neuroscience Needs Behavior: Correcting a Reductionist Bias. *Neuron*, *93*(3), 480–490. https://doi.org/10.1016/j.neuron.2016.12.041

Lengyel, M. (2024). Marr's three levels of analysis are useful as a framework for neuroscience. *The Journal of Physiology*, *602*(9), 1911–1914. https://doi.org/10.1113/JP279549

Linderman, S. W., & Gershman, S. J. (2017). Using computational theory to constrain statistical models of neural data. *Current Opinion in Neurobiology*, *46*, 14–24. https://doi.org/10.1016/j.conb.2017.06.004

Lindsay, G. W. (2021). *Models of the Mind*. Bloomsbury Sigma.

Lindsay, G. W. (2024). Grounding neuroscience in behavioral changes using artificial neural networks. *Current Opinion in Neurobiology*, *84*, 102816. https://doi.org/10.1016/j.conb.2023.102816

Macrides, F., & Chorover, S. L. (1972). Olfactory Bulb Units: Activity Correlated with Inhalation Cycles and Odor Quality. *Science*, *175*(4017), 84–87. https://doi.org/10.1126/science.175.4017.84

Marr, D. (1982). *Vision*. The MIT Press. https://mitpress.mit.edu/9780262514620/vision/

Marshall, W., Baum, B., Fairhall, A., Heisenberg, C.-P., Koslover, E., Liu, A., Mao, Y., Mogilner, A., Nelson, C. M., Paluch, E. K., Trepat, X., & Yap, A. (2024). Where physics and biology meet. *Current Biology*, *34*(20), R950–R960. https://doi.org/10.1016/j.cub.2024.08.022

Mel, B. W. (2000). In the brain, the model is the goal. *Nature Neuroscience*, *3*(11), 1183–1183. https://doi.org/10.1038/81458

Mellon Jr., D. (1997). Physiological characterization of antennular flicking reflexes in the crayfish. *Journal of Comparative Physiology A*, *180*(5), 553–565. https://doi.org/10.1007/s003590050072

Miller, C. T., Gire, D., Hoke, K., Huk, A. C., Kelley, D., Leopold, D. A., Smear, M. C., Theunissen, F., Yartsev, M., & Niell, C. M. (2022). Natural behavior is the language of the brain. *Current Biology*, *32*(10), R482–R493. https://doi.org/10.1016/j.cub.2022.03.031

Murlis, J., Elkinton, J. S., & Cardé, R. (2003). Odor Plumes and How Insects Use Them. *Annual Review of Entomology*, *37*, 505–532. https://doi.org/10.1146/annurev.en.37.010192.002445

Murthy, V. N. (2024). Olfactory navigation in fluctuating environments. *Current Biology*, *34*(20), R1013–R1018. https://doi.org/10.1016/j.cub.2024.07.049

Ngai, J. (2022). BRAIN 2.0: Transforming neuroscience. *Cell*, *185*(1), 4–8. https://doi.org/10.1016/j.cell.2021.11.037

Nobel Committee for Physics. (2024). *The Nobel Prize in Physics 2024*. NobelPrize.Org. https://www.nobelprize.org/prizes/physics/2024/press-release/

Onoda, N., & Mori, K. (1980). Depth distribution of temporal firing patterns in olfactory bulb related to air-intake cycles. *Journal of Neurophysiology*, *44*(1), 29–39. https://doi.org/10.1152/jn.1980.44.1.29

Pereira, T. D., Shaevitz, J. W., & Murthy, M. (2020). Quantifying behavior to understand the brain. *Nature Neuroscience*, 1–13. https://doi.org/10.1038/s41593-020-00734-z

Pillow, J. W. (2024a). Cross Talk opposing view: Marr's three levels of analysis are not useful as a framework for neuroscience. *The Journal of Physiology*, *602*(9), 1915–1917. https://doi.org/10.1113/JP279550

Pillow, J. W. (2024b). CrossTalk rebuttal. *The Journal of Physiology*, *602*(9), 1921–1921. https://doi.org/10.1113/JP286427

Porter, J., Craven, B., Khan, R. M., Chang, S.-J., Kang, I., Judkewitz, B., Volpe, J., Settles, G., & Sobel, N. (2007). Mechanisms of scent-tracking in humans. *Nature Neuroscience*, *10*(1), Article 1. https://doi.org/10.1038/nn1819

Proetz, A. W. (1953). *Essays on the Applied Physiology of the Nose*. Annals Publishing Company.

Ramón y Cajal, S. (1894). *Croonian Lecture: La fine structure des centres nerveux* [Graphic]. doi: 10.1098/rspl.1894.0063

Reddy, G., Murthy, V. N., & Vergassola, M. (2022). Olfactory Sensing and Navigation in Turbulent Environments. *Annual Review of Condensed Matter Physics*, *13*(1), annurev-conmatphys-031720-032754.

https://doi.org/10.1146/annurev-conmatphys-031720-032754
Reinert, J. K., & Fukunaga, I. (2022). The facets of olfactory learning. *Current Opinion in Neurobiology*, *76*, 102623. https://doi.org/10.1016/j.conb.2022.102623
Researchers are embracing visual tools to give fair credit for work on papers. (2021, January 22). Nature Index. https://www.nature.com/nature-index/news/researchers-embracing-visual-tools-contribution-matrix-give-fair-credit-authors-scientific-papers
Rinberg, D., & Gelperin, A. (2006). Olfactory neuronal dynamics in behaving animals. *Seminars in Cell & Developmental Biology*, *17*(4), 454–461. https://doi.org/10.1016/j.semcdb.2006.04.009
Schnitzler, H.-U., Moss, C. F., & Denzinger, A. (2003). From spatial orientation to food acquisition in echolocating bats. *Trends in Ecology & Evolution*, *18*(8), 386–394. https://doi.org/10.1016/S0169-5347(03)00185-X
Schoonover, C. E., Ohashi, S. N., Axel, R., & Fink, A. J. P. (2021). Representational drift in primary olfactory cortex. *Nature*, *594*(7864), 541–546. https://doi.org/10.1038/s41586-021-03628-7
Secundo, L., Snitz, K., & Sobel, N. (2014). The perceptual logic of smell. *Current Opinion in Neurobiology*, *25*, 107–115. https://doi.org/10.1016/j.conb.2013.12.010
Simmons, J. A., Fenton, M. B., & O'Farrell, M. J. (1979). Echolocation and Pursuit of Prey by Bats. *Science*, *203*(4375), 16–21. https://doi.org/10.1126/science.758674
Sobel, N., Thomason, M. E., Stappen, I., Tanner, C. M., Tetrud, J. W., Bower, J. M., Sullivan, E. V., & Gabrieli, J. D. (2001). An impairment in sniffing contributes to the olfactory impairment in Parkinson's disease. *Proceedings of the National Academy of Sciences of the United States of America*, *98*(7), 4154–4159. https://doi.org/10.1073/pnas.071061598
Society for Neuroscience. (2019). *Creation of Neuroscience*. https://www.sfn.org/about/history-of-sfn/the-creation-of-neuroscience/~/media/SfN/Images/History%20of%20SfN/pdf/HistoryofSfN.ashx
Sussillo, D. (2014). Neural circuits as computational dynamical systems. *Current Opinion in Neurobiology*, *25*, 156–163. https://doi.org/10.1016/j.conb.2014.01.008
Sutton, R. (2019). *The Bitter Lesson*. http://www.incompleteideas.net/IncIdeas/BitterLesson.html
Tinbergen, N. (1963). On aims and methods in ethology. *Zeitschrift Für Tierpsychologie*. https://www.esf.edu/biology/faculty/documents/Tinbergen1963onethology.pdf
Tolman, E. C. (1948). *Cognitive maps in rats and men*.
Tsagkogeorga, G., Parker, J., Stupka, E., Cotton, J. A., & Rossiter, S. J. (2013). Phylogenomic Analyses Elucidate the Evolutionary Relationships of Bats. *Current Biology*, *23*(22), 2262–2267. https://doi.org/10.1016/j.cub.2013.09.014
van Rooij, I., Guest, O., Adolfi, F., de Haan, R., Kolokolova, A., & Rich, P. (2024). Reclaiming AI as a Theoretical Tool for Cognitive Science. *Computational Brain & Behavior*. https://doi.org/10.1007/s42113-024-00217-5
Vinograd, A., Nair, A., Kim, J. H., Linderman, S. W., & Anderson, D. J. (2024). Causal evidence of a line attractor encoding an affective state. *Nature*, *634*(8035), 910–918. https://doi.org/10.1038/s41586-024-07915-x
Wachowiak, M. (2011). All in a Sniff: Olfaction as a Model for Active Sensing. *Neuron*, *71*(6),

962–973. https://doi.org/10.1016/j.neuron.2011.08.030
Webster, D. R., & Weissburg, M. J. (2009). The Hydrodynamics of Chemical Cues Among Aquatic Organisms. *Annual Review of Fluid Mechanics*, *41*(Volume 41, 2009), 73–90. https://doi.org/10.1146/annurev.fluid.010908.165240
Yamins, D. L. K., & DiCarlo, J. J. (2016). Using goal-driven deep learning models to understand sensory cortex. *Nature Neuroscience*, *19*(3), 356–365. https://doi.org/10.1038/nn.4244

Olfactory bulb tracks breathing rhythms and place in freely behaving mice

Scott C. Sterrett[1]*, Teresa M. Findley[2]*, Sidney E. Rafilson[2], Morgan A. Brown[2], Aldis P Weible[2], Rebecca Marsden[2], Takisha Tarvin[2], Michael Wehr[2,3], James M. Murray[2,4,5], Adrienne L. Fairhall[1], Matthew C. Smear[2,3,#]

[1] *Department of Neurobiology & Biophysics, University of Washington, Seattle, Washington, United States*

[2] *Institute of Neuroscience, University of Oregon, Eugene, Oregon, United States*

[3] *Department of Psychology, University of Oregon, Eugene, Oregon, United States*

[4] *Department of Biology, University of Oregon, Eugene, Oregon, United States*

[5] *Department of Mathematics, University of Oregon, Eugene, Oregon, United States*

**These authors contributed equally*

[#]Corresponding author: smear@uoregon.edu

Abstract

Vertebrates sniff to control the odor samples that enter their nose. These samples can not only help identify odorous objects, but also locations and events. However, there is no receptor for place or time. Therefore, to take full advantage of olfactory information, an animal's brain must contextualize odor-driven activity with information about when, where, and how they sniffed. To better understand contextual information in the olfactory system, we captured the breathing and movements of mice while recording from their olfactory bulb. In stimulus- and task-free experiments, mice structure their breathing into persistent rhythmic states which are synchronous with statelike structure in ongoing neuronal population activity. These population states reflect a strong dependence of individual neuron activity on variation in sniff frequency, which we display using "sniff fields" and quantify using generalized linear models. In addition, many olfactory bulb neurons have "place fields" that display significant dependence of firing on allocentric location, which were comparable with hippocampal neurons recorded under the same conditions. At the population level, a mouse's location can be decoded from olfactory bulb with similar accuracy to hippocampus. Olfactory bulb place sensitivity cannot be explained by breathing rhythms or scent marks. Taken together, we show that the mouse olfactory bulb tracks breathing rhythms and self-location, which may help unite internal models of self and environment with olfactory information as soon as that information enters the brain.

Introduction

Animals actively sample their environment and explore space, even in lab experiments without experimenter-controlled stimuli and rewards (Berlyne, 1966; Buzsáki, 2019; Crowcroft, 1973; DeBose & Nevitt, 2008; Land & Tatler, 2009; Osborne et al., 1999; Renner, 1990; Wang & Hayden, 2021). Sampling sensory stimuli provides the raw material for constructing and updating internal models of self and the environment (Behrens et al., 2018; Keller & Mrsic-Flogel, 2018; O'Keefe & Nadel, 1978; Tolman, 1948; Weber et al., 2019; S. C.-H. Yang et al., 2016). In turn, internal models inform perceptual inferences and predict the consequences of actions (Buzsáki, 2019; Churchland et al., 1994; Diamanti et al., 2021; Kleinfeld et al., 2014; Parker et al., 2020; Saleem & Busse, 2023; Webb, 2004). How do sensory samples influence internal models and vice versa?

Sampling behavior imposes structure on odor encounters (Chaput et al., 1992; Crimaldi et al., 2022; Gomez-Marin et al., 2011; Huston et al., 2015; Ravel & Pager, 1990; Schmitt & Ache, 1979; Vanderwolf, 2001; Wachowiak, 2011). In terrestrial vertebrates, breathing provides olfactory sensory neurons with access to odorants, and, even in the absence of odor stimuli, olfactory neurons in the nose and olfactory bulb synchronize their activity to the respiratory cycle (Ackels et al., 2020; Adrian, 1950; Chaput et al., 1992; Grosmaitre et al., 2007; Kay et al., 1996; Macrides & Chorover, 1972; Onoda & Mori, 1980; Vanderwolf, 2000). Animals actively vary their respiratory rhythms depending on the novelty of odor stimuli (Verhagen et al., 2007; Wesson et al., 2008), task context (Frederick et al., 2011; Kepecs et al., 2007), and behavioral goals (Bensafi et al., 2003; Findley et al., 2021; Halpern, 1983; Liao & Kleinfeld, 2023; Welker, 1964). As with other senses (Di Lorenzo, 2021; Fenk et al., 2022; Gibson, 1968; Hayhoe & Ballard, 2005; Kim et al., 2020; Kleinfeld et al., 2006; Michaiel et al., 2020; Rucci & Victor, 2015; Stapleton et al., 2006; Yarbus, 1967), animals move their olfactory organs in order to acquire chemosensory information (Bhattacharyya & Bhalla, 2015; Catania, 2013; Findley et al., 2021; Jones & Urban, 2018; Liu et al., 2020; Youngentob et al., 1987). Movement and location influence the dynamics of stimulus availability to odorant receptors, so animals need to unify odor-driven activity with internal models of how, when, and where they sample the environment (Gire et al., 2016; Nevitt et al., 2008; Vergassola et al., 2007; Wallraff, 2004). Understanding this reciprocal interaction requires studying the olfactory system during active exploration of space (Barwich, 2023; Jacobs, 2012; Jacobs & Schenk, 2003; Poo et al., 2022).

Here, we investigated how exploratory behavior in task-free conditions influences activity in the olfactory bulb, specifically how spiking activity tracks sampling behavior and place. To isolate these factors from potential stimulus- or reward-driven activity, we recorded neuronal activity in the absence of explicit odor cues, task, or reward structure. We find that the breathing rhythms of freely behaving mice are structured on long timescales, persisting in rhythmic states that can last for minutes. Furthermore, the

olfactory bulb tracks these breathing rhythms – a statistical model of movement and breathing rhythm can recover stateful structure in the dynamics of neuronal populations. These population dynamics are clearly manifested at the individual neuron level in "sniff fields", which describe the dependence of neuron firing on latency relative to inhalation and the instantaneous sniff frequency. These sniff fields demonstrate that ongoing activity of olfactory bulb neurons depends on sniff frequency. Moreover, we find that the olfactory bulb tracks place; many individual neurons are significantly modulated by position in space, and the mouse's location can be decoded from neuronal populations in the bulb with comparable accuracy to neuronal populations in the hippocampus under the same conditions. Importantly, these place-dependent activity patterns do not depend on scent marks or breathing rhythms. Our results show that the olfactory bulb of freely behaving mice contains information about sampling behavior and place, even in the absence of experimenter-controlled odor cues. Thus the integration of odor information into internal models may begin as soon as olfactory information enters the brain.

Results

Breathing rhythms are richly structured during spontaneous behavior

We hypothesize that the ongoing activity of the mouse olfactory bulb (OB) encodes information about action and environment in order to contextualize odor-driven input from the nose (Freeman, 1978). This hypothesis predicts that the OB tracks variables such as behavioral state and place, even in the absence of an experimental task. To capture spontaneous behavior and neural dynamics, we implanted mice (n=4) with intranasal thermistors and silicon electrode arrays in the OB, and tracked their movements in a 40 by 15 cm behavioral arena from video under ambient light (see Methods; Fig 1a). We did not impose olfactory stimuli, task structure, or rewards, so that mice experienced only ambient stimuli and generated spontaneous behavior. Most of our recording sessions included a period of head fixation on a stationary platform for comparison with prior experiments (Shusterman et al., 2011), followed by a freely moving period, and then a second head-fixed period, which lasted between 60-90 minutes in total.

Figure 1

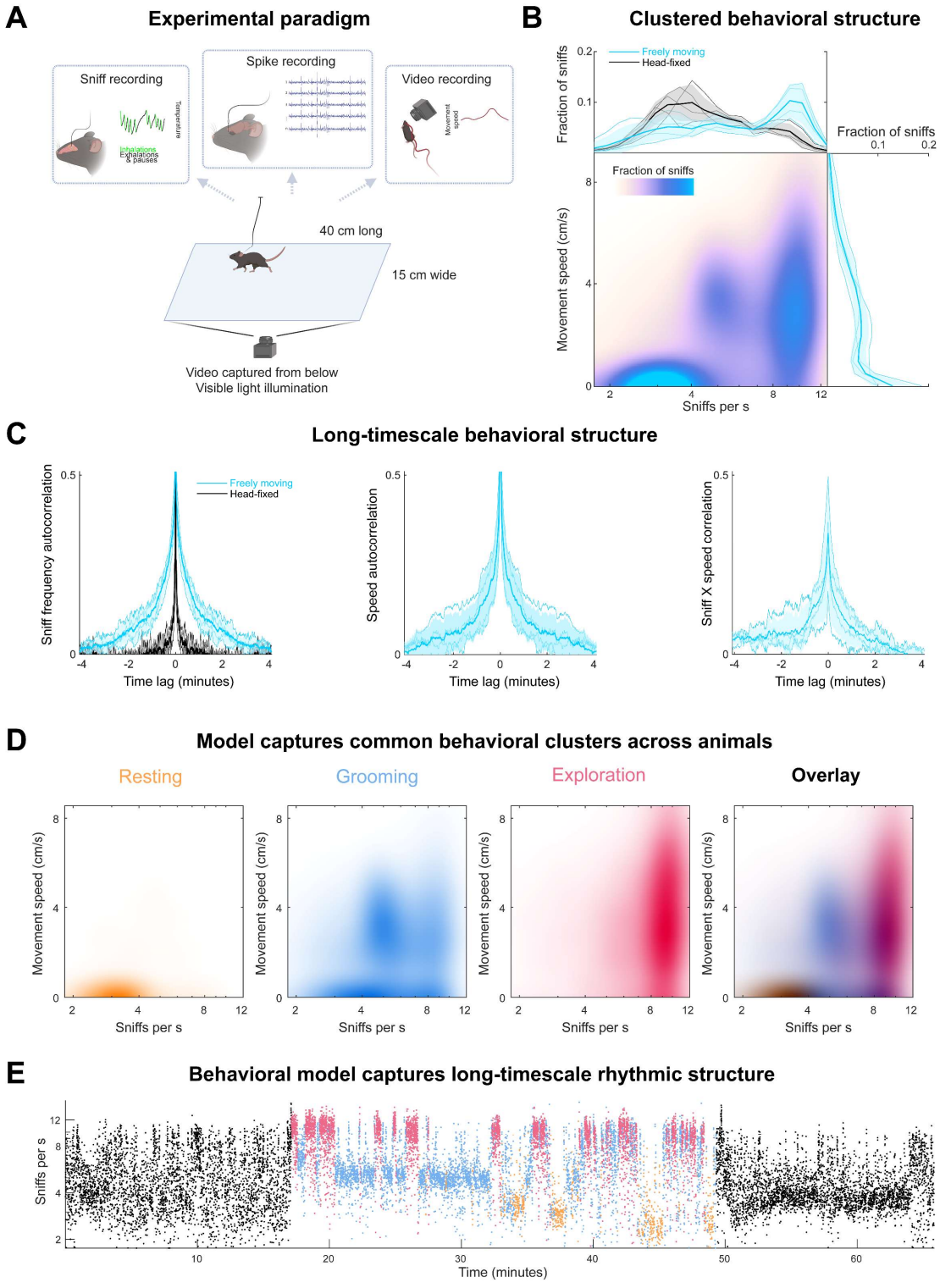

Figure 1: Stateful behavioral structure in an unstructured experimental paradigm. A. Experimental setup. Mice were head-fixed or freely moving in a 40 by 15 cm arena while we recorded respiration and neuronal activity and captured video from below in visible light. **B.** The correlation structure of breathing and movement. *Top,* Histogram of instantaneous sniff frequencies of all mice (n = 4). Thick lines and

shaded regions are mean and ±1 standard deviation, thin lines are individual mice. Blue: freely moving; black: head-fixed. *Right* , Histogram of instantaneous movement speeds, where the movement speed time series was sampled at each inhalation time. *Center,* 2D histogram of breathing frequency and movement speed. **C.** Long-timescale behavioral structure. Autocorrelations of sniff frequency (*Left),* movement speed (*Right)*, and the cross correlation between sniff frequency and speed. Blue: freely moving; black: head-fixed. **D.** A three-state Hidden Markov Model (HMM) fit to the sniff frequency and movement speed time series captures the clustered correlation structure of breathing rhythm and movement. Colormaps show the instantaneous frequency and speed distributions of sniffs in each of three states: Orange: “rest”, blue: “grooming”, red: “exploration”. *Right* Overlay of the distributions from the three states. Overlap is indicated by color mixing and darkness (for colorbars, see Figure 1, supplemental video 2) **E.** The behavioral HMM captures the long-timescale states of breathing rhythms. Each dot indicates an inhalation time with its instantaneous frequency on the vertical axis. Black: head-fixed; other colors as in 1D.

Even in this minimal experimental paradigm, mice exhibited consistently structured behaviors. Mouse breathing is coupled with orofacial and locomotor movements during natural behavior (Findley et al., 2021; Kurnikova et al., 2017; Weinreb, Pearl, et al., 2024). As expected from previous work, breathing rates were overall higher during free movement than during head fixation (Fig 1B, *top*), and breathing rates were correlated with movement speed. In addition to replicating these expected observations, we uncovered novel features of spontaneous behavioral structure. First, we found that instantaneous breathing rates in both conditions were multimodal. During free movement the distribution of sniff frequencies was well fit by a mixture of three log-normal distributions, while during head-fixed conditions, by two (Fig 1B, Fig 1- figure supplement 1). Further, these multiple modes of breathing frequency were associated with distinct movement speeds, such that the joint distribution of sniff frequency and speed formed discrete clusters that recur across sessions and animals (Fig 1B; Fig 1-figure supplement 1). Thus, the relation between sniffing and movement was more complicated than a simple linear correlation.

In addition to the patterning in instantaneous behavior, breathing rhythms and movement speed are structured at longer timescales. The time series of sniff frequency and movement shows stateful organization over timescales of minutes (Fig 1C; Fig 1 - figure supplement 1). In contrast, these persistent states of breathing rhythms are not apparent in head-fixed conditions. To quantify these observations, we computed the autocorrelation of instantaneous breathing frequency and found that the autocorrelation functions had significantly longer timescales in freely moving than head-fixed behavior (Fig 1C). Similar long timescale structure was present in the autocorrelation of movement speed as well as the cross-correlation between breathing and movement. Our analyses demonstrate that even in task-free, ambient-odor conditions, mice perform behaviors structured at multiple timescales.

Continuous, time-varying behaviors can be described as ethograms (Branson et al., 2009; Renner, 2022; Tinbergen, 1965), which divide the time series into discrete behavioral motifs, and provide a useful partition for subsequent analyses (Findley et al., 2021; Markowitz et al., 2023; Weinreb, Pearl, et al., 2024). Motivated by the clustered and long-timescale behavioral structure we observed, we fit the breathing rhythms and movement data from all mice with a Hidden Markov Model (HMM). The model was fit to the behavioral data preprocessed to extract the moving average of speed and the distribution of breathing frequencies, both evaluated in 5 second windows. Model selection was performed using Bayesian Information Criterion (BIC; fig 1 - figure supplement 2). We find that a three-state model well describes free-moving behavioral data and that these three states effectively separate the behavioral clusters (Fig 1D). Through observation of labeled behavioral data, we name these three states “rest”, “grooming”, and “exploration”. These discrete breathing states are seen across all animals but differ in their usage across individual sessions. The average persistence times of states are on the order of tens of seconds to minutes (fig 1 - figure supplement 2). Taken together, these behavioral analyses demonstrate that mice breathe and move in consistently structured ways, even when the experimental paradigm does not impose structure upon their behavior.

A behavioral model captures the structure of neuronal population dynamics

We next recorded spiking activity in the OB during our task-free, ambient-stimulus paradigm. We recorded from OB with extracellular electrodes, including in our analyses units that passed quality control criteria of fewer than 5 % refractory period violations, and fewer than 10% amplitude cutoff violations (see Methods and Fig 2 – figure supplement 1). Comparing mean firing rates of individual units between head-fixed and freely moving conditions, we found that across the population the mean firing rates were only slightly although significantly different (Fig 2A; head-fixed vs freely moving median = 4.51 vs 5.31 spikes per s; p=0.002, rank sum test).

Figure 2

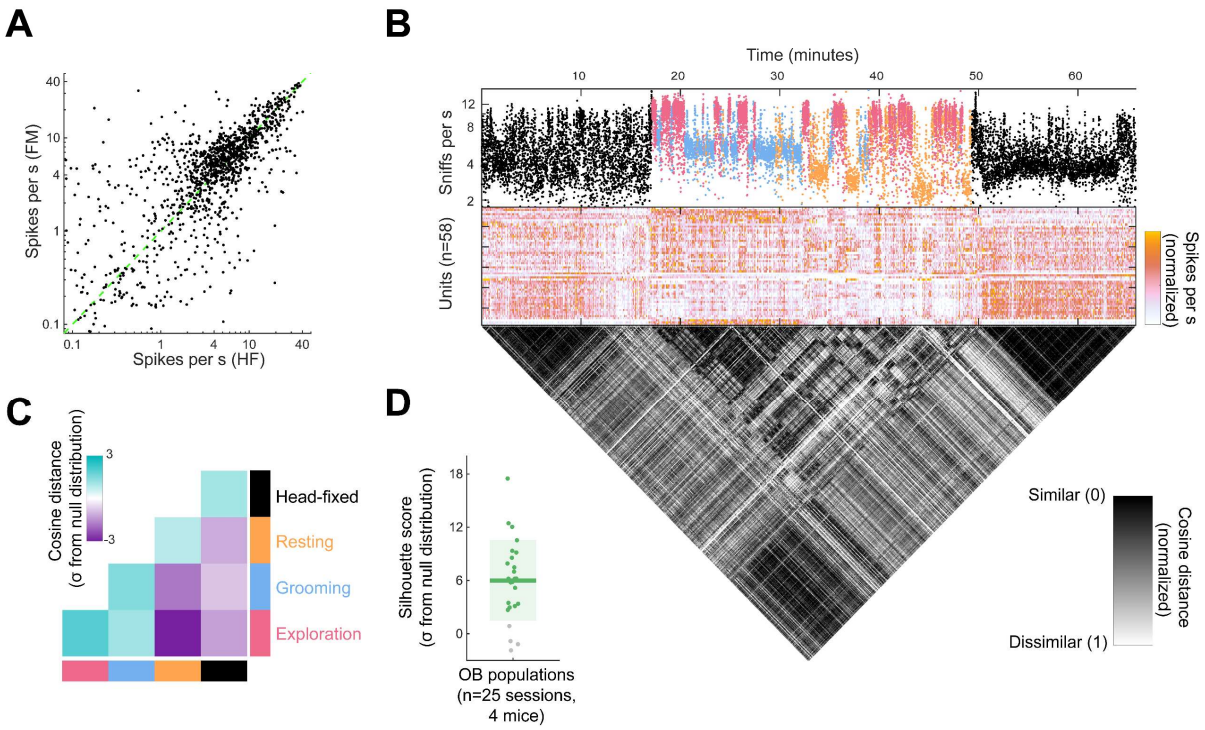

Figure 2: A behavioral model captures the stateful structure of neuronal population activity in Olfactory Bulb. A. Scatter plot of mean firing rates during the head-fixed and freely moving epochs of the recording sessions. Each dot indicates the firing rates of an individual unit (n=1680 units in all sessions; n=1274 in sessions with recordable sniff signals). **B.** Behavior, neuronal population activity, and similarity matrix from an individual session. *Top,* Each dot indicates an inhalation time with its instantaneous frequency on the vertical axis. Black: head-fixed; other colors as in 1D. *Middle,* Whole-session spike rates (5 s bins) of the neuronal population recorded in this session. Each row corresponds to an individual unit (n=58 total), with the color scale indicating the normalized firing rates. Each row is normalized separately between minimum and maximum. *Bottom,* Cosine distance matrix quantifies the similarity between the population activity pattern across time bins. **C.** Grand mean cosine distance matrix between states across mice (n=4). Each session's cosine distance matrix is expressed in units of the number of standard deviations from a null distribution formed by circularly shifting the HMM state time series (see Methods). Positive values indicate greater similarity than expected from the null hypothesis of a "nonsense correlation"; negative indicates less similarity. **D.** Silhouette scores quantifying how well the behavioral states cluster the neuronal population activity patterns in all sessions (4 mice; 25 sessions). Scores are in units of the number of standard deviations from a null distribution formed by circularly shifting the HMM state time series as in 2C.

We predicted that ongoing neuronal activity of OB would reflect the structure of spontaneous behavior. Using the behavioral HMM to partition the sessions, we ask whether behavioral states can describe the similarity of co-occurring population activity. When viewing neural activity alongside behavior, it is apparent that the population vectors are similarly organized into time-varying states (Fig 2B, center). To quantify the

similarity of the activity patterns across different time bins in the recording, we computed the cosine distance between population activity in time bins of 5 seconds width, to form a similarity matrix across time throughout a session (Fig 2B, bottom). The apparent block structure of the similarity matrix supports the impression of statefulness in the neural activity. We next compared this structure to the ethograms generated by our behavioral HMM. Importantly, the slow variation in both the behavioral and neural data raises the possibility of a nonsense correlation (Harris, 2021; Meijer, 2021). To quantify similarity relative to that expected from the slow variation in the data, we scored cosine distance as the number of standard deviations away from the mean of a null distribution formed by circularly shifting the time series (see Methods). Taking the grand mean across animals, we find that within a state, activity patterns overlap more than expected under the null distribution, while across states, activity patterns overlap less than predicted by this null hypothesis (Fig 2C). To quantify how well the behavioral HMM clusters the neural data, we calculated a silhouette score, a measure of consistency within clusters, for each session with respect to a circular shift null distribution (see Methods). Most sessions differed significantly from the null prediction (Fig 2D; mean score 6 sigma; 21/25 $p<0.01$). These analyses show that a model based only on behavioral variables – sniff frequency and movement speed – can effectively cluster neural data from OB, more so than expected from a nonsense correlation arising from the slow variation in behavior and neural activity. Thus, OB activity tracks behavioral structure, even when the behavior is not influenced by experimental stimuli or incentivized by rewards.

Sniff fields (SnFs) describe how neurons track breathing rhythms

OB activity is already known to be strongly modulated by breathing at the level of individual sniffs (Fukunaga et al., 2012; Macrides & Chorover, 1972; Onoda & Mori, 1980). To visualize the relationship between sniff frequency and unit activity, we aligned spike rasters to inhalation times, and sorted inhalations vertically in descending order of instantaneous sniff frequency (Fig 3A). While most units respond at a consistent latency, some fire with uniform amplitude across sniff frequencies (e.g., Fig 3A, Unit 1), while others fire preferentially during specific frequency ranges, around high (>8 sniff per s; Unit 2), middle (4-8 sniffs per s; Unit 3) or low frequencies (<4 sniffs per s; Unit 4). To capture the joint relationship between inhalation timing and breathing frequency, we describe OB unit activity using "sniff fields" (SnFs), the averaged firing rate as a two-dimensional function of latency from inhalation and instantaneous sniff frequency (Fig 4B). Units displayed a diversity of tuning to frequency, demonstrating that this tuning is not merely a monotonic scaling with sniff frequency. Thus, we observe that variation in breathing rhythm modulates the firing rate of inhalation-synchronized responses in OB units.

Figure 3

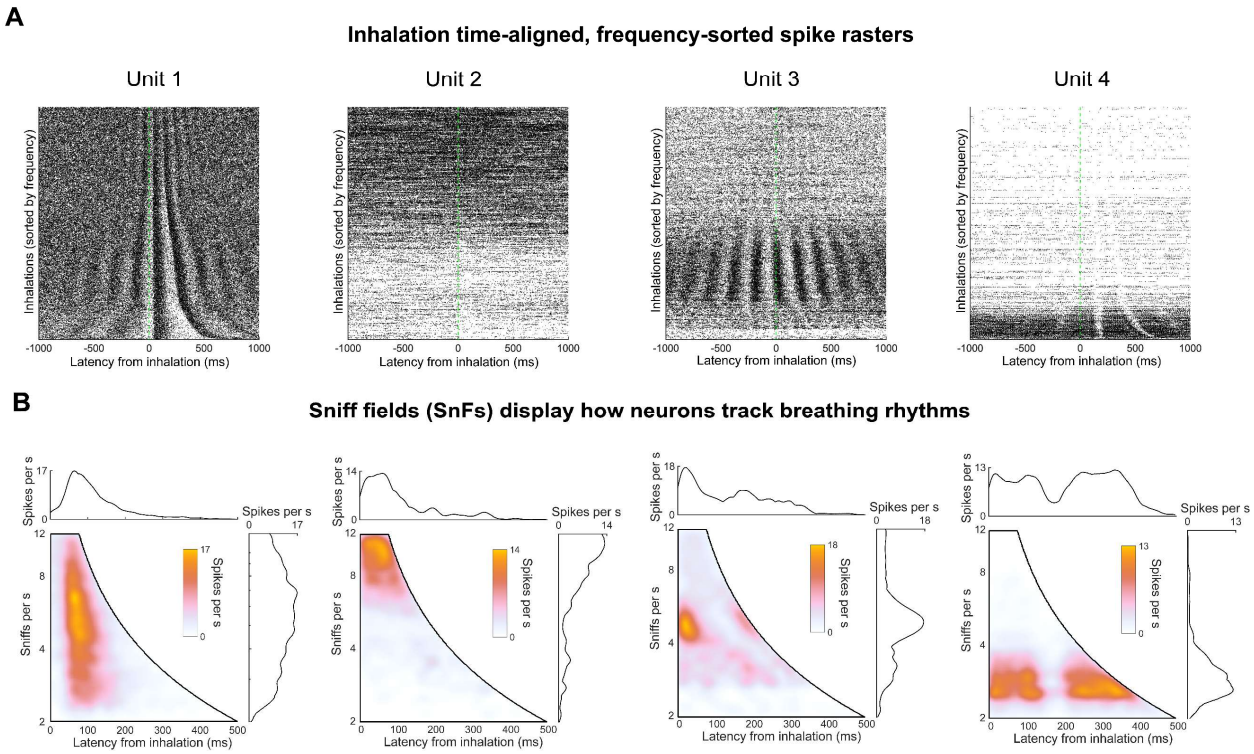

Figure 3: "Sniff fields" (SnFs) display how neurons track breathing rhythms. A. Spike rasters from 4 units simultaneously recorded in the same session. Dots indicate spike times relative to inhalation. Each row shows two seconds of the recording centered at each inhalation time at time 0. Rows are sorted in descending order of sniff frequency **B.** Sniff field (SnF) plots from the same four units. *Bottom left,* Colormap indicates firing rates with respect to latency in the sniff cycle and instantaneous sniff frequency. *Right*, Sniff frequency profile of the SnF calculated by taking the max projection across the horizontal axis of the distribution. *Top*, Latency profile of the SnF calculated by taking the max projection across the vertical axis of the distribution.

Across the population, SnFs can be classified into a limited number of types. We extracted SnF latency and frequency response profiles from all units that were significantly predictable by a latency/frequency Generalized Linear Model (GLM) (913/1111 units from sessions with a head-fixed period; $p<0.01$, sign rank test; see Methods), quantified the similarities of these profiles by calculating earth mover's distance matrices, and used k-means clustering on these matrices to identify subtypes of SnFs. Among units which significantly encoded latency from inhalation (853/913; $p<0.01$, Sign rank test), the variety of SnF latency profiles can be captured with two clusters (Fig 4C). One cluster has one peak at <100 ms after inhalation, and another cluster has two peaks, one at <100 ms, and one >200 ms. These two response profiles

are consistent with those demonstrated in many studies in anesthetized and awake mammals, and have been shown to correspond with tufted and mitral cell morphology, respectively (Fukunaga et al., 2012; Onoda & Mori, 1980). Separately, among the units that significantly encoded sniff frequency (638/913; p<0.01, sign rank test), clustering the SnF frequency profiles revealed three clusters preferring low, medium, or high sniff frequencies (Fig 4B). The latency and frequency profile subtypes are fairly independent; examples of both latency profile types can be found in all three frequency profile types (Fig 4 – figure supplement 1). Further, instantaneous sniff frequency has a smaller, less consistent relationship with spiking during head fixation than during free-moving conditions (Fig 4B). Taken together, we show that OB neurons not only synchronize their spiking to inhalation, but also track variation in the frequency of the breathing rhythm by varying the amplitude of their inhalation-locked ongoing firing.

Figure 4

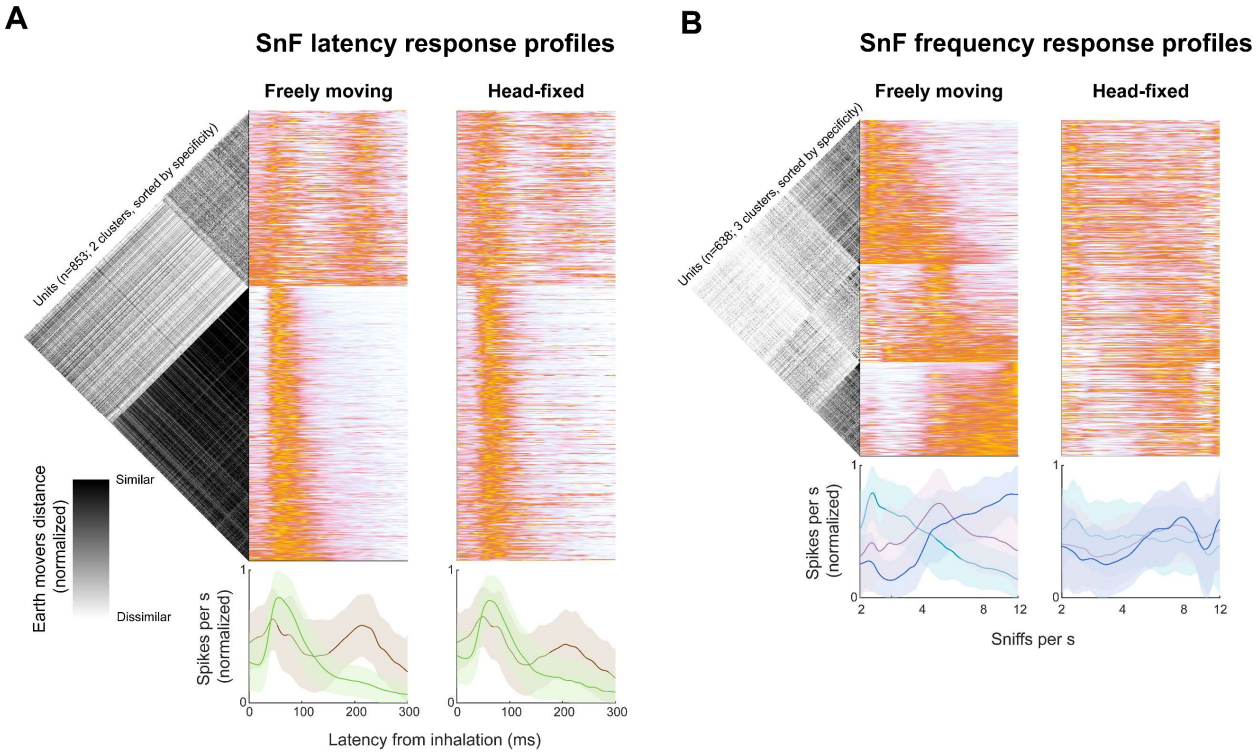

Figure 4: Neuronal sniff field latency and frequency profiles fall into a small number of clusters across the population. A. *Right,* SnF latency profiles of all units that were significantly predictable with a GLM fit to spike latency relative to inhalation (n=853/913 p<0.01, Sign rank test). Freely moving and head-fixed matrices are sorted the same. *Left,* units are segregated into two clusters by k-means clustering of the earth mover's distance matrix quantifying the similarity of SnFs across units. *Bottom,* Within-cluster means for the two clusters. Green: putative tufted cells; Brown: putative mitral cells. Lines and shaded regions are within-cluster means ±1 standard deviation. **B.** *Right,* SnF frequency profiles of all units that were significantly with a GLM trained on instantaneous sniff frequency (n=638/913; p<0.01,

Sign rank test). Freely moving and head-fixed matrices are both sorted according to selectivity index in the freely moving data, and differently than the matrices in 4A. *Left,* units are segregated into three types by k-means clustering of the earth mover's distance matrix quantifying the similarity of SnFs across units. *Bottom,* Within-cluster means for the three clusters. Teal: low frequency units; Purple: medium frequency units; Blue: high frequency units. Lines and shaded regions are within-cluster means ±1 standard deviation.

Statistical models reveal that breathing parameters best predict OB activity

To test the extent to which sniff frequency modulation can be explained by inhalation latency modulation, we used a Generalized Linear Model (GLM) to predict individual unit spiking based on behavioral variables. By comparing variables in isolation and in combination, we can ask whether a given variable uniquely contributes to a predictive model of unit firing. We tested models on held out data compared against a null, mean firing rate model by constructing a log-likelihood increase (LLHi) metric (see Methods; (Hardcastle et al., 2017). We perform 10-fold cross validation and calculate statistics on the distribution of LLHi scores. We compared the LLHi scores of GLMs trained on sniff frequency and latency from inhalation, individually and in combination. Consistent with the strong tuning apparent in SnF visualizations, including frequency in the model significantly improves the prediction in 638/913 units, whereas including latency improves the prediction in 853/913 units (Fig 5A). Thus, the OB correlation with sniff frequency is not simply explained by the previously-established synchronization of unit activity to inhalation.

We next considered how OB units correlate with movement speed. The behavioral model described above (Fig 1) predicts population activity with both sniff frequency and head movement speed. The correlation between these parameters creates a confounding ambiguity: is the correlation between behavior and neural activity best explained by sniffing, movement, or both? To resolve this ambiguity, we used the same GLM approach. Models based on SnF parameters (a combined frequency/latency model; see Methods) predict firing significantly better than the null model in 913/1153 of units. Models based on movement speed predict unit activity in 249/1153 units ($p<0.01$, sign rank test), a smaller but still considerable fraction of the population. Thus, as with many other sensory areas of the brain, activity in OB correlates with movement (Parker et al., 2020). However, if we quantify the contribution of these two variables in a combined sniff field/speed model, we find that movement speed improves the predictions relative to that of a model based on SnF parameters in 102/1153 of units ($p<0.01$, sign rank test; Fig 5B). Further, 12/1153 of the units in our sample were more predictable by speed than by the SnF parameters (Fig 5B *bottom*). Thus, although movement speed is strongly correlated with OB activity, this correlation is largely redundant and reflects more the correlation between breathing and movement than movement itself.

Figure 5

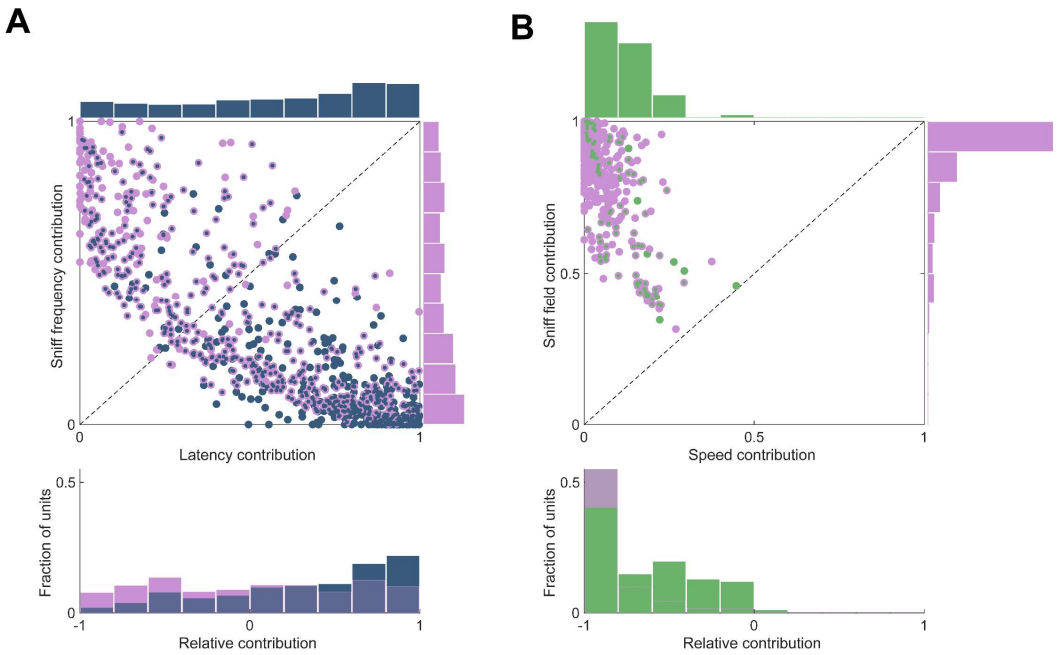

Figure 5: Contribution of behavioral parameters to a predictive model of individual unit firing. A. Both frequency and latency improve a model of individual unit firing. *Top,* Each dot indicates a unit with activity that was significantly predictable from a combined GLM based on both latency and frequency ($p<0.01$, Sign rank test). The contribution is defined as how much including a given parameter improves the model predictions on held-out data (see Methods). Lavender: units for which sniff frequency significantly improved the model prediction; Blue: units for which latency improved the model prediction; Lavender/blue: both parameters improve the model prediction. Marginal distributions of contributions from the two parameters are shown beside and above the scatter plot. *Bottom*, Relative contribution compares the improvement due to the two parameters. **B.** Movement speed minimally improves the predictions of a model incorporating sniff frequency and latency.

Olfactory bulb tracks allocentric place

Motivated by the ethological relevance of the relationship between olfactory signals and internal spatial representations (Baker et al., 2018; Gagliardo, 2013; Jackson et al., 2020; Jacobs, 2023; Matheson et al., 2022; Raithel & Gottfried, 2021), and given previous observations of conjunctive odor/place coding in hippocampus (Fischler-Ruiz et al., 2021; Komorowski et al., 2009) and piriform cortex (Kehl et al., 2024; Mena et al., 2023; Poo et al., 2022), we investigated the relation between OB activity and place. Strikingly, individual OB units show apparent place selectivity during free behavior (Fig 6A): spiking activity is spatially modulated for many units. We wondered how this spatial selectivity compared to that of hippocampal neurons, whose place field properties have been extensively studied (Best et al., 2001). However, direct comparison to hippocampal place fields described in the literature is difficult because most recording studies in the hippocampus use experimental paradigms that differ from ours in important ways. First, the behavioral arena we used is smaller than that of most

hippocampal studies. Second, hippocampal experiments typically incentivize exploration by distributing food pellets or training on a maze task. Lastly, these experiments often exclude data in which the animals are not moving above a criterion speed. While these design choices successfully establish a focus on canonical place cells, they run counter to the goals of our study. We therefore recorded from neurons in the hippocampus (HPC) of mice in the same arena and task-free experimental paradigm as our OB recordings.

We compared place selectivity between OB and HPC. Place fields of units recorded from HPC appeared to be more specific than those of OB (Fig 6b, Methods). To quantify the spatial selectivity of individual units in OB and HPC, we modified a traditional metric of place selectivity, spatial information (Skaggs et al., 1992). This information theoretic measure effectively captures the selectivity of canonical place cells, which have very low ongoing firing rates. In contrast, this measure poorly captures the selectivity apparent in neurons with higher ongoing firing rates, such as hippocampal interneurons (Frank et al., 2001; Wilent & Nitz, 2007) or OB neurons (Fig 2A). To better generalize this metric to neurons with ongoing activity, for each unit we compared spatial information to a null distribution formed by circular shifting the position time series 1000 times, and expressed the selectivity as the Significance of Spatial Information (SSI; Stefanini et al., 2020; C. Yang et al., 2024), defined as the number of standard deviations of the real data from the null distribution. This metric, as illustrated by the example cells in Figure 6A, reveals that a substantial minority of OB neurons are spatially selective (196/1557 units, $p<0.01$), but a significantly smaller fraction than in HPC recorded under the same conditions (270/468 units; Fig 7A).

To evaluate spatial information at the level of OB and HPC populations, we trained a decoder model on simultaneous estimates of location extracted from video tracking and population activity, and tested the model's performance on held-out data at predicting the mouse's position based on the population activity (Fig 7B; Stefanini et al., 2020). We quantified model performance as the mean error between the decoded position and the actual position (see Methods). For 18/31 sessions from OB and 12/13 sessions from HPC, the model decoded the mouse's position better than chance (Fig 7C). These analyses demonstrate that in task-free, ambient stimuli conditions, neuronal activity in HPC tracks an animal's location in an environment. Importantly, we show here, for the first time, that OB neurons also track an animal's location, consistent with the idea that the olfactory system plays an integral role in navigation (Baker et al., 2018; Dittman & Quinn, 1996; Gagliardo, 2013).

Figure 6

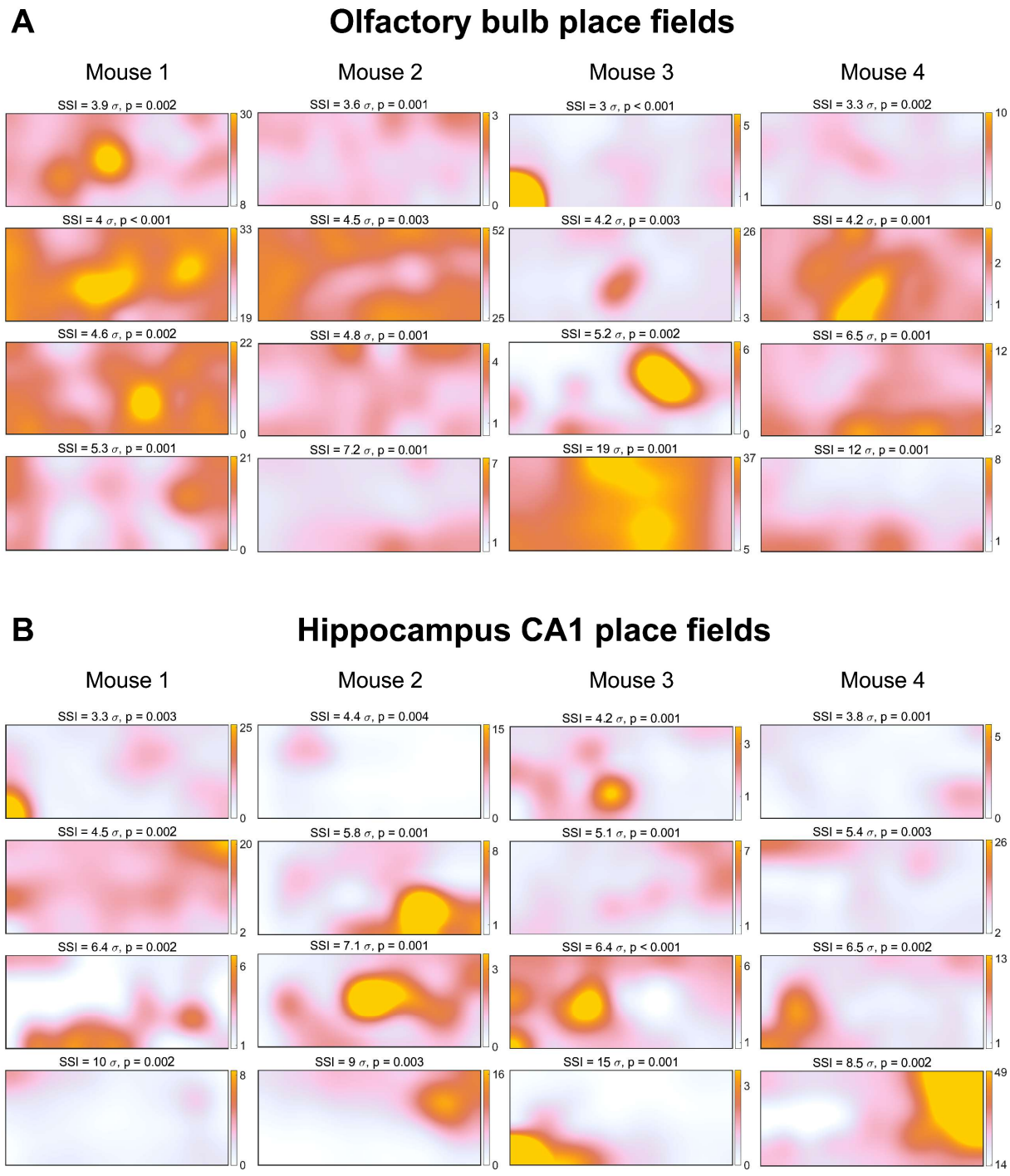

Figure 6: Place fields display allocentric location selectivity of olfactory bulb and hippocampal neurons. Colormaps show occupancy-normalized firing rates as a function of location in the 15 x 40cm experimental arena parsed into a 12 by 5 grid and Gaussian smoothed by one bin width (see Methods). For consistency, OB and HPC colormaps are scaled between the 1st and 99th percentiles of each neuron's firing rate in 10 s bins. Those values are displayed beside each unit's colorbar. **A.** Four example OB units from each of four mice. Significance of Spatial Information (SSI) and p-values are defined

relative to the circular shift null distributions. **B.** Four example HPC units from each of four mice. OB and HC recordings were performed in different animals.

Figure 7

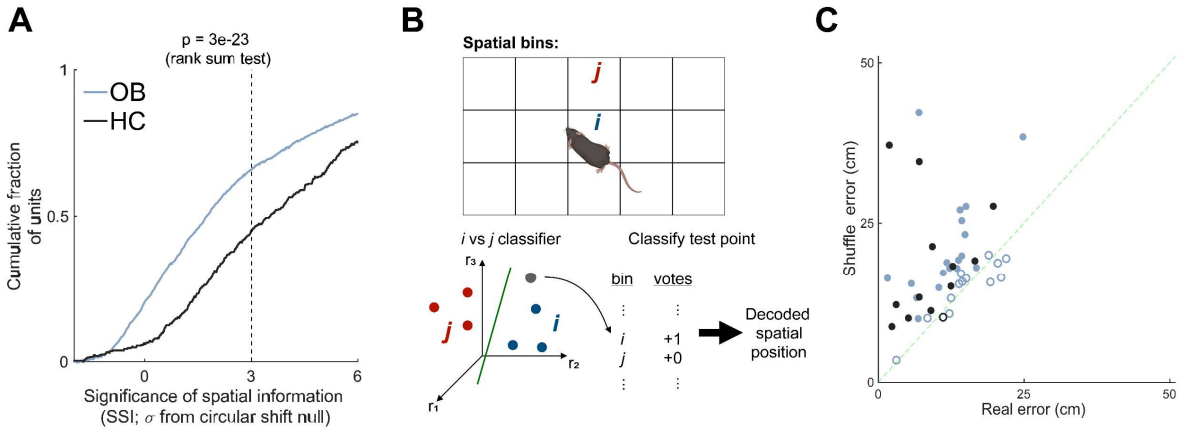

Figure 7: Spatial selectivity of individual neurons and decoding of population activity from olfactory bulb and hippocampus. A. Cumulative distributions of selectivity of OB and HPC units, quantified as the significance of spatial information (SSI), defined relative to circular shift null distributions (see Methods). **B.** Decoder model schematic. A classifier for each pair of spatial bins is trained on neuronal activity (firing rate in 5 s bins) and tested on held out data. The decoded spatial position of the mouse at a given time step is taken as the center of the bin that wins the most "votes", defined as the bin that was predicted by the most pairwise classifiers. **C.** Decoder model performance of OB and HPC populations on real and shuffled controls. Decoding error is defined as the median distance between the decoded spatial position and the mouse's actual position. Points are individual sessions, filled are $p < 0.01$ (sign-rank test).

Figure 8

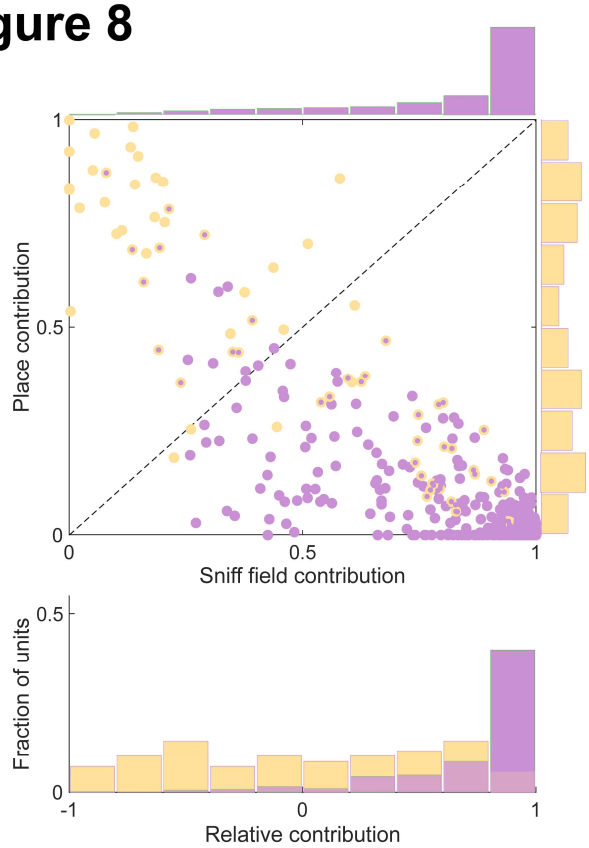

Figure 8: Sniff fields do not explain place selectivity. A. *Top,* Each dot indicates a unit that was significantly predictable from a combined GLM based on both sniff fields and place fields ($p<0.01$, Sign rank test). The contribution is defined as how much including a given parameter improves the model predictions on held-out data (see Methods). Lavender: units for which sniff parameters significantly improved the model prediction; Yellow: units for which place improved the model prediction; Lavender/yellow: both parameters improve the model prediction. Marginal distributions of contributions from the two parameters are shown beside and above the scatter plot. *Bottom*, Relative contribution compares the improvement of the two parameters.

We have shown that OB neurons track breathing rhythms and place. Importantly, breathing rhythms and the states extracted from our behavioral model are not uniformly distributed in allocentric space (Fig 8, figure supplement 1). It is possible that the apparent place information we observe in OB could be explained by differential use of breathing rhythms in different regions in the arena. To test this hypothesis, we used GLMs to ask if inclusion of place significantly improves prediction of single unit spiking activity over a model based on latency from inhalation and sniff frequency (Figs 3 and 4). We found that adding the place covariate to a model with sniff field covariates significantly increased the log-likelihood of held-out data in 160/1153 units ($p<0.01$, sign rank test), and 81/1153 were better predicted by place than by sniff field (Fig 8A).

The unique predictive contribution of place is inconsistent with the hypothesis that place selectivity is an epiphenomenon of the sniff field.

Figure 9

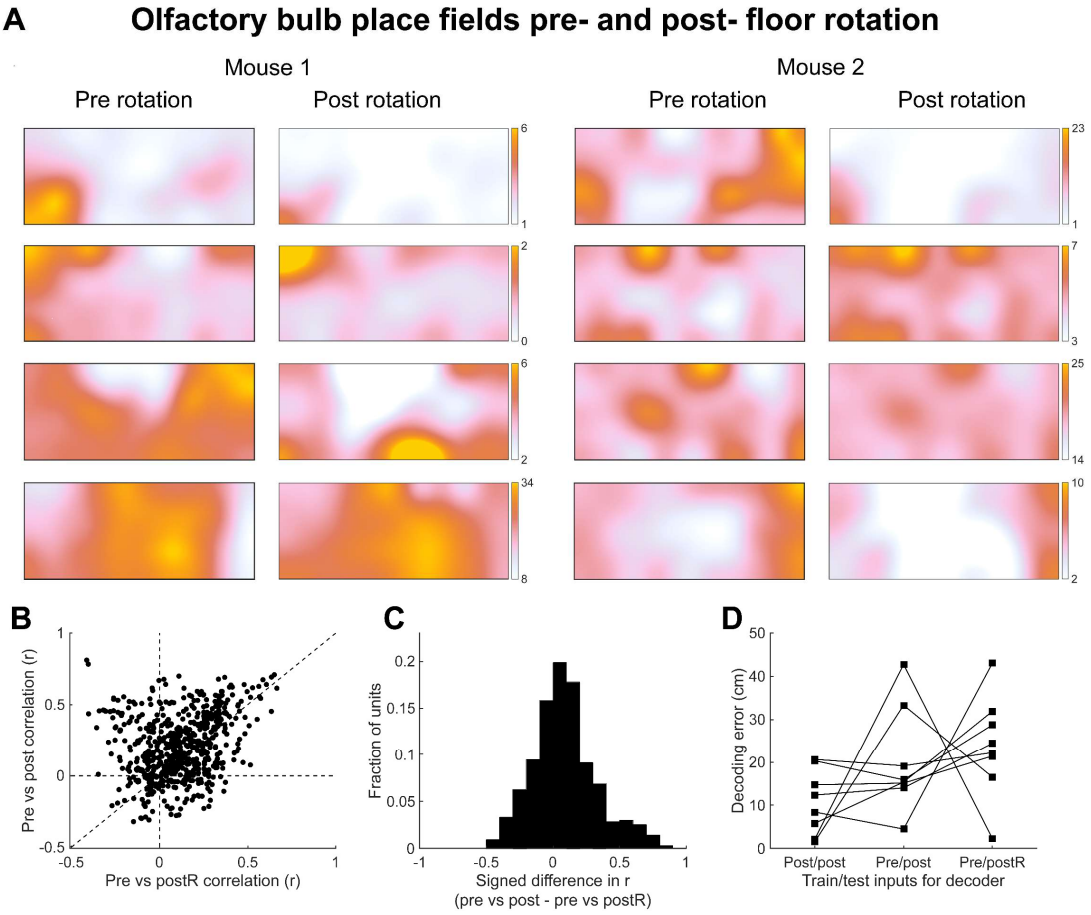

Figure 9: Scent marks do not solely explain place selectivity. In a subset of experiments, we rotated the floor 180 degrees midway through the experiment and compared the resulting place fields. A. Four example units each from OB of two mice. Colormaps are scaled between the 1st and 99th percentiles as in Fig 6. “Pre rotation” shows the place fields calculated from spiking and position time series before the rotation, “post-rotation” shows the place fields from the same units calculated from data after the floor rotation. B. Scatter plot of correlation between pre and post rotation place fields vs pre and virtually rotated post rotation (postR). C. Signed difference in correlations in B reveals that a majority of units’ place fields do not follow the scent marks while others do. D. Population decoding models trained on activity during the post rotation data and tested on post rotation data (Post/post), trained on pre rotation and tested on post rotation (Pre/post), and trained on pre rotation and tested on a 180 degree rotated control of post rotation data (Pre/postR).

We next considered the possibility that apparent place selectivity could result from responses to ambient odorants. Although we did not apply odor stimuli in these experiments, ambient odors from the mouse and the environment are unavoidable and unevenly distributed in space. The most obvious candidate odor source would be the

mouse's own scent marks: mice, along with many organisms, scent mark their environment, and these marks can contribute to navigational behavior (Drickamer, 2001; Hurst et al., 2001; Khan et al., 2012; Means et al., 1992; Wallace et al., 2002). To test whether scent marks influence spatial selectivity, we performed floor rotation control experiments, in which we rotated a transparent floor mat 180 degrees halfway through a recording session. If place selectivity reflected the location of scent marks, then the "place fields" should rotate to reflect the new distribution of scent marks. Inconsistent with this hypothesis, we observed that place fields often maintained the same location selectivity before and after a floor rotation (Fig 9A). Across the population, the place selectivity of most units maintained a higher correlation across the floor rotation rather than correlating with the new position of the scent marks (Fig 9B,C). Additionally, we asked whether the place decoding models generalize across floor rotation conditions (see Methods). If responses to scent marks drove correlations with place, decoders trained on pre- and tested on post-floor rotation should perform significantly worse than those trained and tested on post-floor rotation data. However, we find that these decoders perform equally well (Fig 9D). Taken together, these findings suggest that place selectivity in the OB does not reflect the distribution of scent marks. However, it is important to recognize that these results do not exclude the possibility that other distal sources of ambient odor explain the place selectivity we observe. In either case, we show that OB contains decodable information about place. Inevitably, this activity will combine with odor-driven activity from the nose and be broadcast to the OB's numerous postsynaptic targets, most of which send centrifugal feedback to the OB, and several of which are reciprocally connected with the hippocampus (Aqrabawi & Kim, 2018; Padmanabhan et al., 2019; Price, 1985; Reinert & Fukunaga, 2022; Shipley et al., 2008; Vanderwolf, 2001).

Discussion

In this study, we demonstrate that spontaneous breathing rhythms and olfactory bulb activity share a rich temporal structure in mice. Even during spontaneous behavior and ambient stimuli, mice organize their breathing rhythms into persistent states that evolve in time. Olfactory bulb dynamics are modulated by multiple features of breathing. As previously reported, we show that olfactory bulb spikes synchronize precisely with inhalation onset times, and that this synchronization is very similar between the head-fixed and freely moving states. We also show, for the first time, that many olfactory bulb neurons fire at different rates during different breathing frequencies, and that these activity patterns co-evolve with persistent rhythmic states of breathing behavior.

Further, we find that activity is modulated by the animals' allocentric location at the single unit and population level. We used the rich data available in free behavior preparations to fit statistical models that tease apart the contributions from these variables and show that the OB multiplexes multiple aspects of the animal’s context. This activity will combine with odor-driven activity from the nose and be broadcast to the

OB's numerous postsynaptic targets, many of which are reciprocally connected with the hippocampus (Aqrabawi & Kim, 2018; Padmanabhan et al., 2019).

The presence of neural correlates, however striking, does not prove that they are adaptively beneficial for the animal (Gould et al., 1979), but the metabolic costs of ongoing activity encourage systems to make use of these representations (Sterling & Laughlin, 2015). Animals sample the same stimuli or environment in different contexts and internal dynamics can help reconfigure representations to be relevant to current demands (Asabuki & Clopath, 2024; Berkes et al., 2011). Sniff fields may provide a reference signal allowing animals to use temporal structure in odor-evoked activity and explain how animals can perceive the timing of sniff-locked optogenetic stimuli (Ackels et al., 2021; Chong & Rinberg, 2018; Hopfield, 1995; Kepecs et al., 2006; Lewis et al., 2021; Li et al., 2014; Powers, 1973; Schaefer & Margrie, 2007; Smear et al., 2011, 2013). Place fields in OB may help unify odor-driven activity with putative internal models instantiated in hippocampus and elsewhere (Buzsáki, 2019; Eichenbaum & Cohen, 2014; Jacobs, 2012; Nieh et al., 2021; O'Keefe & Nadel, 1978; Sheffield & Dombeck, 2015; Sugar & Moser, 2019; Tolman, 1948).

What mechanisms may generate sniff fields and place fields in the olfactory bulb? The olfactory epithelium is mechanically stimulated by airflow, which shapes the activity of olfactory bulb neurons (Buonviso et al., 2006; Díaz-Quesada et al., 2018; Grosmaitre et al., 2007; Iwata et al., 2017). In addition to its feedforward inputs, the olfactory bulb receives centrifugal inputs from neuromodulatory centers and cortical areas (Brunert & Rothermel, 2021; Chen & Padmanabhan, 2022; Kapoor et al., 2016; Linster & Cleland, 2002; Nogi et al., 2020; Reinert & Fukunaga, 2022; Shepherd & Greer, 1998; Soria-Gómez et al., 2014; Sullivan et al., 1989; Zak et al., 2024). Our findings encourage follow up experiments to silence sources of centrifugal innervation of OB to test their impact on sniff and place representations in the bulb.

These results contribute to a body of literature demonstrating that primary sensory areas are modulated by behavior-related information. Spontaneous behaviors, including those unrelated to sensory-guided tasks, describe a significant amount of variation in neural recordings from primary sensory areas (Flossmann & Rochefort, 2021; Long & Zhang, 2021; Mertens et al., 2023; Musall et al., 2019; Parker et al., 2020; Saleem & Busse, 2023; Stringer et al., 2019). The olfactory bulb has been shown to be modulated by reward and task contingencies, inhalation, and other aspects of cognition (Doucette & Restrepo, 2008; Freeman, 1978; Kay et al., 1996; Lindeman et al., 2023; Rojas-Líbano et al., 2014; Zak et al., 2024). As in other systems and species, these representations may be multiplexed by cells to adaptively support sensory coding (Fairhall et al., 2001; Fusi et al., 2016; Panzeri et al., 2010; Weber et al., 2019). Our findings underscore the value of studying sensory systems within more naturalistic behavioral paradigms in which animals are released to perform the repertoire of behaviors in which these sensory systems participate (Buzsáki, 2019; Krakauer et al., 2017; Miller et al., 2022). The importance of active sampling mandates a continued emphasis on detailed observation and quantification of behavioral structure (Bialek, 2022; Marshall et al., 2021; Mazzucato, 2022; Weinreb, Osman, et al., 2024; Weinreb, Pearl, et al., 2024).

References

Ackels, T., Erskine, A., Dasgupta, D., Marin, A. C., Warner, T. P. A., Tootoonian, S., Fukunaga, I., Harris, J. J., & Schaefer, A. T. (2021). Fast odour dynamics are encoded in the olfactory system and guide behaviour. *Nature*, 1–6. https://doi.org/10.1038/s41586-021-03514-2

Ackels, T., Jordan, R., Schaefer, A. T., & Fukunaga, I. (2020). Respiration-Locking of Olfactory Receptor and Projection Neurons in the Mouse Olfactory Bulb and Its Modulation by Brain State. *Frontiers in Cellular Neuroscience*, *14*. https://doi.org/10.3389/fncel.2020.00220

Adrian, E. D. (1950). The electrical activity of the mammalian olfactory bulb. *Electroencephalography and Clinical Neurophysiology*, *2*(1–4), 377–388. https://doi.org/10.1016/0013-4694(50)90075-7

Aqrabawi, A. J., & Kim, J. C. (2018). Hippocampal projections to the anterior olfactory nucleus differentially convey spatiotemporal information during episodic odour memory. *Nature Communications*, *9*(1), Article 1. https://doi.org/10.1038/s41467-018-05131-6

Asabuki, T., & Clopath, C. (2024). Embedding stochastic dynamics of the environment in spontaneous activity by prediction-based plasticity. *eLife*, *13*. https://doi.org/10.7554/eLife.95243.1

Baker, K. L., Dickinson, M., Findley, T. M., Gire, D. H., Louis, M., Suver, M. P., Verhagen, J. V., Nagel, K. I., & Smear, M. C. (2018). Algorithms for Olfactory Search across Species. *Journal of Neuroscience*, *38*(44), 9383–9389. https://doi.org/10.1523/JNEUROSCI.1668-18.2018

Barwich, A.-S. (2023). If Proust had whiskers: Recalling locations with smells. *Learning & Behavior*, *51*(2), 121–122. https://doi.org/10.3758/s13420-022-00549-x

Behrens, T. E. J., Muller, T. H., Whittington, J. C. R., Mark, S., Baram, A. B., Stachenfeld, K. L., & Kurth-Nelson, Z. (2018). What Is a Cognitive Map? Organizing Knowledge for Flexible Behavior. *Neuron*, *100*(2), 490–509. https://doi.org/10.1016/j.neuron.2018.10.002

Bensafi, M., Porter, J., Pouliot, S., Mainland, J., Johnson, B., Zelano, C., Young, N., Bremner, E., Aframian, D., Khan, R., & Sobel, N. (2003). Olfactomotor activity during imagery mimics that during perception. *Nature Neuroscience*, *6*(11), 1142–1144. https://doi.org/10.1038/nn1145

Berkes, P., Orbán, G., Lengyel, M., & Fiser, J. (2011). Spontaneous cortical activity reveals hallmarks of an optimal internal model of the environment. *Science (New York, N.Y.)*, *331*(6013), 83–87. https://doi.org/10.1126/science.1195870

Berlyne, D. E. (1966). Curiosity and Exploration. *Science*, *153*(3731), 25–33. https://doi.org/10.1126/science.153.3731.25

Best, P. J., White, A. M., & Minai, A. (2001). Spatial Processing in the Brain: The Activity of Hippocampal Place Cells. *Annual Review of Neuroscience*, *24*(Volume 24, 2001), 459–486. https://doi.org/10.1146/annurev.neuro.24.1.459

Bhattacharyya, U., & Bhalla, U. S. (2015). Robust and Rapid Air-Borne Odor Tracking without Casting. *eNeuro*, *2*(6). https://doi.org/10.1523/ENEURO.0102-15.2015

Bialek, W. (2022). On the dimensionality of behavior. *Proceedings of the National Academy of Sciences*, *119*(18), e2021860119. https://doi.org/10.1073/pnas.2021860119

Bishop, C. M. (2006). *Pattern recognition and machine learning*. Springer.

Branson, K., Robie, A. A., Bender, J., Perona, P., & Dickinson, M. H. (2009). High-throughput ethomics in large groups of Drosophila. *Nature Methods*, *6*(6), 451–457. https://doi.org/10.1038/nmeth.1328

Brunert, D., & Rothermel, M. (2021). Extrinsic neuromodulation in the rodent olfactory bulb. *Cell and Tissue Research*, *383*(1), 507–524. https://doi.org/10.1007/s00441-020-03365-9

Buonviso, N., Amat, C., & Litaudon, P. (2006). Respiratory modulation of olfactory neurons in the rodent brain. *Chemical Senses*, *31*(2), 145–154. https://doi.org/10.1093/chemse/bjj010

Buzsáki, G. (2019). *The Brain from Inside Out*. Oxford University Press. https://doi.org/10.1093/oso/9780190905385.001.0001

Catania, K. C. (2013). Stereo and serial sniffing guide navigation to an odour source in a mammal. *Nature Communications*, *4*(1), Article 1. https://doi.org/10.1038/ncomms2444

Chaput, M. A., Buonviso, N., & Berthommier, F. (1992). Temporal Patterns in Spontaneous and Odour-evoked Mitral Cell Discharges Recorded in Anaesthetized Freely Breathing Animals. *European Journal of Neuroscience*, *4*(9), 813–822. https://doi.org/10.1111/j.1460-9568.1992.tb00191.x

Chen, Z., & Padmanabhan, K. (2022). Top-down feedback enables flexible coding strategies in the olfactory cortex. *Cell Reports*, *38*(12). https://doi.org/10.1016/j.celrep.2022.110545

Chong, E., & Rinberg, D. (2018). Behavioral readout of spatio-temporal codes in olfaction. *Current Opinion in Neurobiology*, *52*, 18–24. https://doi.org/10.1016/j.conb.2018.04.008

Churchland, P. S., Ramachandran, V. S., & Sejnowski, T. J. (1994). A critique of pure vision. In *Large-scale neuronal theories of the brain* (pp. 23–60). The MIT Press.

Cortes, C., & Vapnik, V. (1995). Support-vector networks. *Machine Learning*, *20*(3), 273–297. https://doi.org/10.1007/BF00994018

Crimaldi, J., Lei, H., Schaefer, A., Schmuker, M., Smith, B. H., True, A. C., Verhagen, J. V., & Victor, J. D. (2022). Active sensing in a dynamic olfactory world. *Journal of*

Computational Neuroscience, *50*(1), 1–6. https://doi.org/10.1007/s10827-021-00798-1

Crowcroft, P. (1973). *Mice All Over*. Chicago Zoological Society.

DeBose, J. L., & Nevitt, G. A. (2008). The use of Odors at Different Spatial Scales: Comparing Birds with Fish. *Journal of Chemical Ecology*, *34*(7), 867–881. https://doi.org/10.1007/s10886-008-9493-4

Di Lorenzo, P. M. (2021). Taste in the brain is encoded by sensorimotor state changes. *Current Opinion in Physiology*, *20*, 39–45. https://doi.org/10.1016/j.cophys.2020.12.003

Diamanti, E. M., Reddy, C. B., Schröder, S., Muzzu, T., Harris, K. D., Saleem, A. B., & Carandini, M. (2021). Spatial modulation of visual responses arises in cortex with active navigation. *eLife*, *10*, e63705. https://doi.org/10.7554/eLife.63705

Díaz-Quesada, M., Youngstrom, I. A., Tsuno, Y., Hansen, K. R., Economo, M. N., & Wachowiak, M. (2018). Inhalation Frequency Controls Reformatting of Mitral/Tufted Cell Odor Representations in the Olfactory Bulb. *Journal of Neuroscience*, *38*(9), 2189–2206. https://doi.org/10.1523/JNEUROSCI.0714-17.2018

Dittman, A. H., & Quinn, T. P. (1996). Homing in Pacific Salmon: Mechanisms and Ecological Basis. *Journal of Experimental Biology*, *199*(1), 83–91. https://doi.org/10.1242/jeb.199.1.83

Doucette, W., & Restrepo, D. (2008). Profound Context-Dependent Plasticity of Mitral Cell Responses in Olfactory Bulb. *PLOS Biology*, *6*(10), e258. https://doi.org/10.1371/journal.pbio.0060258

Drickamer, L. C. (2001). Urine marking and social dominance in male house mice (Mus musculus domesticus). *Behavioural Processes*, *53*(1), 113–120. https://doi.org/10.1016/S0376-6357(00)00152-2

Eichenbaum, H., & Cohen, N. J. (2014). Can we reconcile the declarative memory and spatial navigation views on hippocampal function? *Neuron*, *83*(4), 764–770. https://doi.org/10.1016/j.neuron.2014.07.032

Fairhall, A. L., Lewen, G. D., Bialek, W., & de Ruyter van Steveninck, R. R. (2001). Efficiency and ambiguity in an adaptive neural code. *Nature*, *412*(6849), 787–792. https://doi.org/10.1038/35090500

Fenk, L. M., Avritzer, S. C., Weisman, J. L., Nair, A., Randt, L. D., Mohren, T. L., Siwanowicz, I., & Maimon, G. (2022). Muscles that move the retina augment compound eye vision in Drosophila. *Nature*, *612*(7938), 116–122. https://doi.org/10.1038/s41586-022-05317-5

Findley, T. M., Wyrick, D. G., Cramer, J. L., Brown, M. A., Holcomb, B., Attey, R., Yeh, D., Monasevitch, E., Nouboussi, N., Cullen, I., Songco, J. O., King, J. F., Ahmadian, Y., & Smear, M. C. (2021). Sniff-synchronized, gradient-guided

olfactory search by freely moving mice. *eLife*, *10*, e58523. https://doi.org/10.7554/eLife.58523

Fischler-Ruiz, W., Clark, D. G., Joshi, N., Devi-Chou, V., Kitch, L., Schnitzer, M., Abbott, L. F., & Axel, R. (2021). Olfactory landmarks and path integration converge to form a cognitive spatial map. *Neuron*, S0896627321007285. https://doi.org/10.1016/j.neuron.2021.09.055

Flossmann, T., & Rochefort, N. L. (2021). Spatial navigation signals in rodent visual cortex. *Current Opinion in Neurobiology*, *67*, 163–173. https://doi.org/10.1016/j.conb.2020.11.004

Frank, L. M., Brown, E. N., & Wilson, M. A. (2001). A Comparison of the Firing Properties of Putative Excitatory and Inhibitory Neurons From CA1 and the Entorhinal Cortex. *Journal of Neurophysiology*, *86*(4), 2029–2040. https://doi.org/10.1152/jn.2001.86.4.2029

Frederick, D. E., Rojas-Líbano, D., Scott, M., & Kay, L. M. (2011). Rat behavior in go/no-go and two-alternative choice odor discrimination: Differences and similarities. *Behavioral Neuroscience*, *125*(4), 588–603. https://doi.org/10.1037/a0024371

Freeman, W. J. (1978). Spatial properties of an EEG event in the olfactory bulb and cortex. *Electroencephalography and Clinical Neurophysiology*, *44*(5), 586–605. https://doi.org/10.1016/0013-4694(78)90126-8

Fukunaga, I., Berning, M., Kollo, M., Schmaltz, A., & Schaefer, A. T. (2012). Two distinct channels of olfactory bulb output. *Neuron*, *75*(2), 320–329. https://doi.org/10.1016/j.neuron.2012.05.017

Fusi, S., Miller, E. K., & Rigotti, M. (2016). Why neurons mix: High dimensionality for higher cognition. *Current Opinion in Neurobiology*, *37*, 66–74. https://doi.org/10.1016/j.conb.2016.01.010

Gagliardo, A. (2013). Forty years of olfactory navigation in birds. *Journal of Experimental Biology*, *216*(12), 2165–2171. https://doi.org/10.1242/jeb.070250

Gibson, J. J. (1968). What gives rise to the perception of motion? *Psychological Review*, *75*(4), 335–346. https://doi.org/10.1037/h0025893

Gire, D. H., Kapoor, V., Arrighi-Allisan, A., Seminara, A., & Murthy, V. N. (2016). Mice Develop Efficient Strategies for Foraging and Navigation Using Complex Natural Stimuli. *Current Biology*, *26*(10), 1261–1273. https://doi.org/10.1016/j.cub.2016.03.040

Gomez-Marin, A., Stephens, G. J., & Louis, M. (2011). Active sampling and decision making in Drosophila chemotaxis. *Nature Communications*, *2*(1), Article 1. https://doi.org/10.1038/ncomms1455

Gould, S. J., Lewontin, R. C., Maynard Smith, J., & Holliday, R. (1979). The spandrels of San Marco and the Panglossian paradigm: A critique of the adaptationist

programme. *Proceedings of the Royal Society of London. Series B. Biological Sciences*, *205*(1161), 581–598. https://doi.org/10.1098/rspb.1979.0086
Grosmaitre, X., Santarelli, L. C., Tan, J., Luo, M., & Ma, M. (2007). Dual functions of mammalian olfactory sensory neurons as odor detectors and mechanical sensors. *Nature Neuroscience*, *10*(3), 348–354. https://doi.org/10.1038/nn1856
Halpern, B. P. (1983). Tasting and smelling as active, exploratory sensory processes. *American Journal of Otolaryngology*, *4*(4), 246–249. https://doi.org/10.1016/S0196-0709(83)80066-0
Hardcastle, K., Maheswaranathan, N., Ganguli, S., & Giocomo, L. M. (2017). A Multiplexed, Heterogeneous, and Adaptive Code for Navigation in Medial Entorhinal Cortex. *Neuron*, *94*(2), 375-387.e7. https://doi.org/10.1016/j.neuron.2017.03.025
Harris, K. D. (2021). *Nonsense correlations in neuroscience* (p. 2020.11.29.402719). bioRxiv. https://doi.org/10.1101/2020.11.29.402719
Hayhoe, M., & Ballard, D. (2005). Eye movements in natural behavior. *Trends in Cognitive Sciences*, *9*(4), 188–194. https://doi.org/10.1016/j.tics.2005.02.009
Hopfield, J. J. (1995). Pattern recognition computation using action potential timing for stimulus representation. *Nature*, *376*(6535), 33–36. https://doi.org/10.1038/376033a0
Hurst, J. L., Payne, C. E., Nevison, C. M., Marie, A. D., Humphries, R. E., Robertson, D. H. L., Cavaggioni, A., & Beynon, R. J. (2001). Individual recognition in mice mediated by major urinary proteins. *Nature*, *414*(6864), 631–634. https://doi.org/10.1038/414631a
Huston, S. J., Stopfer, M., Cassenaer, S., Aldworth, Z. N., & Laurent, G. (2015). Neural Encoding of Odors during Active Sampling and in Turbulent Plumes. *Neuron*, *88*(2), 403–418. https://doi.org/10.1016/j.neuron.2015.09.007
Iwata, R., Kiyonari, H., & Imai, T. (2017). Mechanosensory-Based Phase Coding of Odor Identity in the Olfactory Bulb. *Neuron*, *96*(5), 1139-1152.e7. https://doi.org/10.1016/j.neuron.2017.11.008
Jackson, B. J., Fatima, G. L., Oh, S., & Gire, D. H. (2020). Many Paths to the Same Goal: Balancing Exploration and Exploitation during Probabilistic Route Planning. *eNeuro*, *7*(3). https://doi.org/10.1523/ENEURO.0536-19.2020
Jacobs, L. F. (2012). From chemotaxis to the cognitive map: The function of olfaction. *Proceedings of the National Academy of Sciences*, *109*(Supplement 1), 10693–10700. https://doi.org/10.1073/pnas.1201880109
Jacobs, L. F. (2023). The PROUST hypothesis: The embodiment of olfactory cognition. *Animal Cognition*, *26*(1), 59–72. https://doi.org/10.1007/s10071-022-01734-1
Jacobs, L. F., & Schenk, F. (2003). Unpacking the cognitive map: The parallel map theory of hippocampal function. *Psychological Review*, *110*(2), 285–315. https://doi.org/10.1037/0033-295X.110.2.285

Jones, P. W., & Urban, N. N. (2018). *Mice follow odor trails using stereo olfactory cues and rapid sniff to sniff comparisons* (p. 293746). bioRxiv. https://doi.org/10.1101/293746

Kapoor, V., Provost, A., Agarwal, P., & Murthy, V. N. (2016). Activation of raphe nuclei triggers rapid and distinct effects on parallel olfactory bulb output channels. *Nature Neuroscience*, *19*(2), 271–282. https://doi.org/10.1038/nn.4219

Kay, L. M., Lancaster, L. R., & Freeman, W. J. (1996). Reafference and attractors in the olfactory system during odor recognition. *International Journal of Neural Systems*, *7*(4), 489–495. https://doi.org/10.1142/s0129065796000476

Kehl, M. S., Mackay, S., Ohla, K., Schneider, M., Borger, V., Surges, R., Spehr, M., & Mormann, F. (2024). Single-neuron representations of odours in the human brain. *Nature*, 1–9. https://doi.org/10.1038/s41586-024-08016-5

Keller, G. B., & Mrsic-Flogel, T. D. (2018). Predictive Processing: A Canonical Cortical Computation. *Neuron*, *100*(2), 424–435. https://doi.org/10.1016/j.neuron.2018.10.003

Kepecs, A., Uchida, N., & Mainen, Z. F. (2006). The Sniff as a Unit of Olfactory Processing. *Chemical Senses*, *31*(2), 167–179. https://doi.org/10.1093/chemse/bjj016

Kepecs, A., Uchida, N., & Mainen, Z. F. (2007). Rapid and Precise Control of Sniffing During Olfactory Discrimination in Rats. *Journal of Neurophysiology*, *98*(1), 205–213. https://doi.org/10.1152/jn.00071.2007

Khan, A. G., Sarangi, M., & Bhalla, U. S. (2012). Rats track odour trails accurately using a multi-layered strategy with near-optimal sampling. *Nature Communications*, *3*(1), Article 1. https://doi.org/10.1038/ncomms1712

Kim, J., Erskine, A., Cheung, J. A., & Hires, S. A. (2020). Behavioral and Neural Bases of Tactile Shape Discrimination Learning in Head-Fixed Mice. *Neuron*, *108*(5), 953-967.e8. https://doi.org/10.1016/j.neuron.2020.09.012

Kleinfeld, D., Ahissar, E., & Diamond, M. E. (2006). Active sensation: Insights from the rodent vibrissa sensorimotor system. *Current Opinion in Neurobiology*, *16*(4), 435–444. https://doi.org/10.1016/j.conb.2006.06.009

Kleinfeld, D., Deschênes, M., Wang, F., & Moore, J. D. (2014). More than a rhythm of life: Breathing as a binder of orofacial sensation. *Nature Neuroscience*, *17*(5), Article 5. https://doi.org/10.1038/nn.3693

Komorowski, R. W., Manns, J. R., & Eichenbaum, H. (2009). Robust conjunctive item-place coding by hippocampal neurons parallels learning what happens where. *The Journal of Neuroscience: The Official Journal of the Society for Neuroscience*, *29*(31), 9918–9929. https://doi.org/10.1523/JNEUROSCI.1378-09.2009

Kovesi, P. (2015). *Good Colour Maps: How to Design Them* (arXiv:1509.03700). arXiv. https://doi.org/10.48550/arXiv.1509.03700

Krakauer, J. W., Ghazanfar, A. A., Gomez-Marin, A., MacIver, M. A., & Poeppel, D. (2017). Neuroscience Needs Behavior: Correcting a Reductionist Bias. *Neuron*, *93*(3), 480–490. https://doi.org/10.1016/j.neuron.2016.12.041

Kurnikova, A., Moore, J. D., Liao, S.-M., Deschênes, M., & Kleinfeld, D. (2017). Coordination of Orofacial Motor Actions into Exploratory Behavior by Rat. *Current Biology*, *27*(5), 688–696. https://doi.org/10.1016/j.cub.2017.01.013

Land, M., & Tatler, B. (2009). *Looking and Acting: Vision and Eye Movements in Natural Behaviour*. OUP Oxford.

Lewis, S. M., Xu, L., Rigolli, N., Tariq, M. F., Suarez, L. M., Stern, M., Seminara, A., & Gire, D. H. (2021). Plume Dynamics Structure the Spatiotemporal Activity of Mitral/Tufted Cell Networks in the Mouse Olfactory Bulb. *Frontiers in Cellular Neuroscience*, *15*. https://doi.org/10.3389/fncel.2021.633757

Li, A., Gire, D. H., Bozza, T., & Restrepo, D. (2014). Precise Detection of Direct Glomerular Input Duration by the Olfactory Bulb. *Journal of Neuroscience*, *34*(48), 16058–16064. https://doi.org/10.1523/JNEUROSCI.3382-14.2014

Liao, S.-M., & Kleinfeld, D. (2023). A change in behavioral state switches the pattern of motor output that underlies rhythmic head and orofacial movements. *Current Biology*, *33*(10), 1951-1966.e6. https://doi.org/10.1016/j.cub.2023.04.008

Lindeman, S., Fu, X., Reinert, J. K., & Fukunaga, I. (2023). *Reward contingency modulates olfactory bulb output via pathway-dependent peri-somatic inhibition* (p. 2023.08.17.553686). bioRxiv. https://doi.org/10.1101/2023.08.17.553686

Linster, C., & Cleland, T. A. (2002). Cholinergic modulation of sensory representations in the olfactory bulb. *Neural Networks*, *15*(4), 709–717. https://doi.org/10.1016/S0893-6080(02)00061-8

Liu, A., Papale, A. E., Hengenius, J., Patel, K., Ermentrout, B., & Urban, N. N. (2020). Mouse Navigation Strategies for Odor Source Localization. *Frontiers in Neuroscience*, *14*. https://doi.org/10.3389/fnins.2020.00218

Long, X., & Zhang, S.-J. (2021). A novel somatosensory spatial navigation system outside the hippocampal formation. *Cell Research*, *31*(6), 649–663. https://doi.org/10.1038/s41422-020-00448-8

Lynch, D., & Frost, M. (Directors). (1990). *Twin Peaks* [Broadcast].

Macrides, F., & Chorover, S. L. (1972). Olfactory Bulb Units: Activity Correlated with Inhalation Cycles and Odor Quality. *Science*, *175*(4017), 84–87. https://doi.org/10.1126/science.175.4017.84

Markowitz, J. E., Gillis, W. F., Jay, M., Wood, J., Harris, R. W., Cieszkowski, R., Scott, R., Brann, D., Koveal, D., Kula, T., Weinreb, C., Osman, M. A. M., Pinto, S. R., Uchida, N., Linderman, S. W., Sabatini, B. L., & Datta, S. R. (2023). Spontaneous behaviour is structured by reinforcement without explicit reward. *Nature*, *614*(7946), Article 7946. https://doi.org/10.1038/s41586-022-05611-2

Marshall, J. D., Aldarondo, D. E., Dunn, T. W., Wang, W. L., Berman, G. J., & Ölveczky, B. P. (2021). Continuous Whole-Body 3D Kinematic Recordings across the Rodent Behavioral Repertoire. *Neuron*, *109*(3), 420-437.e8. https://doi.org/10.1016/j.neuron.2020.11.016

Matheson, A. M. M., Lanz, A. J., Medina, A. M., Licata, A. M., Currier, T. A., Syed, M. H., & Nagel, K. I. (2022). A neural circuit for wind-guided olfactory navigation. *Nature Communications*, *13*, 4613. https://doi.org/10.1038/s41467-022-32247-7

Mazzucato, L. (2022). Neural mechanisms underlying the temporal organization of naturalistic animal behavior. *eLife*, *11*, e76577. https://doi.org/10.7554/eLife.76577

Means, L. W., Alexander, S. R., & O'Neal, M. F. (1992). Those cheating rats: Male and female rats use odor trails in a water-escape "working memory" task. *Behavioral and Neural Biology*, *58*(2), 144–151. https://doi.org/10.1016/0163-1047(92)90387-j

Meijer, G. (2021). Neurons in the mouse brain correlate with cryptocurrency price: A cautionary tale. *Peer Community Journal*, *1*. https://doi.org/10.24072/pcjournal.30

Mena, W., Baker, K., Rubin, A., Kohli, S., Yoo, Y., Ziv, Y., Razaei-Mazinani, C., & Fleischmann, A. (2023). *Differential encoding of odor and place in mouse piriform and entorhinal cortex* (p. 2023.10.05.561119). bioRxiv. https://doi.org/10.1101/2023.10.05.561119

Mertens, P. E. C., Marchesi, P., Ruikes, T. R., Oude Lohuis, M., Krijger, Q., Pennartz, C. M. A., & Lansink, C. S. (2023). Coherent mapping of position and head direction across auditory and visual cortex. *Cerebral Cortex*, *33*(12), 7369–7385. https://doi.org/10.1093/cercor/bhad045

Michaiel, A. M., Abe, E. T., & Niell, C. M. (2020). Dynamics of gaze control during prey capture in freely moving mice. *eLife*, *9*, e57458. https://doi.org/10.7554/eLife.57458

Miller, C. T., Gire, D., Hoke, K., Huk, A. C., Kelley, D., Leopold, D. A., Smear, M. C., Theunissen, F., Yartsev, M., & Niell, C. M. (2022). Natural behavior is the language of the brain. *Current Biology*, *32*(10), R482–R493. https://doi.org/10.1016/j.cub.2022.03.031

Musall, S., Urai, A. E., Sussillo, D., & Churchland, A. K. (2019). Harnessing behavioral diversity to understand neural computations for cognition. *Current Opinion in Neurobiology*, *58*, 229–238. https://doi.org/10.1016/j.conb.2019.09.011

Nevitt, G. A., Losekoot, M., & Weimerskirch, H. (2008). Evidence for olfactory search in wandering albatross, Diomedea exulans. *Proceedings of the National Academy of Sciences*, *105*(12), 4576–4581. https://doi.org/10.1073/pnas.0709047105

Newman, B. (1963). *Canto II* [Graphic].

Nieh, E. H., Schottdorf, M., Freeman, N. W., Low, R. J., Lewallen, S., Koay, S. A., Pinto, L., Gauthier, J. L., Brody, C. D., & Tank, D. W. (2021). Geometry of abstract

learned knowledge in the hippocampus. *Nature*, *595*(7865), 80–84. https://doi.org/10.1038/s41586-021-03652-7

Nogi, Y., Ahasan, M. M., Murata, Y., Taniguchi, M., Sha, M. F. R., Ijichi, C., & Yamaguchi, M. (2020). Expression of feeding-related neuromodulatory signalling molecules in the mouse central olfactory system. *Scientific Reports*, *10*(1), 890. https://doi.org/10.1038/s41598-020-57605-7

O'Keefe, J., & Nadel, L. (1978). *The hippocampus as a cognitive map*. Clarendon Press ; Oxford University Press.

Onoda, N., & Mori, K. (1980). Depth distribution of temporal firing patterns in olfactory bulb related to air-intake cycles. *Journal of Neurophysiology*, *44*(1), 29–39. https://doi.org/10.1152/jn.1980.44.1.29

Osborne, J. l., Clark, S. j., Morris, R. j., Williams, I. h., Riley, J. r., Smith, A. d., Reynolds, D. r., & Edwards, A. s. (1999). A landscape-scale study of bumble bee foraging range and constancy, using harmonic radar. *Journal of Applied Ecology*, *36*(4), 519–533. https://doi.org/10.1046/j.1365-2664.1999.00428.x

Padmanabhan, K., Osakada, F., Tarabrina, A., Kizer, E., Callaway, E. M., Gage, F. H., & Sejnowski, T. J. (2019). Centrifugal Inputs to the Main Olfactory Bulb Revealed Through Whole Brain Circuit-Mapping. *Frontiers in Neuroanatomy*, *12*. https://doi.org/10.3389/fnana.2018.00115

Panzeri, S., Brunel, N., Logothetis, N. K., & Kayser, C. (2010). Sensory neural codes using multiplexed temporal scales. *Trends in Neurosciences*, *33*(3), 111–120. https://doi.org/10.1016/j.tins.2009.12.001

Parker, P. R. L., Brown, M. A., Smear, M. C., & Niell, C. M. (2020). Movement-Related Signals in Sensory Areas: Roles in Natural Behavior. *Trends in Neurosciences*, *43*(8), 581–595. https://doi.org/10.1016/j.tins.2020.05.005

Pereira, T. D., Tabris, N., Matsliah, A., Turner, D. M., Li, J., Ravindranath, S., Papadoyannis, E. S., Normand, E., Deutsch, D. S., Wang, Z. Y., McKenzie-Smith, G. C., Mitelut, C. C., Castro, M. D., D'Uva, J., Kislin, M., Sanes, D. H., Kocher, S. D., Wang, S. S.-H., Falkner, A. L., … Murthy, M. (2022). SLEAP: A deep learning system for multi-animal pose tracking. *Nature Methods*, *19*(4), 486–495. https://doi.org/10.1038/s41592-022-01426-1

Poo, C., Agarwal, G., Bonacchi, N., & Mainen, Z. F. (2022). Spatial maps in piriform cortex during olfactory navigation. *Nature*, *601*(7894), Article 7894. https://doi.org/10.1038/s41586-021-04242-3

Powers, W. T. (1973). *Behavior: The Control of Perception*. Benchmark Pubns Inc.

Price, J. L. (1985). Beyond the primary olfactory cortex: Olfactory-related areas in the neocortex, thalamus and hypothalamus. *Chemical Senses*, *10*(2), 239–258. https://doi.org/10.1093/chemse/10.2.239

Raithel, C. U., & Gottfried, J. A. (2021). Using your nose to find your way: Ethological comparisons between human and non-human species. *Neuroscience &*

Biobehavioral Reviews, *128*, 766–779. https://doi.org/10.1016/j.neubiorev.2021.06.040

Ravel, N., & Pager, J. (1990). Respiratory patterning of the rat olfactory bulb unit activity: Nasal versus tracheal breathing. *Neuroscience Letters*, *115*(2), 213–218. https://doi.org/10.1016/0304-3940(90)90457-K

Reinert, J. K., & Fukunaga, I. (2022). The facets of olfactory learning. *Current Opinion in Neurobiology*, *76*, 102623. https://doi.org/10.1016/j.conb.2022.102623

Renner, M. J. (1990). Neglected aspects of exploratory and investigatory behavior. *Psychobiology*, *18*(1), 16–22. https://doi.org/10.3758/BF03327209

Renner, M. J. (2022). Ethogram. In J. Vonk & T. K. Shackelford (Eds.), *Encyclopedia of Animal Cognition and Behavior* (pp. 2461–2464). Springer International Publishing. https://doi.org/10.1007/978-3-319-55065-7_227

Riley, B. (1990). *Shadowplay* [Graphic].

Rojas-Líbano, D., Frederick, D. E., Egaña, J. I., & Kay, L. M. (2014). The olfactory bulb theta rhythm follows all frequencies of diaphragmatic respiration in the freely behaving rat. *Frontiers in Behavioral Neuroscience*, *8*. https://www.frontiersin.org/articles/10.3389/fnbeh.2014.00214

Rucci, M., & Victor, J. D. (2015). The unsteady eye: An information-processing stage, not a bug. *Trends in Neurosciences*, *38*(4), 195–206. https://doi.org/10.1016/j.tins.2015.01.005

Saleem, A. B., & Busse, L. (2023). Interactions between rodent visual and spatial systems during navigation. *Nature Reviews Neuroscience*, *24*(8), Article 8. https://doi.org/10.1038/s41583-023-00716-7

Schaefer, A. T., & Margrie, T. W. (2007). Spatiotemporal representations in the olfactory system. *Trends in Neurosciences*, *30*(3), 92–100. https://doi.org/10.1016/j.tins.2007.01.001

Schmitt, B. C., & Ache, B. W. (1979). Olfaction: Responses of a Decapod Crustacean Are Enhanced by Flicking. *Science*, *205*(4402), 204–206. https://doi.org/10.1126/science.205.4402.204

Sheffield, M. E. J., & Dombeck, D. A. (2015). The binding solution? *Nature Neuroscience*, *18*(8), 1060–1062. https://doi.org/10.1038/nn.4075

Shepherd, G. M., & Greer, C. A. (1998). Olfactory bulb. In *The synaptic organization of the brain, 4th ed* (pp. 159–203). Oxford University Press.

Shipley, M. T., Ennis, M., & Puche, A. C. (2008). The Olfactory System. In P. M. Conn (Ed.), *Neuroscience in Medicine* (pp. 611–622). Humana Press. https://doi.org/10.1007/978-1-60327-455-5_38

Shusterman, R., Smear, M. C., Koulakov, A. A., & Rinberg, D. (2011). Precise olfactory responses tile the sniff cycle. *Nature Neuroscience*, *14*(8), 1039–1044. https://doi.org/10.1038/nn.2877

Skaggs, W., McNaughton, B., & Gothard, K. (1992). An Information-Theoretic Approach to Deciphering the Hippocampal Code. *Advances in Neural Information Processing Systems*, *5*. https://proceedings.neurips.cc/paper/1992/hash/5dd9db5e033da9c6fb5ba83c7a7ebea9-Abstract.html

Smear, M., Resulaj, A., Zhang, J., Bozza, T., & Rinberg, D. (2013). Multiple perceptible signals from a single olfactory glomerulus. *Nature Neuroscience*, *16*(11), 1687–1691. https://doi.org/10.1038/nn.3519

Smear, M., Shusterman, R., O'Connor, R., Bozza, T., & Rinberg, D. (2011). Perception of sniff phase in mouse olfaction. *Nature*, *479*(7373), 397–400. https://doi.org/10.1038/nature10521

Soria-Gómez, E., Bellocchio, L., Reguero, L., Lepousez, G., Martin, C., Bendahmane, M., Ruehle, S., Remmers, F., Desprez, T., Matias, I., Wiesner, T., Cannich, A., Nissant, A., Wadleigh, A., Pape, H.-C., Chiarlone, A. P., Quarta, C., Verrier, D., Vincent, P., … Marsicano, G. (2014). The endocannabinoid system controls food intake via olfactory processes. *Nature Neuroscience*, *17*(3), 407–415. https://doi.org/10.1038/nn.3647

Stapleton, J. R., Lavine, M. L., Wolpert, R. L., Nicolelis, M. A. L., & Simon, S. A. (2006). Rapid Taste Responses in the Gustatory Cortex during Licking. *Journal of Neuroscience*, *26*(15), 4126–4138. https://doi.org/10.1523/JNEUROSCI.0092-06.2006

Stefanini, F., Kushnir, L., Jimenez, J. C., Jennings, J. H., Woods, N. I., Stuber, G. D., Kheirbek, M. A., Hen, R., & Fusi, S. (2020). A Distributed Neural Code in the Dentate Gyrus and in CA1. *Neuron*, *107*(4), 703-716.e4. https://doi.org/10.1016/j.neuron.2020.05.022

Sterling, P., & Laughlin, S. (2015). *Principles of Neural Design*. The MIT Press. https://doi.org/10.7551/mitpress/9780262028707.001.0001

Stringer, C., Pachitariu, M., Steinmetz, N., Reddy, C. B., Carandini, M., & Harris, K. D. (2019). Spontaneous behaviors drive multidimensional, brainwide activity. *Science*, *364*(6437), eaav7893. https://doi.org/10.1126/science.aav7893

Sugar, J., & Moser, M.-B. (2019). Episodic memory: Neuronal codes for what, where, and when. *Hippocampus*, *29*(12), 1190–1205. https://doi.org/10.1002/hipo.23132

Sullivan, R. M., Wilson, D. A., & Leon, M. (1989). Norepinephrine and learning-induced plasticity in infant rat olfactory system. *Journal of Neuroscience*, *9*(11), 3998–4006. https://doi.org/10.1523/JNEUROSCI.09-11-03998.1989

Tinbergen, N. (1965). *Social Behaviour in Animals*. Springer Netherlands. https://doi.org/10.1007/978-94-011-7686-6

Tolman, E. C. (1948). *Cognitive maps in rats and men*.

Vanderwolf, C. H. (2000). What is the significance of gamma wave activity in the pyriform cortex? *Brain Research*, *877*(2), 125–133. https://doi.org/10.1016/S0006-8993(00)02568-3

Vanderwolf, C. H. (2001). The hippocampus as an olfacto-motor mechanism: Were the classical anatomists right after all? *Behavioural Brain Research*, *127*(1), 25–47. https://doi.org/10.1016/S0166-4328(01)00354-0

Vergassola, M., Villermaux, E., & Shraiman, B. I. (2007). 'Infotaxis' as a strategy for searching without gradients. *Nature*, *445*(7126), Article 7126. https://doi.org/10.1038/nature05464

Verhagen, J. V., Wesson, D. W., Netoff, T. I., White, J. A., & Wachowiak, M. (2007). Sniffing controls an adaptive filter of sensory input to the olfactory bulb. *Nature Neuroscience*, *10*(5), 631–639. https://doi.org/10.1038/nn1892

Wachowiak, M. (2011). All in a Sniff: Olfaction as a Model for Active Sensing. *Neuron*, *71*(6), 962–973. https://doi.org/10.1016/j.neuron.2011.08.030

Wallace, D. G., Gorny, B., & Whishaw, I. Q. (2002). Rats can track odors, other rats, and themselves: Implications for the study of spatial behavior. *Behavioural Brain Research*, *131*(1–2), 185–192. https://doi.org/10.1016/s0166-4328(01)00384-9

Wallraff, H. G. (2004). Avian olfactory navigation: Its empirical foundation and conceptual state. *Animal Behaviour*, *67*(2), 189–204. https://doi.org/10.1016/j.anbehav.2003.06.007

Wang, M. Z., & Hayden, B. Y. (2021). Latent learning, cognitive maps, and curiosity. *Current Opinion in Behavioral Sciences*, *38*, 1–7. https://doi.org/10.1016/j.cobeha.2020.06.003

Webb, B. (2004). Neural mechanisms for prediction: Do insects have forward models? *Trends in Neurosciences*, *27*(5), 278–282. https://doi.org/10.1016/j.tins.2004.03.004

Weber, A. I., Krishnamurthy, K., & Fairhall, A. L. (2019). Coding Principles in Adaptation. *Annual Review of Vision Science*, *5*, 427–449. https://doi.org/10.1146/annurev-vision-091718-014818

Weinreb, C., Osman, M. A. M., Jay, M., & Datta, S. R. (2024). Systems Neuro Browser (SNUB). *Journal of Open Source Software*, *9*(95), 6187. https://doi.org/10.21105/joss.06187

Weinreb, C., Pearl, J. E., Lin, S., Osman, M. A. M., Zhang, L., Annapragada, S., Conlin, E., Hoffmann, R., Makowska, S., Gillis, W. F., Jay, M., Ye, S., Mathis, A., Mathis, M. W., Pereira, T., Linderman, S. W., & Datta, S. R. (2024). Keypoint-MoSeq: Parsing behavior by linking point tracking to pose dynamics. *Nature Methods*, *21*(7), 1329–1339. https://doi.org/10.1038/s41592-024-02318-2

Welker, W. I. (1964). *Analysis of Sniffing of the Albino Rat*. https://doi.org/10.1163/156853964X00030

Wesson, D. W., Carey, R. M., Verhagen, J. V., & Wachowiak, M. (2008). Rapid Encoding and Perception of Novel Odors in the Rat. *PLOS Biology*, *6*(4), e82. https://doi.org/10.1371/journal.pbio.0060082

Wilent, W. B., & Nitz, D. A. (2007). Discrete Place Fields of Hippocampal Formation Interneurons. *Journal of Neurophysiology*, *97*(6), 4152–4161. https://doi.org/10.1152/jn.01200.2006

Yang, C., Mammen, L., Kim, B., Li, M., Robson, D. N., & Li, J. M. (2024). A population code for spatial representation in the zebrafish telencephalon. *Nature*, 1–10. https://doi.org/10.1038/s41586-024-07867-2

Yang, S. C.-H., Wolpert, D. M., & Lengyel, M. (2016). Theoretical perspectives on active sensing. *Current Opinion in Behavioral Sciences*, *11*, 100–108. https://doi.org/10.1016/j.cobeha.2016.06.009

Yarbus, A. L. (1967). *Eye Movements and Vision*. Springer US. https://doi.org/10.1007/978-1-4899-5379-7

Youngentob, S. L., Mozell, M. M., Sheehe, P. R., & Hornung, D. E. (1987). A quantitative analysis of sniffing strategies in rats performing odor detection tasks. *Physiology & Behavior*, *41*(1), 59–69. https://doi.org/10.1016/0031-9384(87)90131-4

Zak, J. D., Reddy, G., Konanur, V., & Murthy, V. N. (2024). Distinct information conveyed to the olfactory bulb by feedforward input from the nose and feedback from the cortex. *Nature Communications*, *15*(1), 3268. https://doi.org/10.1038/s41467-024-47366-6

Methods

Animal housing and care

All procedures were conducted in accordance with the ethical guidelines of the National Institutes of Health and were approved by the Institutional Animal Care and Use Committee at the University of Oregon. Animals were maintained on a reverse 12/12 h light/dark cycle. All recordings were performed during the dark phase of the cycle. Mice were C57Bl6/J background and were 8–12 weeks of age at the time of surgery.

Surgical procedures

Animals were anesthetized with isoflurane (3% concentration initially, altered during surgery depending on response of the animal to anesthesia). Incision sites were numbed prior to incision with 20 mg/mL lidocaine.

Thermistors were implanted between the nasal bone and inner nasal epithelium (Findley et al., 2021). A custom titanium head bar and Janelia micro drive were implanted.

For olfactory bulb array implantation, we administered atropine (0.03 mg/kg) preoperatively to reduce inflammation and respiratory irregularities. Surgical anesthesia was induced and maintained with isoflurane (1.25–2.0%). Skin overlying the skull between the lambdoid and frontonasal sutures was removed. A rectangular window was cut through the skull overlying the lateral half of the left bulb for insertion of the recording array. The array was lowered to a depth of 1mm and cemented in place with Grip Cement. For hippocampus electrode implantation, an array of 8 tetrodes was inserted vertically through a small, 1mm2 craniotomy overlying the dorsal CA1 cell field of the left hemisphere. To minimize postoperative discomfort, Carpofen (10 mg/kg) was administered 45 minutes prior to the end of surgery. Mice were housed individually after the surgery and allowed 7 days of post-operative recovery.

Behavioral recordings

Mice were restrained by head fixation then placed in a 15 cm by 40cm behavioral arena. After a period of head-fixation, mice were released to move around the arena, without explicit training or reward structure, while breathing (sampling rate 1kHz), neural data (sampling rate 30kHz), and video (frame rate 100 Hz) were recorded. In a subset of sessions the mice were recorded for 20 min and then the floor was rotated 180 deg and the mice were recorded for an additional 20 min.

The mice were imaged from below to reduce errors due to cable and implant obstruction. A one-direction privacy film was placed on the floor to prevent mice from viewing the open platform which could introduce confounds such as fear responses. A transparent removable flooring was placed directly over this to allow rotation.

We record sniffing using intranasally implanted thermistors (TE Sensor Solutions, #GAG22K7MCD419), amplified initially with custom-built op amp (Texas Instruments, #TLV2460, circuit available upon request) and then a CYGNAS, FLA 01 amplifier fed into the analog input of an open ephys box.

Pose estimation

The location of the head, center of mass, and base of tail of the mouse were tracked via SLEAP (Pereira et al., 2022). A random set of 1000 frames were hand labeled and compared to the assigned head location to assess error rates. Movement speeds are calculated from the distance the head travels per unit time, smoothed with a 1 s Savitsky-Golay filter. In addition, a head speed limit was placed on the resulting tracking data (10 pix/s = cm/s), and violations were smoothed by linear interpolation.

Electrophysiology

Following a 3 day recovery period post surgery mice were head fixed and the custom microdrive was advanced to the regions of interest (ROI) while recording. Either Si probes (Diagnostic Biochips P-64-7) or a custom implanted array of 8 tetrodes passed in pairs through 4 linearly-aligned 27-gauge stainless steel hypodermic tubes. Tetrodes were made of 18 µm (25 µm coated) tungsten wire (California Fine Wire). Once the ROI

was reached a minimum of 24 hours was allowed prior to data collection to increase recording stability.

Data were acquired via a 128-channel data acquisition system (RHD2000; Intan Technologies) at a 30 kHz sampling frequency and Open Ephys software (http://open-ephys.org). A camera positioned 90cm above the arena floor was used to recording movement around the arena with Bonsai video acquisition software (http://bonsai-rx.org).

Custom Bonsai code was used to align the TTL triggers from the camera frames, the sniff, and the electrophysiology recording captured with no filters applied in the OpenEphys software.

Spike and sniff data preprocessing and inclusion criteria

Analysis of spikes and sniffing were performed in MATLAB. Electrophysiological data were preprocessed via Kilosort, Phy2, and custom software. Inhalation and exhalation times were extracted by finding peaks and troughs in the temperature signal after downsampling to 1000 samples per s, and smoothing with a 25 ms moving window. All sniffs' instantaneous frequencies are inverse intersniff intervals. Sniffs with instantaneous frequencies greater than 17 and less than 0.5 sniffs per s were excluded from the analysis. Autocorrelations of sniff frequency and speed and their cross correlation were calculated after mean subtraction and de-trending.

Single units were curated with criteria of 5% refractory period violations (refractory period = 1.5 ms) and an amplitude loss cutoff of 10%. Amplitudes were calculated by first calculating the mean spike waveform on the channel giving the largest spike amplitude and finding its peak and trough times. Then, for each spike time, amplitude was calculated as the difference between the peak and trough times of the mean. The cutoff criterion was this amplitude being less than or equal to zero, so that the fraction of lost spikes can be estimated. This criterion greatly reduces the potential of significant electrode drift over the recording.

Neuronal population similarity analysis (Matlab)

For population analysis with respect to breathing rhythms (Fig 2), we first calculated each unit's firing rate time series in 5 s bins, normalized to scale those values between 1 and 0, and smoothed with a 15 s Savitzky-golay filter. For visualization, the units were then sorted according to k-means clustering on the earth movers distances between all units' time series. These were then colored according to the spike rate colormap used throughout the paper (see below). The resulting matrix is displayed beneath the HMM state-colored sniff frequency plot (Fig 2B). To calculate the similarity matrix over time, we took the cosine distance between all time bins' population vector (Fig 2B). To compare the neuronal population similarity to the behavioral HMM states, for each session we built a state similarity matrix with the mean cosine distance for comparing

every combination of states. To determine whether the distance matrices differed from the prediction of a nonsense correlation null hypothesis, we calculated the state similarity matrix between the neural population vectors when the behavioral HMM states were circularly shifted for the number of 5 s bins in the entire session minus two bins on either side for padding (sessions varied from approximately 30 to 90 minutes). For each session the state similarity matrix values were converted to the number of standard deviations between the real value and the mean of the circular shift null distribution. These similarity matrices were then averaged within animals, and a grand mean was calculated across the within-animal means (Fig 2C). To assess how well the behavioral HMM clustered the neural population vectors, we calculated a silhouette score for the free-moving period of each session. These were then expressed as the number of standard deviations from the mean of a circular shift null distribution.

Sniff field visualizations (Matlab)

To depict the relationship between individual unit activity and breathing rhythms, we devised sniff fields to portray the relationship between inhalation latency, sniff frequency, and spike probability (Fig 3). For every spike, we assigned a latency as the difference between the spike time and the nearest preceding inhalation time (250 linear spaced bins between 0 and 500 ms), and a frequency as the inverse duration of that sniff (250 log2 spaced bins between 2 and 13 sniffs per s; sniffs with instantaneous frequencies less than 2 were assigned to bin 1, and those greater than 13 to bin 250). Then, to build the joint distribution, we calculated the latency histogram for all spikes that occurred in sniffs within a given frequency bin. We then smoothed the resulting two dimensional matrix with a gaussian filter of width 6. We acknowledge that this smoothing is a questionable choice, given that the latency and frequency axes are in different units, but we nevertheless smoothed in order to reduce the perceptual artifacts of square bins and for aesthetic purposes. These sniff fields were then colored according to the spike rate colormap used throughout the paper (see below).

To analyze sniff fields across the population (Fig 4), we calculated the joint distributions at lower resolution (latency: 30 linear spaced bins between 0 and 300 ms; frequency: 30 log2 spaced bins between 1.75 and 14 sniffs per s). We then took the max projections along the latency and frequency axes for each unit to reduce their information to two "profiles": latency and frequency. To select for only units with significant selectivity, we then included only those units for which a GLM incorporating the single-variable profiles' parameter improved the predictions of a latency/frequency model (see below). To compare and cluster these profiles, we calculated the earth movers distance between each pair of profiles (normalized between 0 and 1), and sorted them into types by k-means clustering. We imposed two clusters on the latency profiles and three clusters on the frequency profiles. Including additional clusters did not appreciably change the results. To display these profiles across the population, we stacked the units' profiles

vertically, separated by cluster and sorted by selectivity (the mean of the profile after normalization). These profile stacks were then colored according to the spike rate colormap used throughout the paper (see below).

Place field visualizations and analysis (Matlab)

To visualize and test the relationship between spiking and place, we assigned each spike to the simultaneous head's position estimate in a 12 by 5 array of spatial bins (approximately 3 cm squared). Place fields were calculated as the two dimensional distribution of spike positions divided by the occupancy distribution. For visualization, these 12 by 5 maps were scaled to 1200 by 500 pixels and smoothed by a 71 pixel gaussian (about 2 cm squared). This smoothing is intended to reduce the high spatial frequency artifacts resulting from square bins and for aesthetic purposes. These place fields were then colored according to the spike rate colormap used throughout the paper (see below).

To assess the significance of place selectivity, we used the traditional measure of Spatial Information (Skaggs and McNaughton, 1992). The slow variation in position and spike rate time series raise the danger of a nonsense correlation in this metric. Furthermore this metric does not work well for units with high ongoing firing rates. For these reasons, we express spatial information as the Significance of Spatial Information (SSI; Stefanini et al, 2020) calculated as the number of standard deviations from a circular shift null distribution.

Place Decoding

For place decoding, neural data was binned into 200 ms time windows, and the spatial arena was divided into 60 uniform regions arranged in a 12x5 grid. To account for potential variability over the recording duration, each session was divided into 10 intervals of approximately 4-8 minutes each. Within each interval, a modified 10-fold cross-validation was applied: the interval was subdivided into 10 folds, and the model was trained on 9 folds from each interval while testing on the held-out fold. This cross-validation process was repeated across all intervals, allowing the model to leverage data from the entire session for training and spatial predictions. To classify neural activity by location, we adapted the method from Stefanini et al. (2020) using all identified cells. A Support Vector Machine (SVM) classifier with a linear kernel (implemented via svm.SVC in Python) was used to associate firing patterns with location (Cortes & Vapnik, 1995). Input vectors were non-linearly mapped into a high-dimensional feature space, where a linear decision surface (hyperplane) was constructed. This SVM-based approach enabled pairwise classification across each of the 60 regions in the arena. The classifier employed a majority-vote rule across pairwise outputs to determine the most likely location of the animal, yielding an instantaneous position estimate (Bishop, 2006). The decoded position, set as the center of the

selected region, was then used to compute the decoding error between actual and predicted locations.

In a subset of the OB sessions, the arena floor mat was rotated by 180 degrees midway through the session, effectively rotating floor-borne scent marks while leaving distal cues unaffected. For analysis, each session was further partitioned into 10 intervals before the rotation and 10 intervals after, creating 20 intervals in total. To establish baseline decoding accuracy within each half, we applied the original place decoding analysis independently for both pre-rotation and post-rotation periods (Pre-Pre and Post-Post Decoding). To test the generalization of spatial encoding across the rotation, the decoder was trained on 9 folds from each of the 10 pre-rotation intervals and tested on the corresponding 1 fold from the 10 post-rotation intervals (Pre-Post Decoding), with the reverse applied for post-rotation training and pre-rotation testing (Post-Pre Decoding). Additionally, we introduced a fictive 180-degree rotation in the predicted trajectory to evaluate the influence of scent-based versus distal cues. In this fictive rotation analysis (Pre/Post-Rotated and Post/Pre-Rotated Decoding), the model trained on pre-rotation intervals was tested on post-rotation intervals using a fictive 180-degree rotation of the predicted trajectory, and vice versa. This analysis allowed us to evaluate the decoder's reliance on scent-based versus distal cues.

To assess the significance of decoding error within individual sessions and across all floor rotation conditions, we generated a shuffled baseline by circularly shifting the reversal of the position data by a pseudorandom integer within the middle 80% of the session duration. For each of the 10 folds of this circularly shifted data, we computed 10 median decoding errors. These shuffled errors served as a comparison to the true decoding errors, and statistical significance was assessed using a Wilcoxon rank-sum test.

Nested Generalized Linear Models (GLMs)

We use Poisson generalized linear models (GLMs) to predict spiking activity of each unit based on sniff parameters and place (Hardcastle et al., 2017). Models were assessed using ten-fold cross-validation. Each session is divided into 50 equal sized bins and ten train test splits are performed on five equally spaced test samples to find representative training and testing sets. Statistical model performance was quantified using a Log-Likelihood Increase (LLHi) metric, which is the change in log-likelihood of held out test data under the fit model compared with a null, mean-rate model. This metric is similar to an F-test, but agnostic to penalization terms. To quantify the non-redundant predictivity of each of these parameters, we calculated a relative predictivity index as the LLHi gained from adding a parameter divided by the total LLHi of the full model. Importantly, because of the redundancy between predictive parameters, these relative predictivity indices do not sum to 1.

Hidden Markov Models (HMMs)

We fit a gaussian HMM to all sessions from all mice to find behavior states present across mice. The HMM models the observed behavioral data as a gaussian random variable with mean and variance dependent on a time-varying latent state. Behavior observations were formatted as a 5 second moving average of nose speed and a 5 second moving average of the distribution of breathing frequencies. HMM parameters are fit using the Expectation Maximization algorithm. Model selection was performed using Bayesian Information Criterion (BIC), which adds a penalty for increasing the number of model parameters to the likelihood of the data under the model. Lower BIC scores are preferred. BIC scores for 1-10 hidden states are reported as the lowest score of 5 random initializations because EM often finds local maximum in the log posterior. Most likely states were assigned to all sessions from the best performing three-state model using the Viterbi algorithm.

Colormaps (Matlab)

To make continuous colormaps, we started from a rainbow colormap designed to be perceptually uniform (Kovesi, 2015); colorcet.com). To complement the chromatic variation afforded by this colormap with luminance variation, we multiplied its values with a smooth ramp between 0 and 1. This gives a colormap in which the minimum value is black. Because these figures will be displayed on a white background (i.e., on a website or a piece of paper), we prefer to represent the minimum value as white. To make the minimum value white, we subtracted the colormap from 1. We used the resulting colormap to represent sniffs per s, and by exchanging its red and blue values we made a colormap to represent spikes per s.

To make categorical color maps, we sample colors from paintings or other popular images. Colors were sampled from painters Bridget Riley (Figs 1, 2, 4, 5, and 8; Riley, 1990), Barnett Newman (Fig 7; Newman, 1963), and the credits of the television series Twin Peaks (Fig 4; Lynch & Frost, 1990). We provide a simple Matlab script for sampling colors into colormaps that can be saved and used later for plotting.

Data and Code Availability

Data and code will be made publicly available at the time of publication.

Acknowledgements

This work was supported by NIH NINDS R01NS123903, NIH NIDCD R01DC018789, and the Simons Collaboration on the Global Brain (SCGB).

Author Contributions

	SCS*	TMF*	SER	MAB	APW	TT	RM	MW	JMM	ALF	MCS
Contributor Role											
Conceptualization	x	x		x					x	x	x
Data Curation		x	x	x							x
Formal Analysis	x		x						x	x	x
Funding Acquisition	x	x		x					x	x	x
Investigation		x			x	x	x				
Methodology	x	x	x	x					x	x	x
Project Administration		x							x	x	x
Resources								x	x	x	x
Software	x	x	x	x							
Supervision								x	x	x	x
Validation	x	x	x	x					x	x	x
Visualization	x										x
Writing – Original Draft Preparation	x									x	x
Writing – Review & Editing	x	x	x		x			x	x	x	x

Supplemental Information

Figure 1 - Figure supplement 1

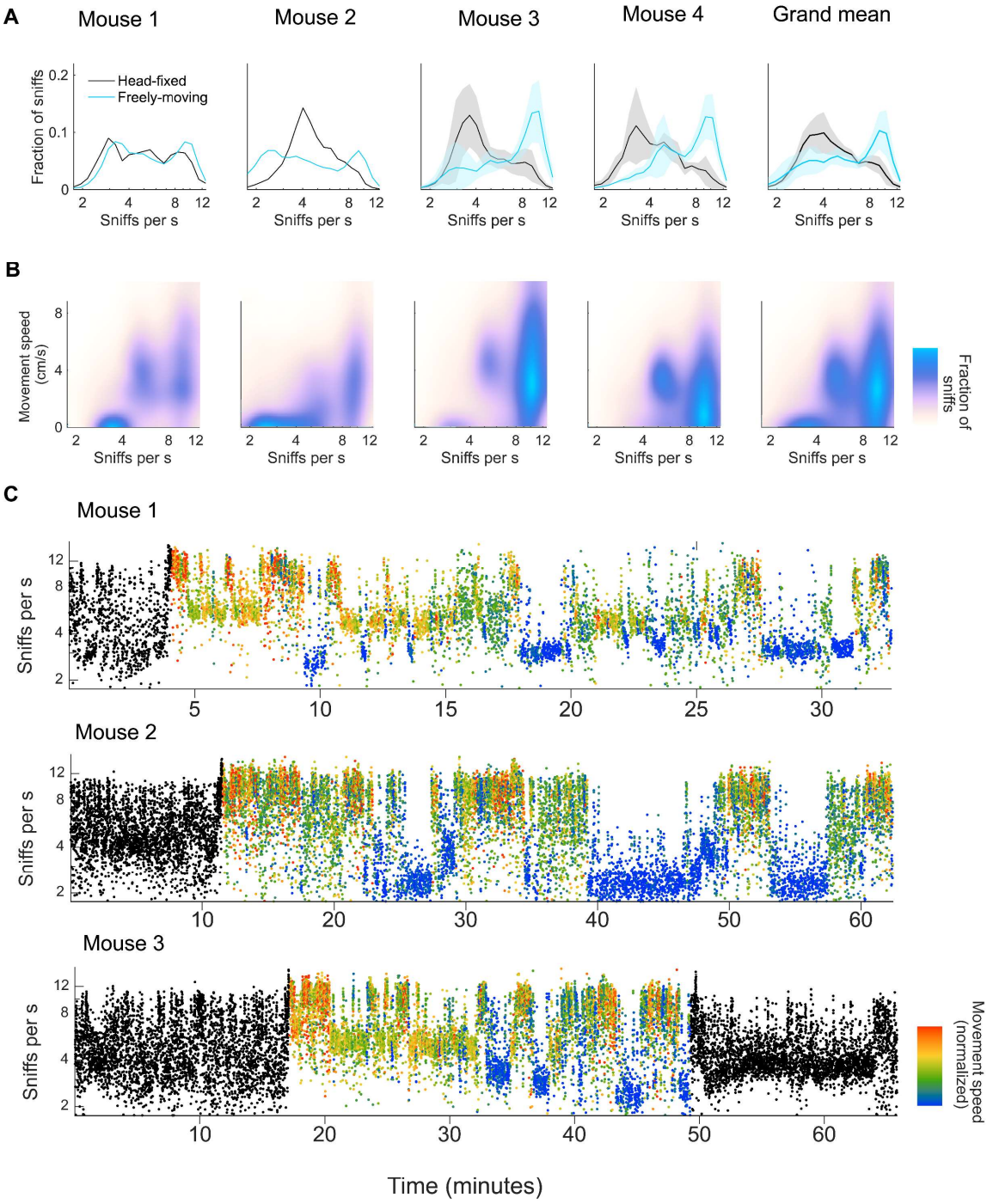

Figure 1 - Figure Supplement 1: A. Histogram of instantaneous sniff frequencies for each individual mouse and grand mean (*n* = 4). Thick lines and shaded regions are mean and ±1 standard deviation. Blue: freely moving; black: head-fixed. **B.** 2D histogram of breathing frequency and movement speed for

each individual mouse and grand mean (n=4). **C.** Sniff rasters for three example sessions where each dot indicates an inhalation time with its instantaneous frequency on the vertical axis. Black: head-fixed; Colors based on movement speed during the freely-moving condition.

Figure 1 - Figure supplement 2

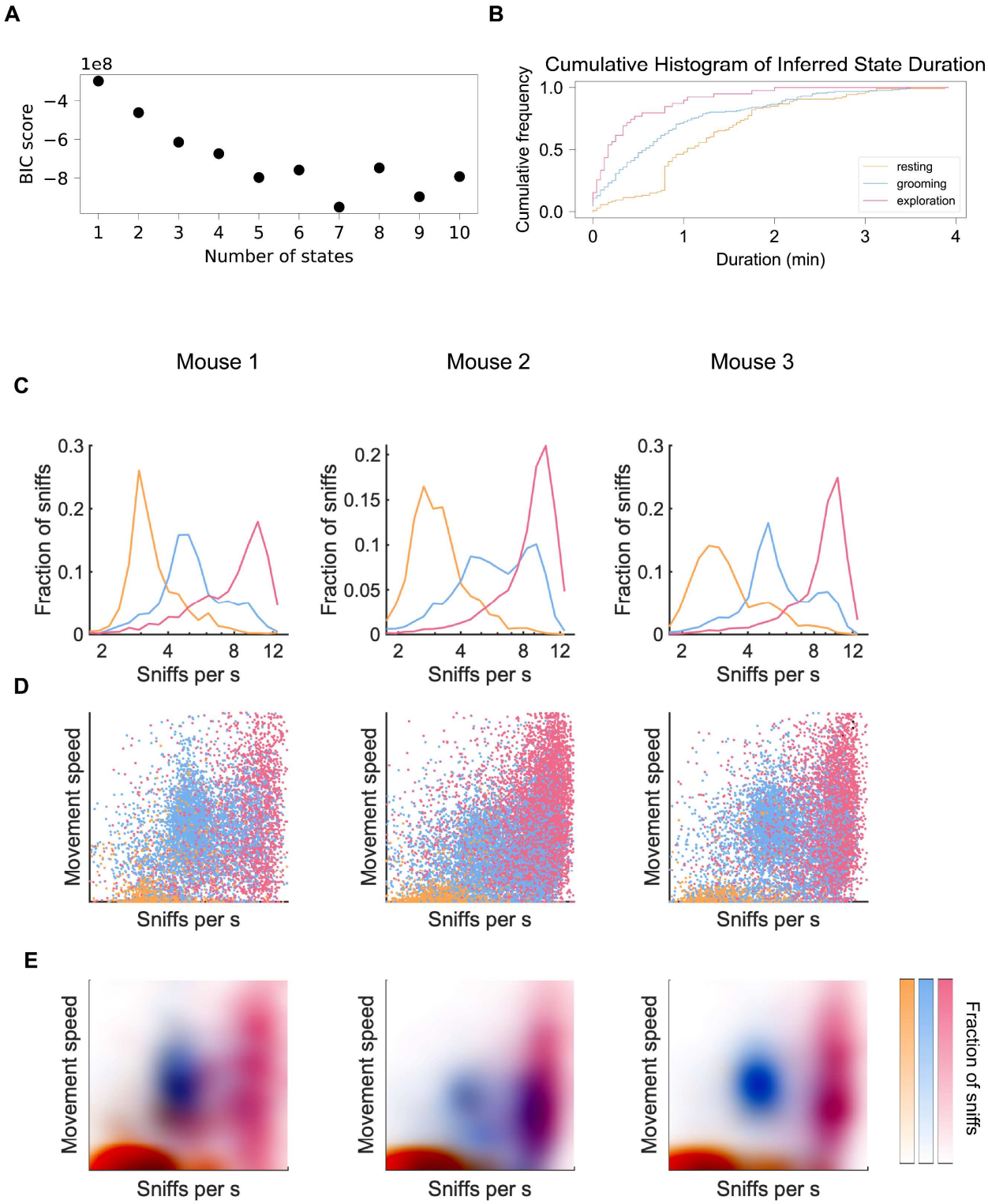

Figure 1 - Figure Supplement 2: A. Bayesian Information Criterion (BIC) scores for HMMs with increasing numbers of hidden states. Scores drop substantially until three states. **B.** Cumulative histogram of inferred state durations across all sessions show that states typically last tens of seconds to minutes. **C.** Sniff Frequency histograms across inferred states for three individual sessions from three mice. **D.** Joint movement speed and sniff frequency scatter plots colored by state assignments for the same three sessions. **E.** Probability density estimates of joint movement speed and sniff frequency for the same three sessions.

Figure 2 - Figure supplement 1

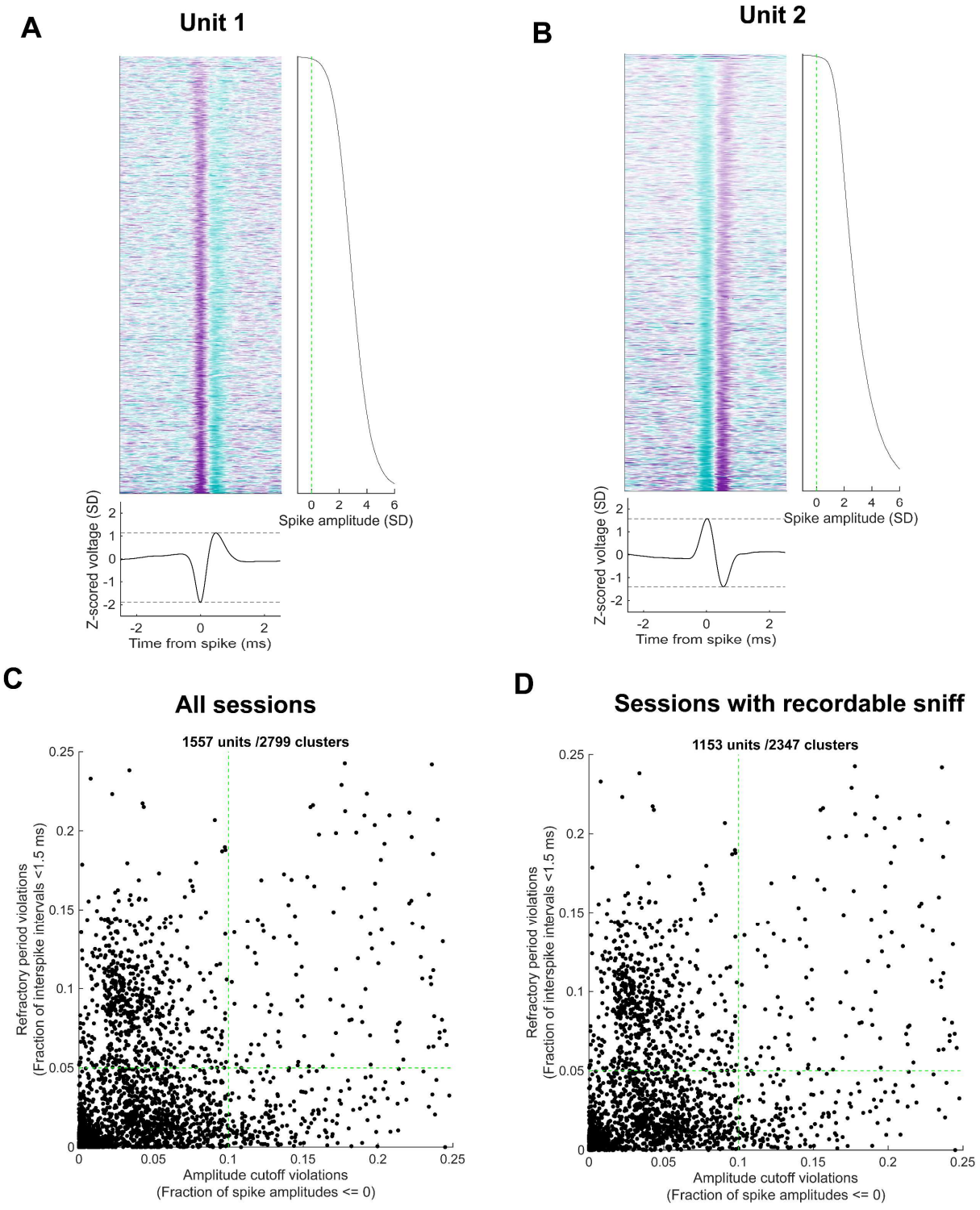

Figure 2 - Figure supplement 1: Unit inclusion criteria A. All spike waveforms for an example unit, their corresponding z-scored spike amplitudes, and mean waveform shape. To calculate amplitude on a spike by spike basis, we took the difference between the signal at the peak time and the trough time. **B.** Same as in **A.** for an example unit with positive leading waveform. **C.** Scatter of all cluster's amplitude

cutoff violations and refractory period violations. Green dashed lines show criteria for inclusion (amplitude cutoff violations < 10%, refractory period violations < 5%). **D.** As in **C.** for all clusters in sessions with simultaneous sniff recording.

Figure 4 - Figure supplement 1

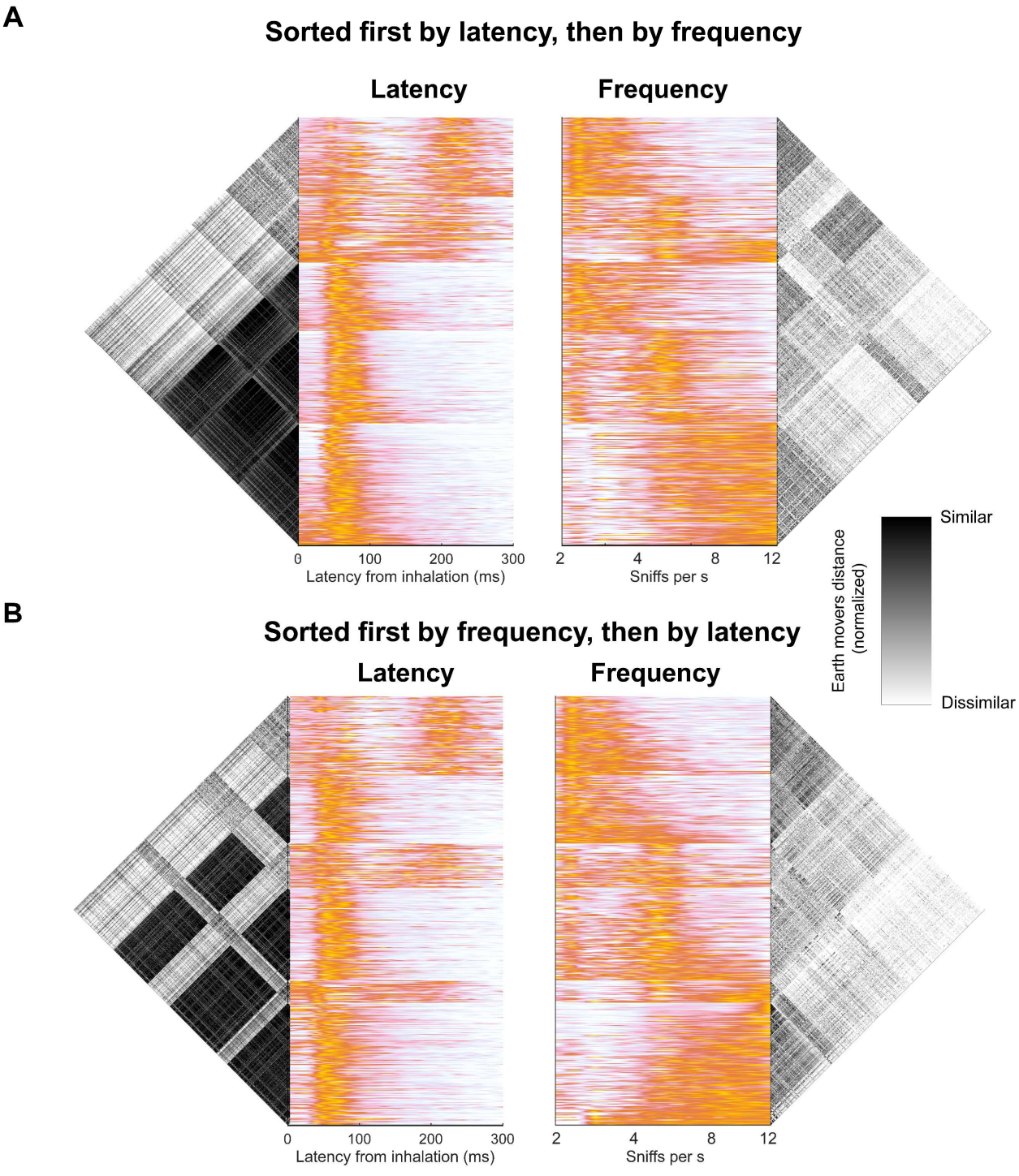

Figure 4 - Figure supplement 1: Overlap between sniff latency and frequency clusters. A. (Left) SnF latency profiles of all units sorted by latency (Right) SnF frequency profiles separately clustered within latency clusters show a diversity of frequency profiles exist within each functional latency cluster. Earthmovers distance matrices show clustered structure of profiles. **B.** As above, but sorted first by SnF frequency then latency clustered within frequency clusters.

Figure 8 - Figure supplement 1

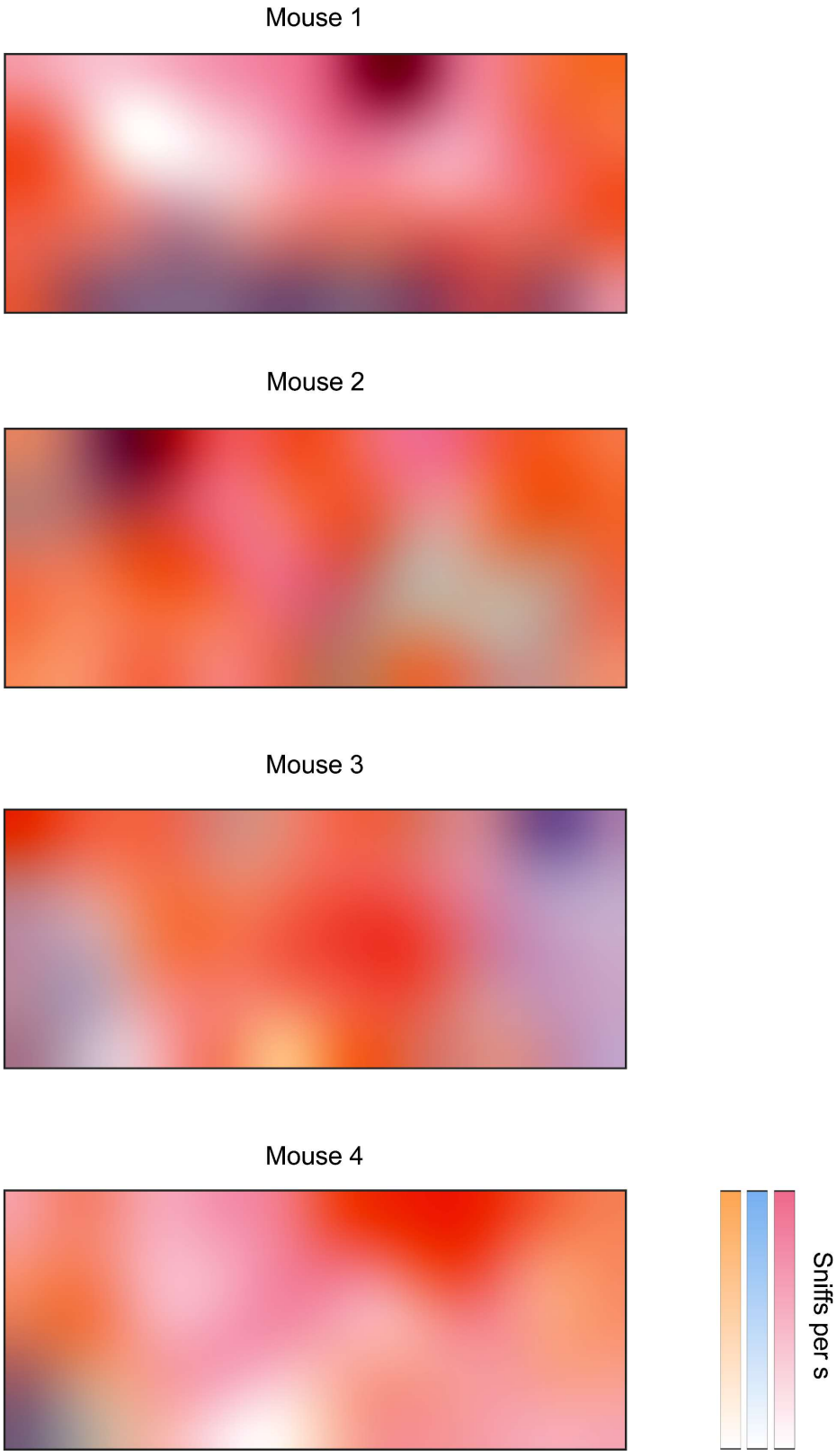

Figure 8 – Figure supplement 1: Spatial distribution of behavioral state usage. The spatial distribution of behavioral state usage for each OB mouse. Colormap overlays the usage of each state, normalized by sniffs, into a composite color as in Figure 1 (Figure 1 – Supplemental video 2).

Figure 1 - Supplemental Video 1: Visualizing and sonifying neurodata (ViSoND) from a representative recording session. To provide an observable demonstration of neural recordings during freely moving behavior, we developed a tool called ViSoND, in which sniff and spike events are rendered to MIDI notes, so that different events can be identified by different sounds. The top panel shows video of the mouse, the center panel shows the synchronous raw thermistor signal, colored according to the current behavioral HMM state, and the bottom panel animates a population raster that is also synchronous with the behavior video. Inhalation times are indicated visually by peaks in the thermistor signal and sonically by occurrences of a kick drum sample. Visually, spikes from each unit are indicated by marks on each row of the raster plot. Sonically, spikes from each unit are mapped to a different note of a virtual piano.
Accessible
at https://www.dropbox.com/scl/fi/2kae0qnftw052e9gcn7ig/Sniff_OB_ViSoND.mp4?rlkey=cq926o6ntazlw4oq4dzguwju0&dl=0

Figure 1 - Supplemental Video 2: 3D color map visualization for distribution-weighted color mixing. In order to indicate the distributions for three populations, defined by our behavioral states, we developed distribution-weighted color mixing. Here, each state is identified by a basis color from Riley (1990), and multiplied with the distribution of sniffs for a given set of parameters. Colors range from white to full color for a given state, and overlap is indicated by darkening. This color scheme can be conceptualized as a cube, with the three axes defined by the three states (“Explore”, “Groom”, and “Rest”) and represented by their respective basis colors. Video animates sections from this cube along each of the three axes, where each subplot indicates sections taken from a different angle. Accessible at https://www.dropbox.com/scl/fi/qofn0fh593xjy2myqspwa/Figure-1-Extended-video-2.mp4?rlkey=n3w9g7q0w18h81ftxgb64g7br&dl=0

Recurrent neural networks balance sensory- and memory-guided policies for spatial foraging.

Scott C. Sterrett[1], David H. Gire[2], Adrienne L. Fairhall[1]

[1] *Department of Neurobiology & Biophysics, University of Washington, Seattle, Washington, United States*

[2] *Department of Psychology, University of Washington, Seattle, Washington, United States*

Abstract

Animal foraging relies on spatial navigation under uncertainty; searchers can use sensory information to explore for new rewarding patches or use spatial memory to exploit previous reward patches. How do neural systems balance search strategies in the face of uncertainty in the environment? *Deep reinforcement learning* (RL) combines the powerful function approximation of neural networks with traditional reinforcement learning to find optimal policies in complex environments and tasks. We train recurrent actor-critic networks using meta-RL to solve a 2D spatial foraging task. We show that network training constructs population dynamics which carry out inference within a trial to perform adaptive strategies that maximize reward. The population dynamics execute single-episode switching between sensory-guided exploration and memory-guided exploitation strategies. Additionally, agents learn efficient strategies to navigate non-stationary reward distributions. These representations correlate with belief-state inference, which emerges from a model-free learning algorithm. The representational geometry of these solutions provide hypotheses for the dynamics underlying adaptive, continuous spatial decision-making strategies in neural systems.

Introduction

Foraging relies on spatial navigation under uncertainty of exploiting remembered reward locations and exploring new rewarded locations. Exploiting remembered reward locations relies on spatial memory systems such as the hippocampus and entorhinal cortex, which have been shown to construct internal models of the world. Exploring for new rewarded locations relies more on sensory cues and sensorimotor search strategies, like gradient climbing or surge-cast. How do spatial memory and sensory cues dynamically inform exploration-exploitation tradeoffs in goal-directed olfactory navigation in unpredictable environments?

The olfactory system is bidirectionally coupled with spatial memory systems like hippocampus and entorhinal cortex, anatomically, functionally, and evolutionarily. Olfactory cues are useful for hippocampal-entorhinal circuits constructing cognitive maps and these maps in turn modulate representations of cues in olfactory areas.

Goal-directed spatial navigation requires representations of goals and the intermediate landscape in order plan and execute routes from the current location to the goal (Nyberg et al., 2022; Pfeiffer & Foster, 2013). Representations of goals influence entorhinal maps (Boccara et al., 2019; Butler et al., 2019). Rodents represent multiple aspects of their environment in order to adaptively plan routes to resources and avoid predators (Byers et al., 2019; Jackson et al., 2020). Sequential, egocentric navigation, like gradient-climbing, requires less representational load, but is less robust.

There are multiple sources of information present in odor plumes which characteristically vary relative to the source which could be used to associate odor inputs with spatial information (Boie et al., 2018; Crimaldi & Koseff, 2001; Demir et al., 2020; Rigolli, Magnoli, et al., 2021). Navigation can also be multisensory, with visual and wind cues in particular being used in conjunction with odor cues to guide strategies like cast and surge (Álvarez-Salvado et al., 2018; Balkovsky & Shraiman, 2002; Kennedy & Marsh, 1974; Ouyang et al., 2024; van Breugel & Dickinson, 2014). Each model captures some aspects of animal behavior but making comparisons across models demonstrates that no model captures all aspects of behavior (Pang et al., 2018). Reinforcement learning models have captured various aspects of search behaviors: cast-surge, head-casting, alternation (Loisy & Eloy, 2022; Rando et al., 2024; Rigolli, Reddy, et al., 2021; Singh et al., 2023). What many sensorimotor algorithms cannot capture is that when rodents gain knowledge about the spatial distribution of sources, they often switch from sensory-guided strategies to spatial-memory guided strategies (Gire et al., 2016; Jackson et al., 2020). Often models ignore the embodied respiratory dynamics (Severino & Barwich, 2024). Toroidal structure for mapping two-dimensional space (Gardner et al., 2022; Giocomo et al., 2011; Guanella et al., 2007; Wen et al., 2024). Continuous attractor networks for navigation (Mcnaughton et al., 1989; McNAUGHTON et al., 1996; McNaughton et al., 2006).

Artificial neural networks (ANNs) have been trained to solve a variety of challenging navigation problems (Banino et al., 2018; Miconi et al., 2018; Zintgraf et al., n.d.). These networks can be used as fully observable models to be reverse engineered in search of mechanistic hypotheses for how neural systems might solve these challenging computations (Burak & Fiete, 2009; El-Gaby et al., 2024; Fang & Stachenfeld, 2023; Foster et al., 2000; Nakahara & Doya, n.d.; Pedamonti et al., 2023; Sorscher et al., 2023; Voigts et al., 2022; Whittington et al., 2020).

Task trained neural networks are a useful paradigm for computational and systems neuroscience as they provide fully observable models of neural circuits for complex behaviors (Driscoll et al., 2022; Fetz, 1994; Sussillo et al., 2015; Yamins & DiCarlo, 2016). Deep reinforcement learning has recently emerged to combine the powerful function approximation of neural networks with traditional reinforcement learning to find optimal policies in complex environments and tasks (Botvinick et al., 2020).

Meta-learning is a common approach to solving the exploration-exploitation trade off (Beck et al., 2023; Wang et al., 2017). Trained neural networks can be reverse engineered to unravel the dynamics that support behavior. What representations are learned that allow for the hidden population dynamics to carry out the inference task?

What are belief states? In the case where an agent receives ambiguous observations, that is observations that do not directly correspond with a specific state, it becomes impractical to use a policy which defines a transformation from observations to actions. In this scenario, often formalized mathematically as a partially observable markov decision process (POMDP), it is advantageous to construct a belief about the current state from the ambiguous observations, termed a *belief state*. Belief states are often defined as a probability distribution over possible states (Funamizu et al., 2016). A policy can then be used to map these belief states to actions (Babayan et al., 2018; Dayan & Daw, 2008; Kaelbling et al., 1998; Rao, 2010).. Belief states in deep reinforcement learning (Alver & Precup, 2021; Beck et al., 2023; Hennig et al., 2023).

We take a normative approach to this question by leveraging recent theoretical work in Deep Meta Reinforcement Learning (meta-RL) to train recurrent neural networks (RNNs) to perform a simulated task that requires a dynamic tradeoff between sensory guided exploration and spatial memory guided exploitation strategies. Across training, RNN agents must learn a meta-strategy of exploration for new rewarded locations informed by sensory-guided search as well as exploitation of remembered reward locations and deploy this meta-strategy to novel task iterations. We find that RNN agents learn a flexible, but structured representation of task information that allows them to quickly discover new reward locations and efficiently exploit this information in subsequent episodes. We find that local “odor” cues modify exploration strategies and are not necessary for exploitation of remembered rewards.

Results

We developed a simulated foraging task in a 2D grid world (arena). The arena has open squares and walls, as well as closed boundaries. Agents do not receive global position information. Local 3x3 wall inputs can be ambiguous, which requires agents to integrate inputs and actions in order to localize their position in the arena. Agents receive a positive reward each time they enter a hidden reward state. In a given trial, agents start in a center square and must explore the arena to find a single, hidden reward square. In the stationary task, this reward square will remain fixed for the duration of the trial. In the non-stationary condition, this reward square can change between episodes within a trial. Once an agent finds a reward, the episode ends and they are teleported to a

random open square to start the next episode. A trial lasts 100 timesteps and can contain multiple episodes.

We use an actor critic recurrent neural network. Inputs are delivered to a recurrent neural network which has two readout layers: an actor arm which produces a distribution over possible actions, and a critic layer which produces a scalar-estimate of the value. We use a gated recurrent unit in the RNN. We enforce weight and activity penalties to encourage simple solutions. We use the advantage actor critic (A2C) loss as well as an entropy bonus to encourage exploration during training.

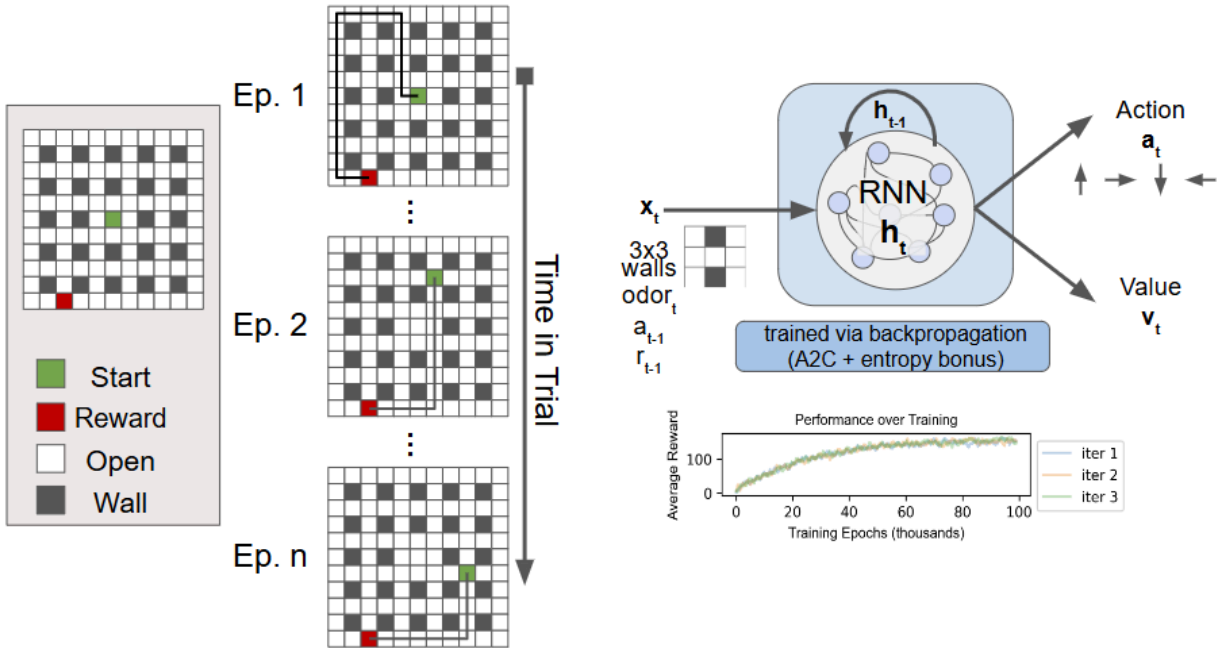

Figure 1: Dynamic spatial foraging task and deep meta-reinforcement learning agents. (A) Agents move throughout a bounded two dimensional grid world arena with internal walls to find a hidden reward location. A trial, which contains multiple episodes, starts with the agent at a central start square. Agents can navigate the arena until they enter the hidden reward square, where they receive a positive reward, are teleported to a new location to start the next episodes. Episodes repeat until the trial times out. Hidden reward states can be fixed for the duration of the trial ("stationary") or change across episodes ("non-stationary"). Reward states can also have local "odor" cues which provide local information about reward location. **(B)** Recurrent neural network (RNN) architecture which controls agents. Inputs include the local, 3x3 wall structure, "odor" cues, the previous action and reward. A recurrent layer of gated-recurrent units receives inputs and provides outputs to an actor and critic arm. All weights are trained via backpropagation using the advantage actor critic (A2C) loss. **(C)** Three representative training curves for the stationary task show reliable learning of the task.

During training, agents are teleported to random locations in the arena. When trained on a simpler task where agents are teleported only to the start square, agents perform worse on the test task. The random teleportation requires agents to construct multiple paths to the same goal, thus learning a more robust representation of the rewarded location. This is a central principle in cognitive map representations for goal-directed navigation. After training, all weights are frozen, which requires all inference within a trial to be performed by the hidden dynamics in the network.

In the stationary task, the optimal policy is to efficiently explore the arena, which is most efficiently done by a spiral trajectory (Hayes et al., 2002; Singh et al., 2023; Zintgraf et al., n.d.). How do agents learn the structure of a 2D environment and plan optimal routes within that environment? In our task, agents do not receive explicit spatial location information and must integrate noisy, possible ambiguous inputs about the local environment to perform this computation.

Once the reward square has been found, agents should repeat the shortest possible trajectory back to the reward square for the remainder of the episode. This is what we find agents do. This is intriguing as the shortest possible path is not the same as the one that was performed during exploration, which suggests model-based behavior, which has emerged from the model-free learning algorithm (Alver & Precup, 2021). We can quantify this trade-off by looking at the ratio of the initial episode length and the subsequent episode lengths. Across the population this is much less than one and significantly lower than in random networks. Vanilla-RNNs seem capable of efficient exploration but are unable to efficiently use in-trial adaptation (plot episode 1 vanilla rnn vs gru and episode 2-N for vanilla rnn vs gru).

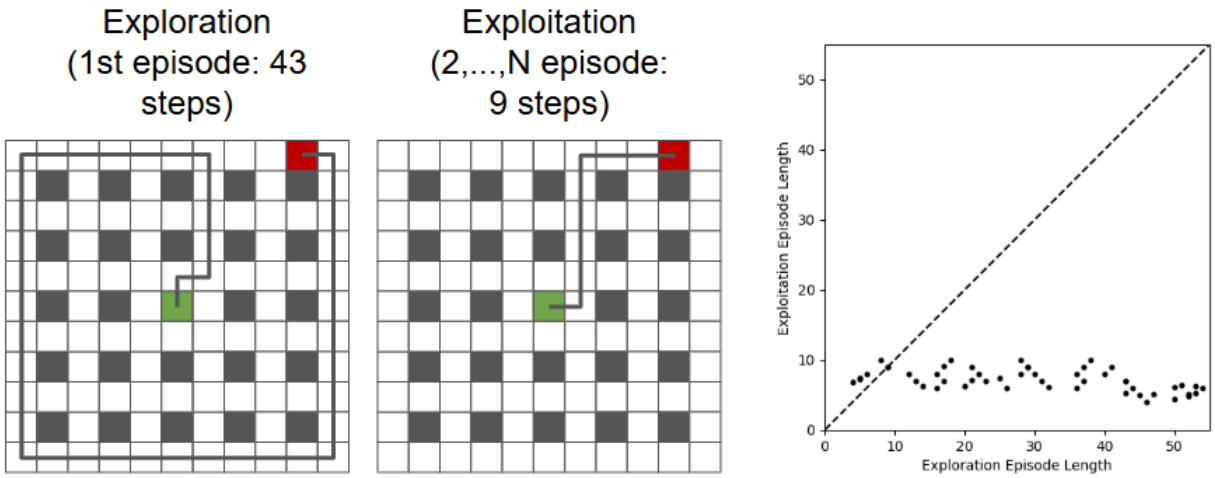

Figure 2: Efficient inference and exploitation of within-task information. (A) A representative trajectory for the first episode “explore” where agents must explore the arena to discover which state is the hidden reward state in this trial. (B) A representative trajectory for

subsequent episodes (“exploit”) where agents use the within-trial information to take shorter trajectories back to the reward state. (C) The ratio of the length of the first episode to the average of all subsequent episodes, a metric to quantify the agent’s have learned to take shorter paths after inferring within trial information in episode 1.

We next take advantage of the fully observed, trained networks to analyze the representations learned to perform the task. A simple approach is to ask if we can decode the reward location within a trial from the hidden activities of the RNN. We hypothesize that this decoding should be no better than chance during episode 1 and significantly higher during all subsequent episodes. We generate 1000 example trials and construct a training set from 70% of these trials and test on a heldout 30%. We find that decoding performance is non better than chance during exploration and significantly better during exploitation than during exploration.

We look at single trial decoder performance to gain an intuition about the form of these representations of space. We exploit the logistic decoder outputs to look at the outputed probability of reward across each timestep in a trial. We find an initially uniform prior over the gridworld, which is updated to sequentially remove unrewarded sites, and ultimately maximally predict the rewarded square, which is stable across subsequent episodes. This representation is akin to an optimal belief-state. We can test this intuition by correlating hidden activity with an optimal belief state using linear regression in probe experiments where there is no reward square and find that R2=0.59.

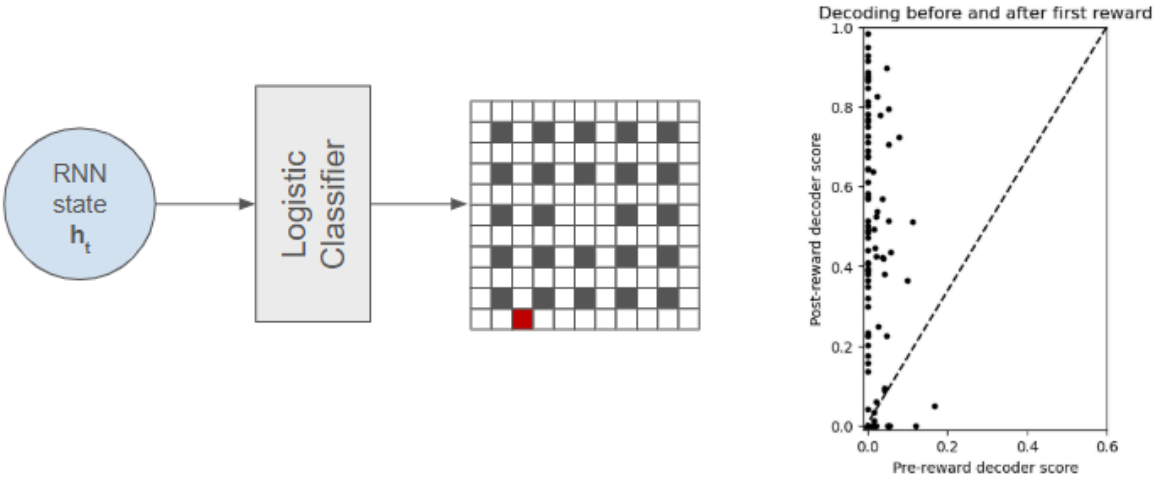

Figure 3: RNN hidden states are approximate belief states of reward information. (A) Logistic decoder accuracy scores for multiple trials, separated into scores during the first episode, explore accuracy, and scores during subsequent episodes, exploit accuracy. Exploit accuracy is significantly higher, demonstrating that networks gain decodable information about reward location only after the first episode. **(B)** An optimal belief model for reward location, demonstrated in a representative trial. As agents visit unrewarded states, they are removed

from the belief, until eventually the reward state is found and the belief collapses to a single state. **(C)** Logistic decoder outputs for an example trial show RNN hidden states approximate an optimal belief (R2=0.59).

To further examine the representations learned to perform this task, we explored the state-space of activity during trials. By visualizing the principal components of RNN hidden units during trials, we find that networks learn to separate exploration and exploitation policies in state space, but reuse a spiral map of 2D space to encode reward locations across an entire trial.

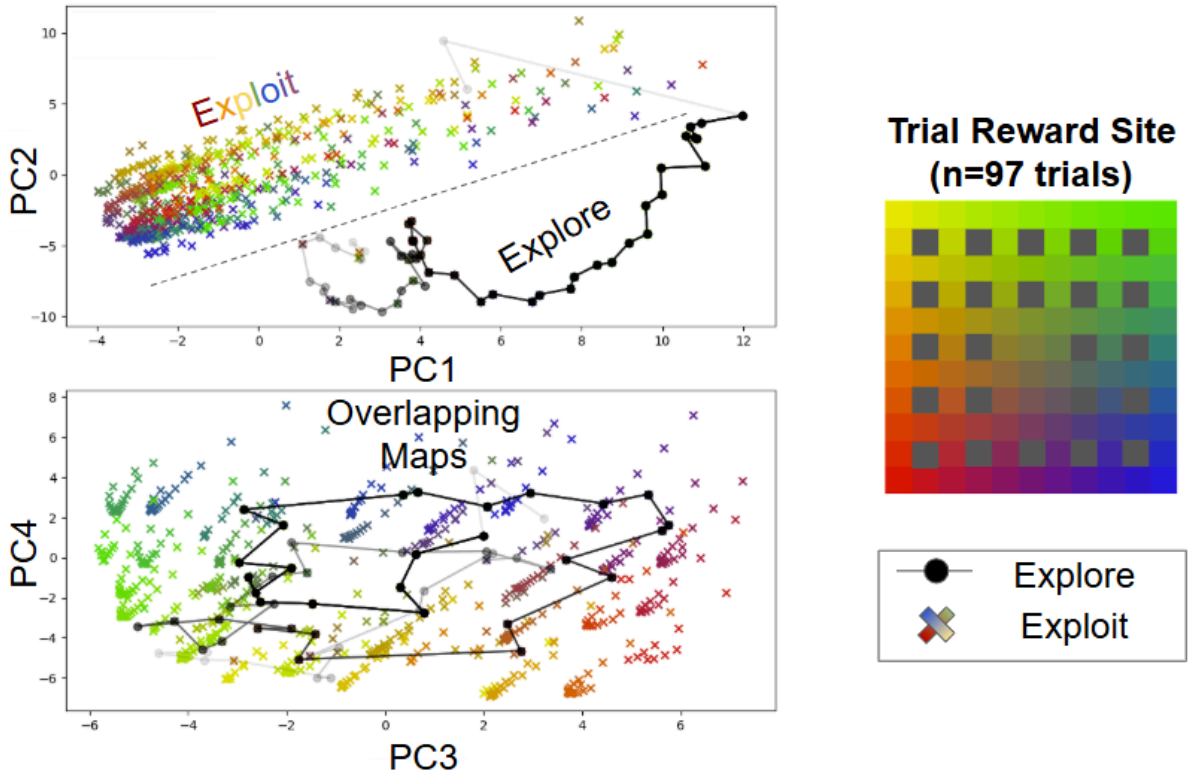

Figure 4: Hidden dynamics support within trial inference and adaptive explore-exploit policies. (A) The first two principal components of network dynamics separate exploration and exploitation policies. Black shows overlapping exploration hidden state trajectories for all 40 possible trial types (colored according to the colormap *right*). Colored crosses are the hidden state at the start of all exploitation episodes. (B) The third and fourth principal components reveal the network constructs a map of reward sites which maintains allocentric spatial relationships, which is reused in both exploration and exploitation.

Odor cues impact exploration strategies

To examine how local sensory gradients inform foraging strategies, we implement a version of the task where agents receive a scalar input that is proportional to the distance to target, within a truncated distance.This changes exploration behavior as the

most efficient trajectory now only needs to traverse the region of the gridworld that would place the agent within the detectable range of local-gradients. Indeed, we find agents now only explore a reduced radius of the arena. We find that agents can find an initial reward site significantly faster than when there are no odor cues present; agents use local cues about reward to perform more efficient exploration.

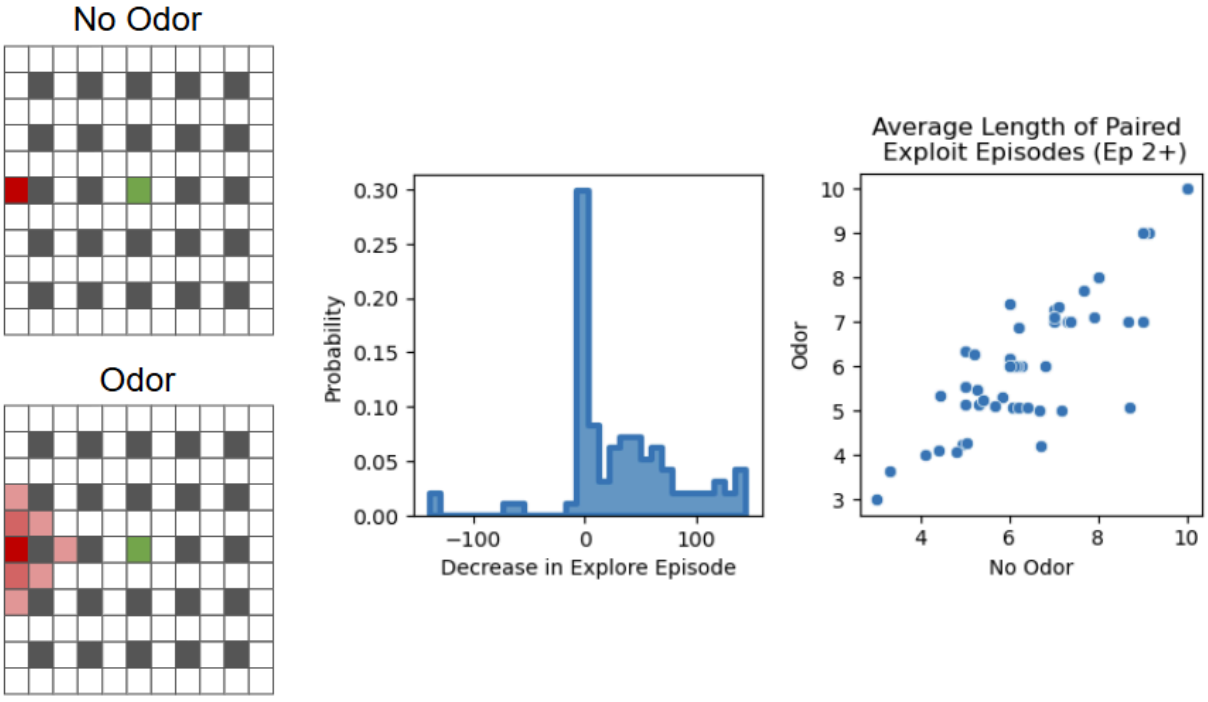

Figure 5: Odor inputs improve exploration, but not exploitation behaviors. (A) distribution of first episode length, a measure of how quickly agents find the reward on the first trial for networks trained with no odor cues or odor cues **(B)** Difference in first episode length between odor/no-odor agents for pairs of trials with the same reward location. Positive values mean no odor agents had a longer episode. **(C)** Change in number of rewards found (in progress) representative odor trajectories compared with no-odor trials. Supplement:[Anosmia exploration video]

Additionally, we performed ‘anosmia’ perturbation experiments where we removed odor inputs during testing on agents that had received odor inputs during training. We find that agents' exploration is greatly impacted, but can often still perform shorter trajectories back to reward locations, suggesting exploitation strategies are orthogonalized from exploration policies.

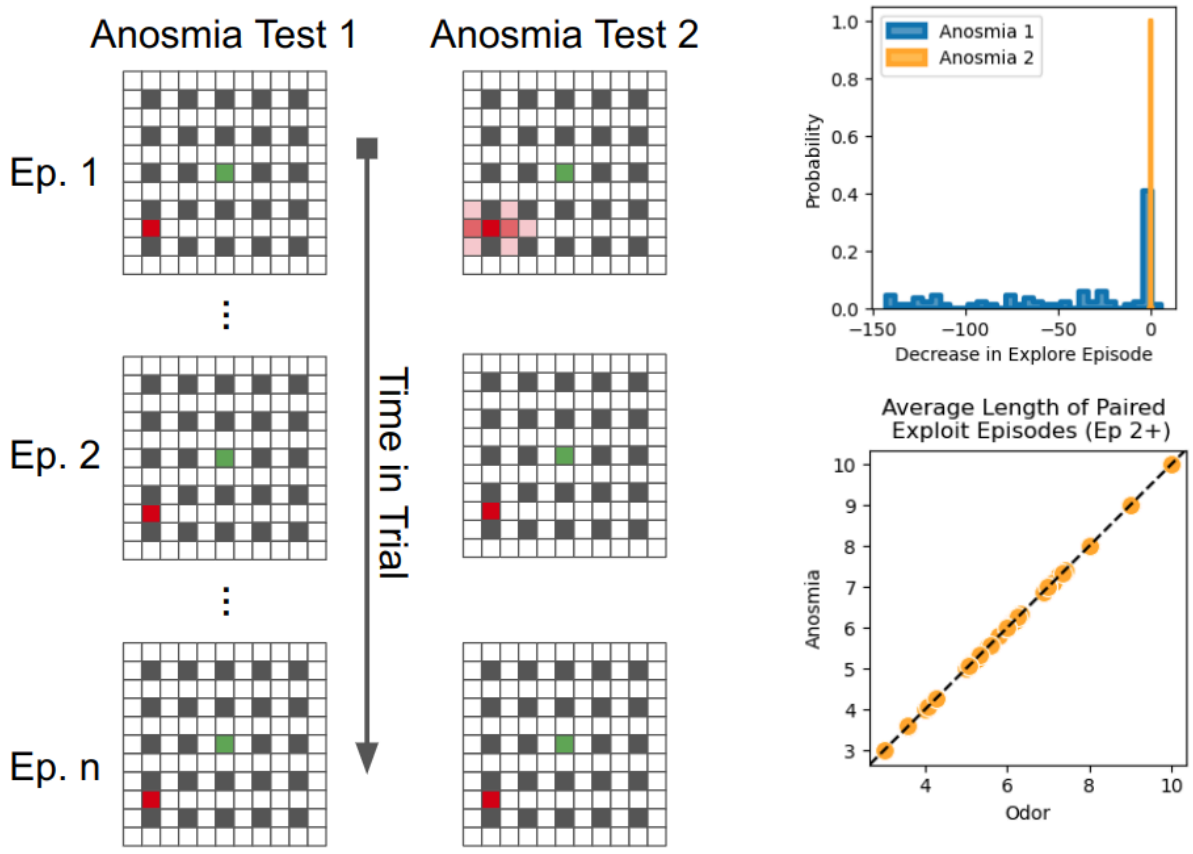

Figure 6: Ablating odor inputs impairs exploration but not exploitation

Discussion

We cast the problem of olfactory navigation as a meta-learning problem where exploration is driven by sensory cues and exploitation is facilitated by spatial memory. We find that RNNs can learn the task via deep meta-reinforcement learning. Odor cues are key to exploration strategies but not essential for exploitation strategies. Network dynamics construct belief-like states of task information, which are orthogonalized across exploration-exploitation, but shared in 2D grid space. This allows for behavior which is both efficient and flexible.

Methods

Deep Meta Reinforcement Learning

Meta reinforcement learning describes the class of machine learning algorithms which learn how to reinforcement learn. That is, they are a subset of meta-learning, or learning to learn, that deals with normative models of learning to maximize rewards (Beck et al., 2023). Reinforcement learning is a process of learning how to act within a given environment to maximize rewards

More formally, RL algorithms learn a policy which maps states, or observations, to actions which maximizes the expected reward with an environment, often a Markov decision process (MDP). MDP is defined by a tuple $\langle S, A, P, P_0, R, \gamma, T \rangle, where S$ is the set of states, A is the set of actions, $P(s_{t+1}|s_t, a_t) : S \times A \times S \rightarrow R+$ is the probability of transitioning from state s_t to state s_{t+1} after taking action a_t, $P_0(s_0) : S \rightarrow R^+$ is a distribution over initial states, $R(s_t, a_t) : S \times A \rightarrow R$ is a reward function, $\gamma \in [0, 1]$ is a discount factor, and T is the horizon

A policy maps states to action probabilities $\pi(a|s) : S \times A \rightarrow R^+$. Through the interaction of the policy and the MDP, we can describe the distribution of trajectories as:

$$P(\tau) = P_0(s_0) \prod_{t=0}^{T} \pi(a_t|s_t) P(s_{t+1}|s_t, a_t)$$

The policy will learn to maximize the expected reward:

$$J(\pi) = E_{\tau \sim P(\tau)} \left[\sum_{t=0}^{T} \gamma^t r_t \right]$$

Over a series of episodes of length H, we collect multiple trajectories $\mathcal{D} = {\tau^h}_{h=0}^{H}$. Therefore, we define an RL algorithm as the function:

$$f(\mathcal{D}) : ((S \times A \times R)^T)^H \rightarrow \Phi$$

We will learn this function f through a meta-training framework. Meta-training relies on a set of tasks, or MDPs, which are drawn from a distribution of tasks $p(M)$. This distribution will contain a shared set of states and actions, but contain different reward and state-transition functions. In our case, we will parameterize this function with a Recurrent Neural Network (RNN). An important distinction between Deep RL and Deep Meta-RL

is that RNNs receive states as inputs as well as previous actions and rewards, which allows them to learn an adaptive policy.
In our study, we will define a set of partially observable MDPs, called $p(M)$, which arise from a shared grid-world environment. The observations o are the set of: 3x3 binary wall structure, olfactory cue [0,1], r_{t-1}, a_{t-1} - up, down, left, right Reward functions will contain a single rewarded state at any given time t, which is hidden from the agent, and returns a reward of +R when the agent enters the state. In the course of an episode, the reward location may change, that is to say it can be non-stationary. The state transition function is defined such that agents have deterministic transitions in the grid-world environment, except in the special case where an agent moves to a rewarded state, which causes a transition to the teleported state. Episodes are 150 timesteps in duration.
Networks
We use actor-critic RNNs, a popular architecture in deep RL which uses neural networks to simultaneously approximate both a policy and value function. An RNN contains a set of hidden units h, a linear input layer, and two linear output layers, an actor arm and a value arm. All the weights and biases are initialized from $U(-k, k)$ where $k = \frac{1}{hiddensize}$. Weights are updated using Adam. Networks are trained over 200k iterations of 30 batched trials using the Advanced Actor Critic (A2C) algorithm.
Advantage Actor Critic
Advantage Actor Critic (A2C) is an asynchronous, deterministic policy gradient algorithm for deep RL (Mnih et al., 2016). A2C calculates an advantage function

$$A(s, a) = r + \gamma * V(s') - V(s)$$

We also use an entropy bonus, which encourages exploration by encouraging entropy in the action distributions.

References

Álvarez-Salvado, E., Licata, A. M., Connor, E. G., McHugh, M. K., King, B. M., Stavropoulos, N., Victor, J. D., Crimaldi, J. P., & Nagel, K. I. (2018). Elementary sensory-motor transformations underlying olfactory navigation in walking fruit-flies. *eLife*, *7*, e37815. https://doi.org/10.7554/eLife.37815

Alver, S., & Precup, D. (2021). *What is Going on Inside Recurrent Meta Reinforcement Learning Agents?* (arXiv:2104.14644). arXiv. https://doi.org/10.48550/arXiv.2104.14644

Babayan, B. M., Uchida, N., & Gershman, S. J. (2018). Belief state representation in the dopamine system. *Nature Communications*, *9*(1), 1891. https://doi.org/10.1038/s41467-018-04397-0

Balkovsky, E., & Shraiman, B. I. (2002). Olfactory search at high Reynolds number. *Proceedings of the National Academy of Sciences of the United States of America*, *99*(20), 12589–12593. https://doi.org/10.1073/pnas.192393499

Banino, A., Barry, C., Uria, B., Blundell, C., Lillicrap, T., Mirowski, P., Pritzel, A., Chadwick, M. J., Degris, T., Modayil, J., Wayne, G., Soyer, H., Viola, F., Zhang, B., Goroshin, R., Rabinowitz, N., Pascanu, R., Beattie, C., Petersen, S., … Kumaran, D. (2018). Vector-based navigation using grid-like representations in artificial agents. *Nature*, *557*(7705), 429–433. https://doi.org/10.1038/s41586-018-0102-6

Beck, J., Vuorio, R., Liu, E. Z., Xiong, Z., Zintgraf, L., Finn, C., & Whiteson, S. (2023). *A Survey of Meta-Reinforcement Learning* (arXiv:2301.08028). arXiv. http://arxiv.org/abs/2301.08028

Boccara, C. N., Nardin, M., Stella, F., O'Neill, J., & Csicsvari, J. (2019). The entorhinal cognitive map is attracted to goals. *Science*, *363*(6434), 1443–1447. https://doi.org/10.1126/science.aav4837

Boie, S. D., Connor, E. G., McHugh, M., Nagel, K. I., Ermentrout, G. B., Crimaldi, J. P., & Victor, J. D. (2018). Information-theoretic analysis of realistic odor plumes: What cues are useful for determining location? *PLOS Computational Biology*, *14*(7), e1006275. https://doi.org/10.1371/journal.pcbi.1006275

Botvinick, M., Wang, J. X., Dabney, W., Miller, K. J., & Kurth-Nelson, Z. (2020). Deep Reinforcement Learning and its Neuroscientific Implications. *arXiv:2007.03750 [Cs, q-Bio]*. http://arxiv.org/abs/2007.03750

Burak, Y., & Fiete, I. R. (2009). Accurate Path Integration in Continuous Attractor Network Models of Grid Cells. *PLOS Computational Biology*, *5*(2), e1000291. https://doi.org/10.1371/journal.pcbi.1000291

Butler, W. N., Hardcastle, K., & Giocomo, L. M. (2019). Remembered reward locations restructure entorhinal spatial maps. *Science*, *363*(6434), 1447–1452. https://doi.org/10.1126/science.aav5297

Byers, K. A., Lee, M. J., Patrick, D. M., & Himsworth, C. G. (2019). Rats About Town: A Systematic Review of Rat Movement in Urban Ecosystems. *Frontiers in Ecology and Evolution*, *7*. https://doi.org/10.3389/fevo.2019.00013

Crimaldi, J. P., & Koseff, J. R. (2001). High-resolution measurements of the spatial and temporal scalar structure of a turbulent plume. *Experiments in Fluids*, *31*(1), 90–102. https://doi.org/10.1007/s003480000263

Dayan, P., & Daw, N. D. (2008). Decision theory, reinforcement learning, and the brain. *Cognitive, Affective, & Behavioral Neuroscience*, *8*(4), 429–453. https://doi.org/10.3758/CABN.8.4.429

Demir, M., Kadakia, N., Anderson, H. D., Clark, D. A., & Emonet, T. (2020). *Walking Drosophila navigate complex plumes using stochastic decisions biased by the timing of odor encounters* [Preprint]. Neuroscience. https://doi.org/10.1101/2020.03.23.004218

Driscoll, L., Shenoy, K., & Sussillo, D. (2022). *Flexible multitask computation in recurrent networks utilizes shared dynamical motifs* (p. 2022.08.15.503870). bioRxiv. https://doi.org/10.1101/2022.08.15.503870

El-Gaby, M., Harris, A. L., Whittington, J. C. R., Dorrell, W., Bhomick, A., Walton, M. E., Akam, T., & Behrens, T. E. J. (2024). A cellular basis for mapping behavioural structure. *Nature*, 1–10. https://doi.org/10.1038/s41586-024-08145-x

Fang, C., & Stachenfeld, K. (2023, October 13). *Predictive auxiliary objectives in deep RL mimic learning in the brain*. The Twelfth International Conference on Learning Representations. https://openreview.net/forum?id=agPpmEgf8C

Fetz, E. E. (1994). Are movement parameters recognizably coded in the activity of single neurons? In P. Cordo & S. Harnad (Eds.), *Movement Control* (1st ed., pp. 77–88). Cambridge University Press. https://doi.org/10.1017/CBO9780511529788.008

Foster, D. j., Morris, R. g. m., & Dayan, P. (2000). A model of hippocampally dependent navigation, using the temporal difference learning rule. *Hippocampus*, *10*(1), 1–16. https://doi.org/10.1002/(SICI)1098-1063(2000)10:1<1::AID-HIPO1>3.0.CO;2-1

Funamizu, A., Kuhn, B., & Doya, K. (2016). Neural substrate of dynamic Bayesian inference in the cerebral cortex. *Nature Neuroscience*, *19*(12), 1682–1689. https://doi.org/10.1038/nn.4390

Gardner, R. J., Hermansen, E., Pachitariu, M., Burak, Y., Baas, N. A., Dunn, B. A., Moser, M.-B., & Moser, E. I. (2022). Toroidal topology of population activity in grid cells. *Nature*, *602*(7895), 123–128. https://doi.org/10.1038/s41586-021-04268-7

Giocomo, L. M., Moser, M.-B., & Moser, E. I. (2011). Computational Models of Grid Cells. *Neuron*, *71*(4), 589–603. https://doi.org/10.1016/j.neuron.2011.07.023

Gire, D. H., Kapoor, V., Arrighi-Allisan, A., Seminara, A., & Murthy, V. N. (2016). Mice Develop Efficient Strategies for Foraging and Navigation Using Complex Natural Stimuli. *Current Biology*, *26*(10), 1261–1273. https://doi.org/10.1016/j.cub.2016.03.040

Guanella, A., Kiper, D., & Verschure, P. (2007). A model of grid cells based on a twisted torus topology. *International Journal of Neural Systems*, *17*(4), 231–240. https://doi.org/10.1142/S0129065707001093

Hayes, A. T., Martinoli, A., & Goodman, R. M. (2002). Distributed odor source localization. *IEEE Sensors Journal*, *2*(3), 260–271. https://doi.org/10.1109/JSEN.2002.800682

Hennig, J. A., Pinto, S. A. R., Yamaguchi, T., Linderman, S. W., Uchida, N., & Gershman, S. J. (2023). *Emergence of belief-like representations through reinforcement learning* (p. 2023.04.04.535512). bioRxiv. https://doi.org/10.1101/2023.04.04.535512

Jackson, B. J., Fatima, G. L., Oh, S., & Gire, D. H. (2020). Many Paths to the Same Goal: Balancing Exploration and Exploitation during Probabilistic Route Planning. *eNeuro*, *7*(3). https://doi.org/10.1523/ENEURO.0536-19.2020

Kaelbling, L. P., Littman, M. L., & Cassandra, A. R. (1998). Planning and acting in partially

observable stochastic domains. *Artificial Intelligence*, *101*(1), 99–134. https://doi.org/10.1016/S0004-3702(98)00023-X

Kennedy, J. S., & Marsh, D. (1974). Pheromone-Regulated Anemotaxis in Flying Moths. *Science*, *184*(4140), 999–1001. https://doi.org/10.1126/science.184.4140.999

Loisy, A., & Eloy, C. (2022). Searching for a source without gradients: How good is infotaxis and how to beat it. *Proceedings of the Royal Society A: Mathematical, Physical and Engineering Sciences*, *478*(2262), 20220118. https://doi.org/10.1098/rspa.2022.0118

McNAUGHTON, B. L., Barnes, C. A., Gerrard, J. L., Gothard, K., Jung, M. W., Knierim, J. J., Kudrimoti, H., Qin, Y., Skaggs, W. E., Suster, M., & Weaver, K. L. (1996). Deciphering The Hippocampal Polyglot: The Hippocampus as a Path Integration System. *Journal of Experimental Biology*, *199*(1), 173–185. https://doi.org/10.1242/jeb.199.1.173

McNaughton, B. L., Battaglia, F. P., Jensen, O., Moser, E. I., & Moser, M.-B. (2006). Path integration and the neural basis of the “cognitive map.” *Nature Reviews Neuroscience*, *7*(8), 663–678. https://doi.org/10.1038/nrn1932

Mcnaughton, B. L., Leonard, B., & Chen, L. (1989). Cortical-hippocampal interactions and cognitive mapping: A hypothesis based on reintegration of the parietal and inferotemporal pathways for visual processing. *Psychobiology*, *17*(3), 230–235. https://doi.org/10.1007/BF03337774

Miconi, T., Stanley, K., & Clune, J. (2018). Differentiable plasticity: Training plastic neural networks with backpropagation. *Proceedings of the 35th International Conference on Machine Learning*, 3559–3568. https://proceedings.mlr.press/v80/miconi18a.html

Mnih, V., Badia, A. P., Mirza, M., Graves, A., Lillicrap, T. P., Harley, T., Silver, D., & Kavukcuoglu, K. (2016). *Asynchronous Methods for Deep Reinforcement Learning* (arXiv:1602.01783). arXiv. https://doi.org/10.48550/arXiv.1602.01783

Nakahara, H., & Doya, K. (n.d.). *Dynamics of Attention as Near Saddle-Node Bifurcation Behavior*.

Nyberg, N., Duvelle, É., Barry, C., & Spiers, H. J. (2022). Spatial goal coding in the hippocampal formation. *Neuron*, *110*(3), 394–422. https://doi.org/10.1016/j.neuron.2021.12.012

Ouyang, B., True, A. C., Crimaldi, J. P., & Ermentrout, B. (2024). Simple olfactory navigation in air and water. *Journal of Theoretical Biology*, *595*, 111941. https://doi.org/10.1016/j.jtbi.2024.111941

Pang, R., Breugel, F. van, Dickinson, M., Riffell, J. A., & Fairhall, A. (2018). History dependence in insect flight decisions during odor tracking. *PLOS Computational Biology*, *14*(2), e1005969. https://doi.org/10.1371/journal.pcbi.1005969

Pedamonti, D., Mohinta, S., Dimitrov, M. V., Malagon-Vina, H., Ciocchi, S., & Costa, R. P.

Chapter 4: Computational Ethology

Abstract

Modern systems neuroscience is incorporating increasingly more complex behavioral experiments in large part due to technological advances in the field of computational ethology. This field uses advances in machine learning to track animal behavior from video and automatically segment behavior into time-varying descriptions, called ethograms. These methods allow experimenters to quantify behavior at increasingly precise spatiotemporal scales, which allow the field to understand the neural control of behavior. This chapter contains vignettes from multiple projects where I applied tools from computational ethology in collaboration with experimentalists. I have extracted figures and methods I contributed to convey key concepts of the ways computational ethology can be used, but the full texts of each paper can be found at the DOI in each section.

Introduction

An essential problem in the study of behavior, ethology, is the construction of an ethogram. Ethograms define the set of discrete behavior labels of the organism under study. What is the alphabet of the behavior under study? Decades of ethology have defined qualitative ways to observe behavior and some early quantitative studies (Berman, 2018; Heiligenberg, 1973; Tinbergen, 1965). However, in the last ten years, computational tools have revolutionized the study of behavior making it far more precise, efficient, and widely used (Datta et al., 2019; Pereira et al., 2020).

Tinbergen laid out an approach that sequentially goes from descriptions, to qualitative, and finally quantitative understandings of animal behavior (Tinbergen, 1965). With the proliferation of computation methods which automate the process of constructing ethograms and labeling behavior, investigators run the risk of passing up on the first two steps in the process to arrive at quantitative descriptions. Despite the allure of “automated behavioral analysis”, all computational ethology investigators will benefit from many hours of raw video (or better yet, in-person) observation of animal behavior. From these observations and notes, an investigator can begin to formulate a qualitative description of the behavior in question. It is at this point that tools from computational ethology become useful - to quantify these qualitative observations. Blindly throwing modern pose estimation and segmentation algorithms at a problem is not an answer unto itself. This can be useful, for example in behavioral phenotyping for drug discovery (Wiltschko et al., 2020), but often leaves one with dozens to hundreds of abstractly defined “clusters”. When viewing cluster 66 and cluster 87 side by side, could you succinctly describe the difference between these? Often the answer is no. Additionally,

you many lock yourself into a specific timescale of analysis, when there will be interesting behavioral structure on multiple timescales (10s of milliseconds, 100s of milliseconds, seconds, minutes, hours, days, years; (Azabou et al., 2023; Weinreb et al., 2024; Zhang, 2023).

Pose Estimation

A main driving force has been markerless pose estimation: the ability to infer postural keypoints from an organism without the use of attached markers. This revolution has been powered by machine vision advances, namely convolutional neural networks and transfer learning. With these tools, markerless pose estimation has become an out-of-the-box tool with point-and-click interfaces that is used in labs throughout the world. Deeplabcut, SLEAP, and Lightning pose are three of the most popularly used methods, each with slightly different methods, but the same underlying goal: to take raw video data and transform it into a time-series of keypoint locations (Biderman et al., 2024; Mathis et al., 2018; Pereira et al., 2022).

3D pose estimation has proved to be a considerably more challenging problem than 2D pose estimation and the field is still working out methods for this.

The output of a pose estimation analysis is a time series of size number of keypoints by number of timestamps. While these keypoint estimates can be useful for some analyses, like time spent occupying certain regions of space or inter-organism distances, many labs will want to perform analyses on top of pose estimation outputs. The most common goal is to construct an ethogram and label new data, which requires a behavioral segmentation algorithm.

Behavioral segmentation and dynamics: How to construct a behavior?

The essential task of a behavioral segmentation method is to take a timeseries of keypoint estimates and return a time series of behavior labels. This is a considerably less well defined problem than pose estimation. What behaviors are you interested in describing? With a specific set of behaviors in mind, you can use supervised methods which take a set of hand-labeled data points to train a classifier, which can then be applied to larger datasets (Bohnslav et al., 2021; Nilsson et al., 2020). However, many investigators are interested in discovering the set of behaviors that exist in their dataset. This means unsupervised methods, which constructs the set of possible behavioral labels as well as assigns labels to the time series, will be desired (Berman et al., 2014; Hsu & Yttri, 2021; Luxem et al., 2022; Weinreb et al., 2024; Wiltschko et al., 2015). Once behavioral data has been segmented, subsequent analyses can be used to determine: behavioral phenotypes (Wiltschko et al., 2020), neural correlates (Markowitz et al., 2023), etc. These analyses can be tuned to the analytic needs of individual labs, but efforts exist to provide general purpose algorithms for these as well (Sun et al., 2023; von Ziegler et al., 2024)

While behavioral segmentation algorithms are powerful tools for large-scale data analysis, they are not replacements for careful observation and do not provide unbiased answers to scientific questions. Statistical or predictive objectives can provide a means by which to define a “best” model, but can be disconnected from interpretable models. Prediction is often in tension with understanding when using computational models (Chirimuuta, 2021).

An exciting frontier in computational ethology is 3D pose estimation and whole-body biomechanical models. These tools are being combined to simulate animal behavior at unprecedented resolution to construct “virtual twins” of flies, mice, and rats. Through a combination of learning algorithms like imitation learning and reinforcement learning, neural network controllers can construct realistic goal-directed behaviors, creating simulated data at the level of joint kinematics (Aldarondo et al., 2024; DeWolf et al., 2024; Marshall et al., 2022; Vaxenburg et al., 2024).

Results

Dynamics of odor-source localization: Insights from real-time odor plume recordings and head-motion tracking in freely moving mice
Mohammad F. Tariq, Scott C. Sterrett, Sidney Moore, Lane, David J. Perkel, David H. Gire
Plos One 2024 https://doi.org/10.1371/journal.pone.0310254

Abstract
Animals navigating turbulent odor plumes exhibit a rich variety of behaviors, and employ efficient strategies to locate odor sources. A growing body of literature has started to probe this complex task of localizing airborne odor sources in walking mammals to further our understanding of neural encoding and decoding of naturalistic sensory stimuli. However, correlating the intermittent olfactory information with behavior has remained a long-standing challenge due to the stochastic nature of the odor stimulus. We recently reported a method to record real-time olfactory information available to freely moving mice during odor-guided navigation, hence overcoming that challenge. Here we combine our odor-recording method with head-motion tracking to establish correlations between plume encounters and head movements. We show that mice exhibit robust head-pitch motions in the 5-14Hz range during an odor-guided navigation task, and that these head motions are modulated by plume encounters. Furthermore, mice reduce their angles with respect to the source upon plume contact. Head motions may thus be an important part of the sensorimotor behavioral repertoire during naturalistic odor-source localization.

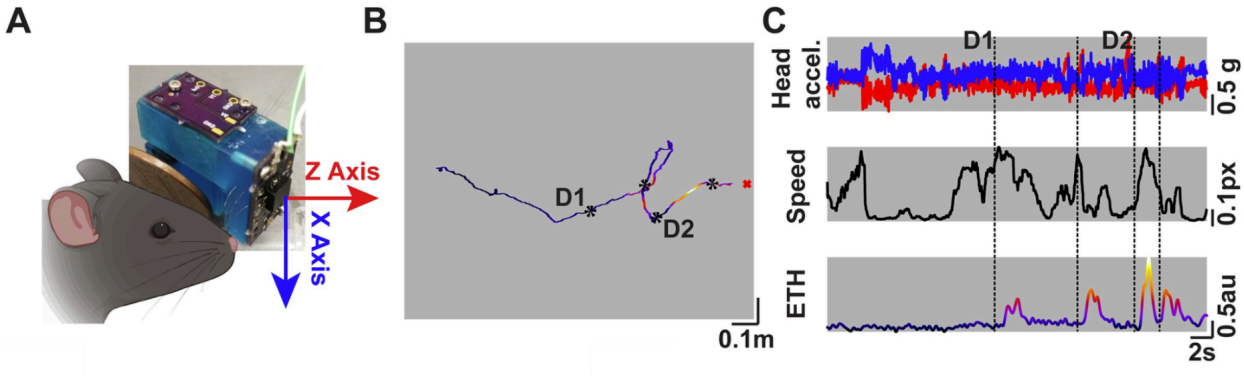

Fig 1. Concurrent head-motion tracking with real-time odor plume monitoring.(A) The designed 3D-printed part with a custom designed PCB to monitor the plume information along with an accelerometer. The arrows correspond to the axis of orientation of the accelerometer and the color corresponds with panel C. (B) An individual trajectory of a mouse engaged in plume-tracking to locate the odor source for a water reward. Overlaid on the trajectory is the colormap of the real-time plume signal experienced by the mouse. The color-scale goes from dark (low signal) to lighter (higher signal) and corresponds with the colors shown in C. The black asterisks represent the locations of plume encounters. The red “x” marks the location of the odor source. (C) (Top) The read-out over time from the Z- and X- axis channels of the accelerometer (red & blue, respectively) from the trajectory shown in B. (Middle) The speed of the animal over time during the trial shown in B. (Bottom) The plume signal experienced by the mouse during its search. The color-scale, same as B, goes from dark (low) to light (high). Black dashed lines represent the times of plume encounters.

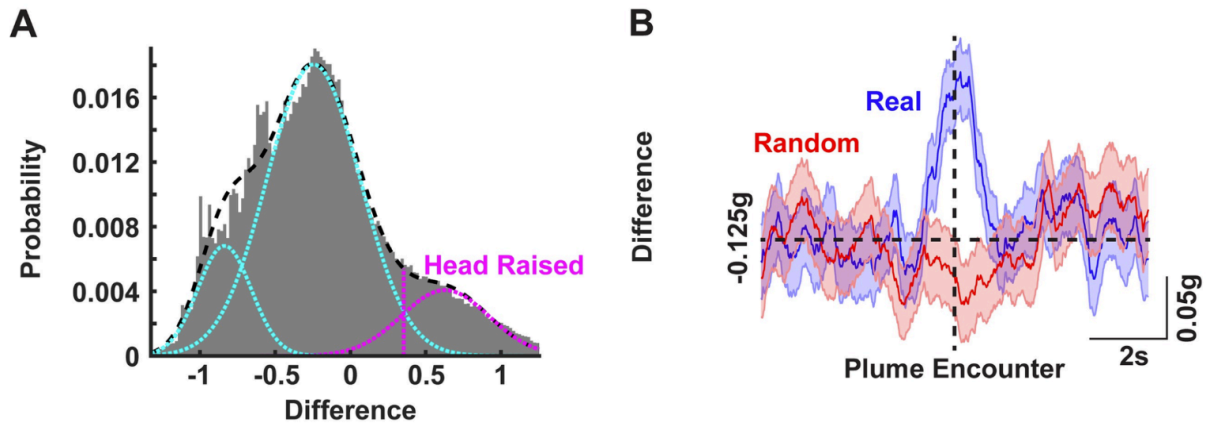

Fig 2. Plume encounter results in a lowering of the head with a corresponding increase in the frequency of head-pitch motion.
A) The difference in the median Z- and X-axes read out from the accelerometer pooled over all trials and all animals. The resulting distribution was then fit with the sum of three Gaussians (black dashed curve). The mean-S.D. (magenta dashed line) of the third Gaussian (magenta curve) was then set as a threshold to classify the head as either raised (values greater than the

dashed magenta line) or lowered. B) Mean ± SEM of the difference of median of Z- and X-axes readings for real (blue) and randomly selected (red) trajectories (same plume encounter events as those presented in Fig 2C–2E)

Psychedelics impact active sampling and odor perception in freely moving mice
Amanda C. Welch, Scott C. Sterrett, K.R. Jones, Matt C. Smear
(in preparation) 2024
Olfactory hallucinations occur in many disorders, including Parkinson's disease, epilepsy, schizophrenia, and migraines, but the mechanisms underlying these hallucinations are unknown. Mechanistic studies of hallucination in animal models are fundamentally limited, since animals do not verbalize what they perceive. However, in lieu of a verbal report, internal states can be inferred from an animal's externally observable behavior. Using computational tools, we have shown that a mouse's perceptual states can be inferred from close analysis of strategic sniffing behavior. We have found that injection of the psychedelic DOI alters the rhythmic structure of sniffing behavior and the accuracy of odor report. In ongoing work, we are investigating how DOI impacts population dynamics in the olfactory bulb. This work will provide fresh insights into the link between active sampling, olfaction, and psychedelics.

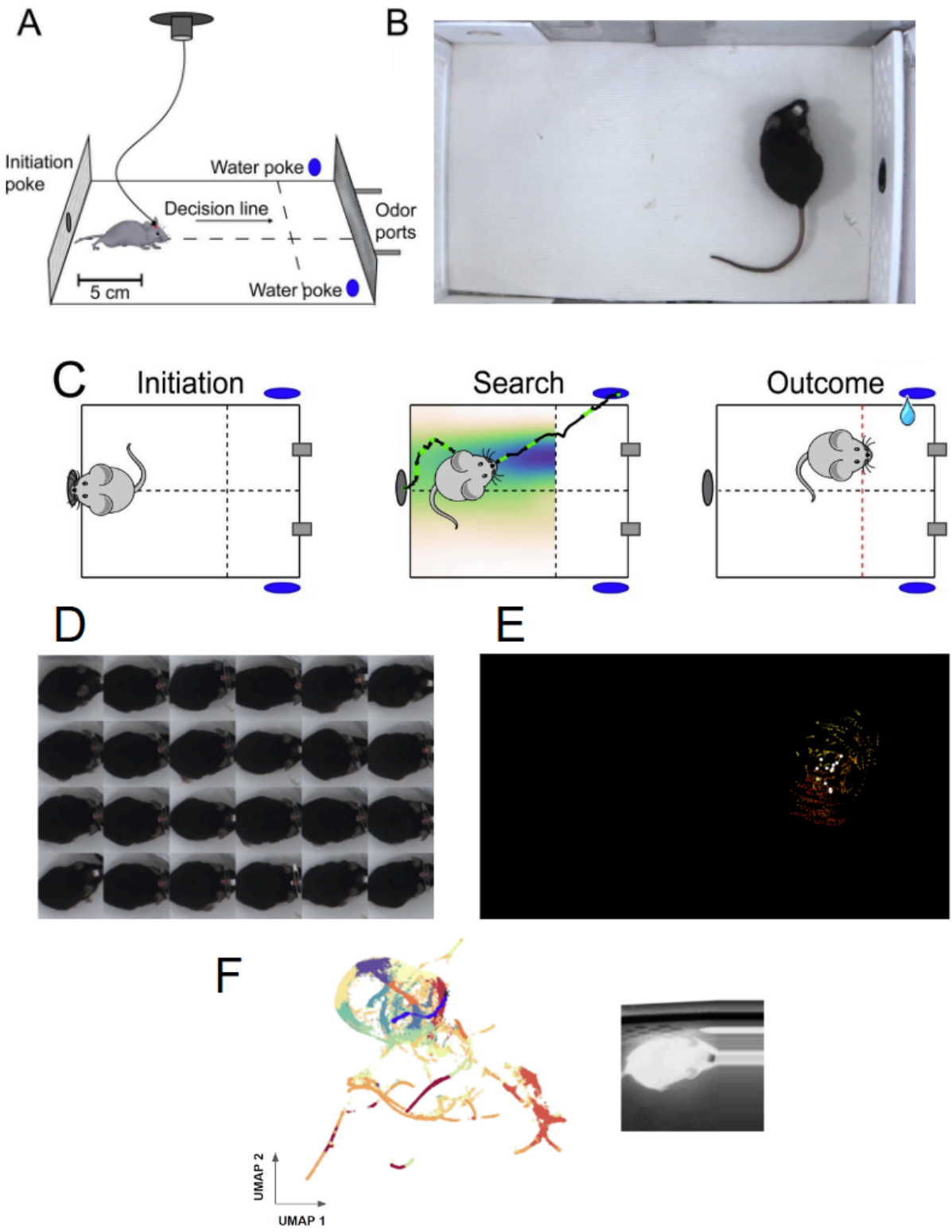

(A) Olfactory localization task in mice. (B) Overhead video recording is used for behavioral analyses. (C) Task performance (D-E) an example discrete behavioral motif identified via

keypoint-moseq used at the initiation port to sample the left side of the box (F) *left* Continuous latent behavioral visualizations using VAME show the structure of initiation port (orange), left sample (yellow/green), and right sample (yellow/red) motifs form a looped structure. *right* synchronized video frame.

Dimensionality of locomotor behaviors in developing *C. elegans*

Cera W. Hassinan*, Scott C. Sterrett*, Brennan Summy, Arnav Khera, Angie Wang, Jihong Bai
*these authors contributed equally
Plos Computational Biology 2024 https://doi.org/10.1371/journal.pcbi.1011906

Abstract
Adult animals display robust locomotion, yet the timeline and mechanisms of how juvenile animals acquire coordinated movements and how these movements evolve during development are not well understood. Recent advances in quantitative behavioral analyses have paved the way for investigating complex natural behaviors like locomotion. In this study, we tracked the swimming and crawling behaviors of the nematode Caenorhabditis elegans from postembryonic development through to adulthood. Our principal component analyses revealed that adult C. elegans swimming is low dimensional, suggesting that a small number of distinct postures, or eigenworms, account for most of the variance in the body shapes that constitute swimming behavior. Additionally, we found that crawling behavior in adult C. elegans is similarly low dimensional, corroborating previous studies. Further, our analysis revealed that swimming and crawling are distinguishable within the eigenworm space. Remarkably, young L1 larvae are capable of producing the postural shapes for swimming and crawling seen in adults, despite frequent instances of uncoordinated body movements. In contrast, late L1 larvae exhibit robust coordination of locomotion, while many neurons crucial for adult locomotion are still under development. In conclusion, this study establishes a comprehensive quantitative behavioral framework for understanding the neural basis of locomotor development, including distinct gaits such as swimming and crawling in C. elegans.

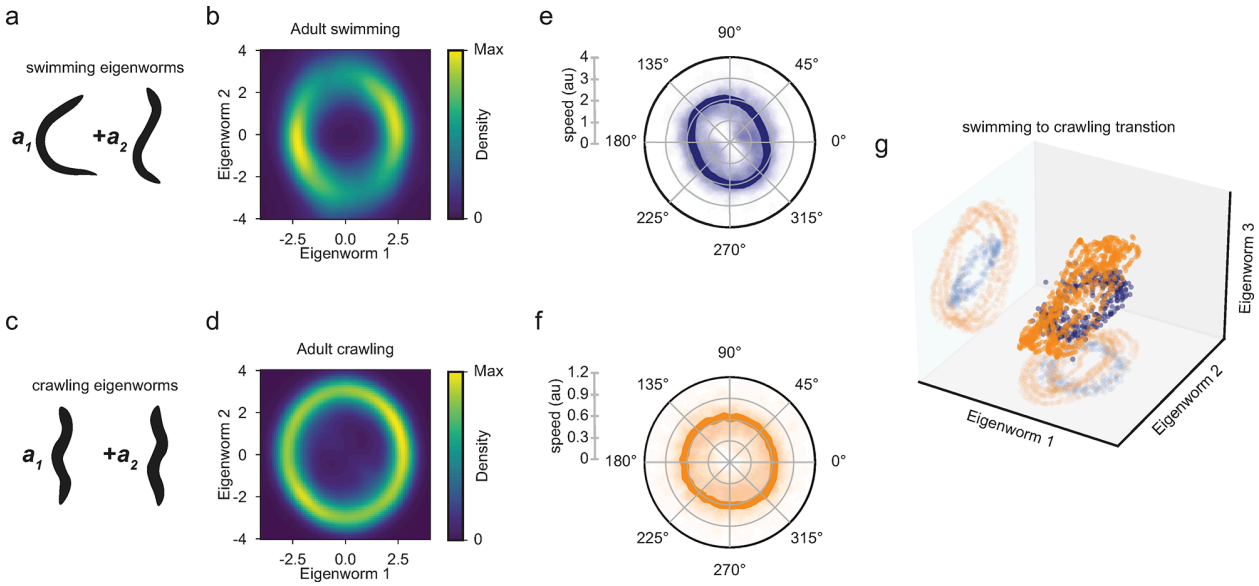

Fig 3. C. elegans adult swimming and crawling are distinct gaits.
(a) Schematics of the first two principal eigenworms from adult swimming as shown in Fig 1C. (b) Swimming eigenworm amplitude distributions show a stereotyped ring structure which captures the coordination of swimming eigenworms one and two to produce swimming locomotion in adult C. elegans (n = 43). (c) Schematics of the first two principal eigenworms of adult crawling behavior. (d) Crawling eigenworm amplitude distributions show a stereotyped ring structure of coordination between crawling eigenworms one and two in adult C. elegans (n = 38). (e and f) Polar plots of eigenworm amplitude (b and d) speeds as a function of phase in the ring. Speed data across all animals are plotted as scatter points, and the mean is overlayed. (e) In swimming, speed is bimodal and is slowest when in the “C” shape, or eigenworm one, whereas in crawling (f) the speed is constant along the ring. (g) 3D scatter plot of the first three eigenworm amplitudes from a representative worm tracked during a swimming-to-crawling transition. The ring structure of swimming (blue) is distinct from the ring structure associated with crawling (orange).

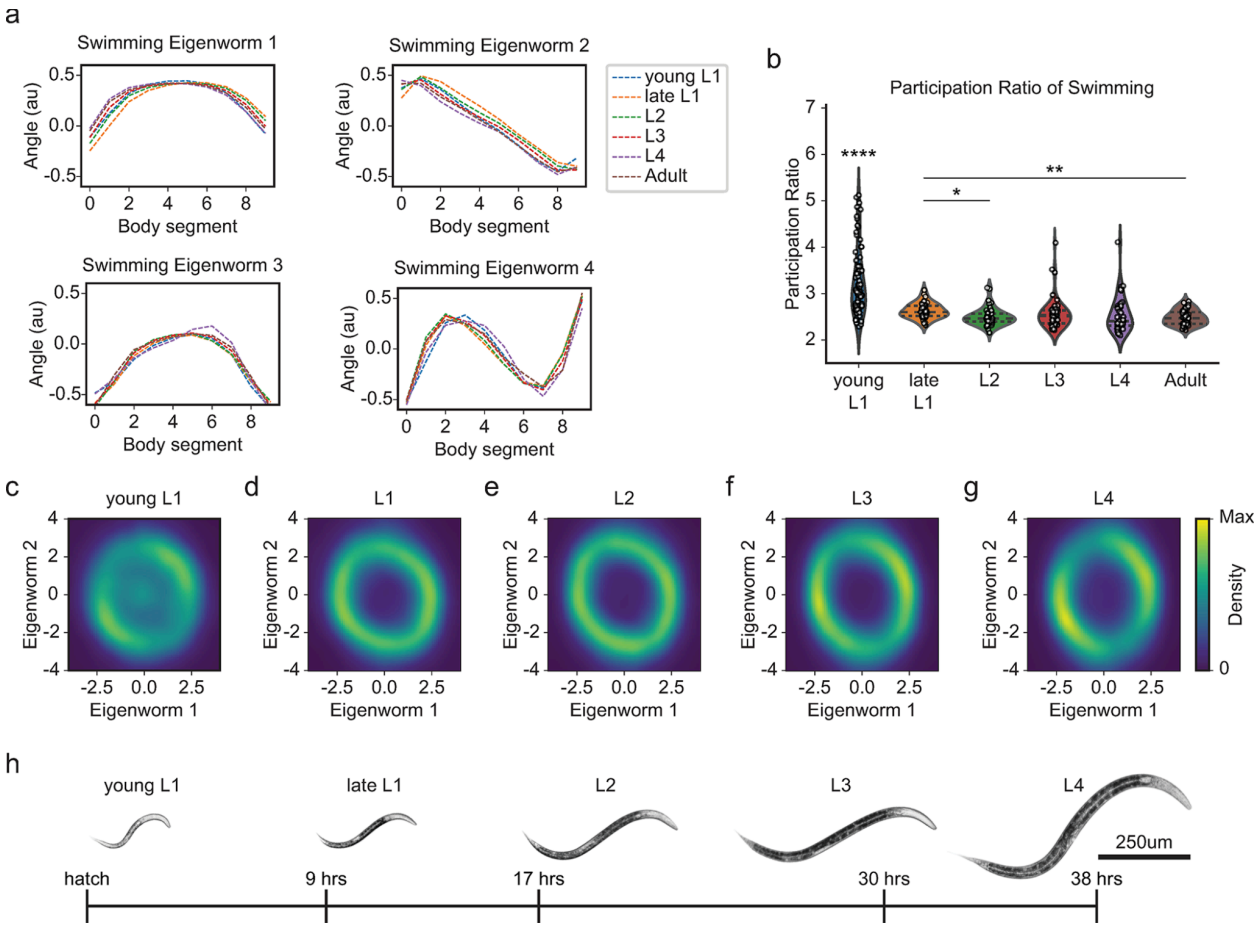

Fig 4. Rhythmic swimming is present at birth and matures throughout development.
(a) Swimming eigenworms 1–4 across developmental stages: young L1 (blue), late L1 (orange), L2 (green), L3 (red), L4 (purple), adult (brown). (b) Participation ratios (PRs) representing the dimensionality for each swimming tracking session of young L1 (n = 86), late L1 (n = 40), L2 (n = 47), L3 (n = 48), L4 (n = 39), and adult (n = 43) C. elegans. Young L1 and adult C. elegans swimming PRs show a significant difference in means (p = 9.07e-08, t-test). (c-g) Swimming locomotion represented by eigenworm one and two amplitude distributions across developmental stages: young L1 (c), late L1 (d), L2 (e), L3 (f), and L4 (g) demonstrate coordination of these eigenworms is present across development, however young L1 worms also produce uncoordinated postures not represented by the first two eigenworms. (h) The developmental stages, young L1, late L1, L2, L3, L4 of N2 C. elegans recorded in this study. Dashed lines in (b) represent means and interquartile range. Statistical significance in (b) was determined using Bonferroni adjusted alpha levels of 0.03 (0.05/15). Young L1 PRs showed ****p statistical significance compared to all other stages. Significance: *p<0.0033, **p<0.00067, ****p<0.0000067.

Attentional Switching in Larval Zebrafish

Kumaresh Krishnan, Akila Muthukumar, Scott Sterrett, Paula Pflitsch, Adrienne Fairhall, Mark Fishman, Armin Bahl, Hanna Zwaka, Florian Engert

Preprint (under revision) 2023 https://doi.org/10.21203/rs.3.rs-3486824/v1

Abstract
Decision making strategies in the face of conflicting or uncertain sensory input have been successfully described in many different species. Here we analyze large behavioral datasets of larval zebrafish engaged in a 'coherent dot' optomotor assay. We find that animal performance is bimodal and can be separated into two 'states', an engaged state where performance is high and fish consistently turn into the direction of the coherent motion, and a second, disengaged state, where performance drops to chance. We find that a simple Hidden Markov Model (HMM) is sufficient to model these transitions and fits our experimental data well. Moreover, this addition can be incorporated into an existing Drift Diffusion Model (DDM) framework that has previously been used to model perceptual decision making in larval zebrafish. Further, we leverage the large behavioral data sets to fit a mixture model of performance distributions and extract two latent variables which we term 'focus' and 'competence'. Whereas 'competence' quantifies performance while the fish is in the engaged state, the 'focus' variable captures the relative duration for which each animal persists in the engaged state. We show that 'focus' may be largely inherited from the parents, while 'competence' is more likely to be influenced by environmental context. This quantitative framework for analyzing decision making can be used to screen genetic perturbations for their impact on these two aspects of performance, and potentially help to identify a genetic basis and a neural mechanism for attention that extends across organisms.

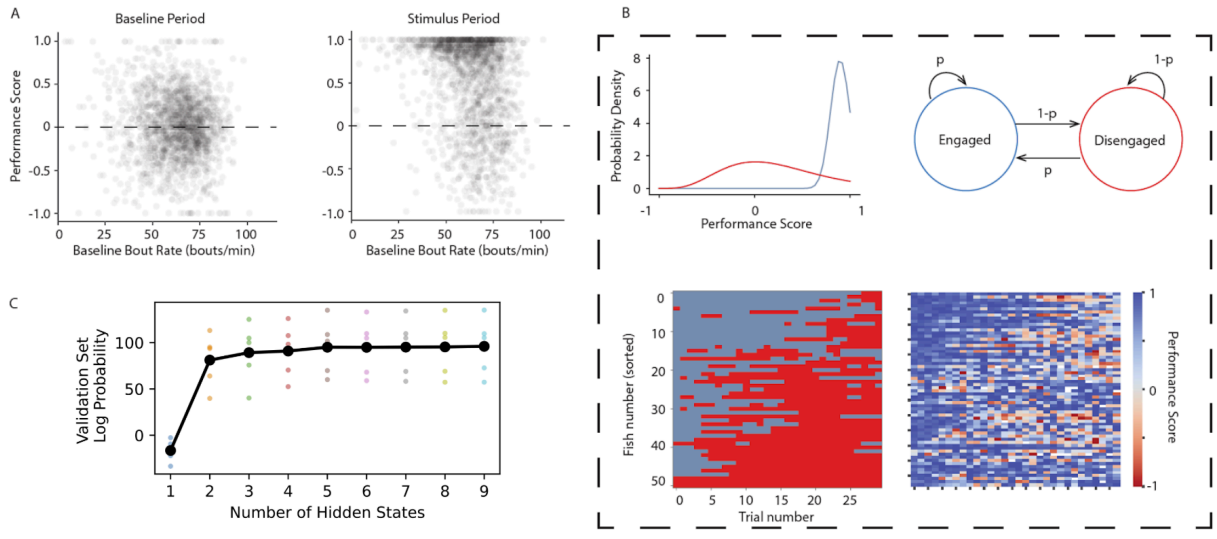

Figure 5. Attentional switching in zebrafish optomotor responses (A) Point cloud of all 1920 trials showing distribution of performance scores against bout rate in the baseline period for (left) performance evaluated against a random target in the baseline period (right) performance evaluated in the stimulus period (B) (top left) Gamma distributions inferred from HMM that best

fits the experimental data (top right) Compact description of the proposed attentional switching framework (bottom left) trials classified as attentive (blue) and inattentive (red) based on HMM (bottom right) performance score across trials for each fish sorted by average score (C) HMM validation set log likelihood for increasing number of hidden states of five cross-validated folds

Discussion

Computational ethology is an exciting interdisciplinary field which has changed not just the way we quantify behavioral experiments, but also how we think about the brain. With large-scale behavioral and neural data becoming increasingly common, the field is faced with a theoretical challenge of how to connect the two, and what counts as understanding (Anderson & Perona, 2014; Krakauer et al., 2017; Urai et al., 2022).

References

Aldarondo, D., Merel, J., Marshall, J. D., Hasenclever, L., Klibaite, U., Gellis, A., Tassa, Y., Wayne, G., Botvinick, M., & Ölveczky, B. P. (2024). A virtual rodent predicts the structure of neural activity across behaviours. *Nature*, *632*(8025), 594–602. https://doi.org/10.1038/s41586-024-07633-4

Anderson, D. J., & Perona, P. (2014). Toward a Science of Computational Ethology. *Neuron*, *84*(1), 18–31. https://doi.org/10.1016/j.neuron.2014.09.005

Azabou, M., Mendelson, M., Ahad, N., Sorokin, M., Thakoor, S., Urzay, C., & Dyer, E. (2023). Relax, it doesn't matter how you get there: A new self-supervised approach for multi-timescale behavior analysis. *Advances in Neural Information Processing Systems*, *36*, 28491–28509.

Berman, G. J. (2018). How to Build a Behavior. *Neuron*, *100*(6), 1275–1277. https://doi.org/10.1016/j.neuron.2018.12.007

Berman, G. J., Choi, D. M., Bialek, W., & Shaevitz, J. W. (2014). Mapping the stereotyped behaviour of freely moving fruit flies. *Journal of The Royal Society Interface*, *11*(99), 20140672. https://doi.org/10.1098/rsif.2014.0672

Biderman, D., Whiteway, M. R., Hurwitz, C., Greenspan, N., Lee, R. S., Vishnubhotla, A., Warren, R., Pedraja, F., Noone, D., Schartner, M. M., Huntenburg, J. M., Khanal, A., Meijer, G. T., Noel, J.-P., Pan-Vazquez, A., Socha, K. Z., Urai, A. E., Cunningham, J. P., Sawtell, N. B., & Paninski, L. (2024). Lightning Pose: Improved animal pose estimation via semi-supervised learning, Bayesian ensembling and cloud-native open-source tools. *Nature Methods*, *21*(7), 1316–1328. https://doi.org/10.1038/s41592-024-02319-1

Bohnslav, J. P., Wimalasena, N. K., Clausing, K. J., Dai, Y. Y., Yarmolinsky, D. A., Cruz, T., Kashlan, A. D., Chiappe, M. E., Orefice, L. L., Woolf, C. J., & Harvey, C. D. (2021). DeepEthogram, a machine learning pipeline for supervised behavior classification from raw pixels. *eLife*, *10*, e63377. https://doi.org/10.7554/eLife.63377

Chirimuuta, M. (2021). Prediction versus understanding in computationally enhanced neuroscience. *Synthese*, *199*(1–2), 767–790. https://doi.org/10.1007/s11229-020-02713-0

Datta, S. R., Anderson, D. J., Branson, K., Perona, P., & Leifer, A. (2019). Computational Neuroethology: A Call to Action. *Neuron*, *104*(1), 11–24.

https://doi.org/10.1016/j.neuron.2019.09.038
DeWolf, T., Schneider, S., Soubiran, P., Roggenbach, A., & Mathis, M. W. (2024). *Neuro-musculoskeletal modeling reveals muscle-level neural dynamics of adaptive learning in sensorimotor cortex* (p. 2024.09.11.612513). bioRxiv. https://doi.org/10.1101/2024.09.11.612513
Heiligenberg, W. (1973). Random processes describing the occurrence of behavioural patterns in a cichlid fish. *Animal Behaviour*, *21*(1), 169–182. https://doi.org/10.1016/S0003-3472(73)80057-0
Hsu, A. I., & Yttri, E. A. (2021). B-SOiD, an open-source unsupervised algorithm for identification and fast prediction of behaviors. *Nature Communications*, *12*(1), Article 1. https://doi.org/10.1038/s41467-021-25420-x
Krakauer, J. W., Ghazanfar, A. A., Gomez-Marin, A., MacIver, M. A., & Poeppel, D. (2017). Neuroscience Needs Behavior: Correcting a Reductionist Bias. *Neuron*, *93*(3), 480–490. https://doi.org/10.1016/j.neuron.2016.12.041
Luxem, K., Mocellin, P., Fuhrmann, F., Kürsch, J., Miller, S. R., Palop, J. J., Remy, S., & Bauer, P. (2022). Identifying behavioral structure from deep variational embeddings of animal motion. *Communications Biology*, *5*(1), Article 1. https://doi.org/10.1038/s42003-022-04080-7
Markowitz, J. E., Gillis, W. F., Jay, M., Wood, J., Harris, R. W., Cieszkowski, R., Scott, R., Brann, D., Koveal, D., Kula, T., Weinreb, C., Osman, M. A. M., Pinto, S. R., Uchida, N., Linderman, S. W., Sabatini, B. L., & Datta, S. R. (2023). Spontaneous behaviour is structured by reinforcement without explicit reward. *Nature*, *614*(7946), Article 7946. https://doi.org/10.1038/s41586-022-05611-2
Marshall, J. D., Li, T., Wu, J. H., & Dunn, T. W. (2022). Leaving flatland: Advances in 3D behavioral measurement. *Current Opinion in Neurobiology*, *73*, 102522. https://doi.org/10.1016/j.conb.2022.02.002
Mathis, A., Mamidanna, P., Cury, K. M., Abe, T., Murthy, V. N., Mathis, M. W., & Bethge, M. (2018). DeepLabCut: Markerless pose estimation of user-defined body parts with deep learning. *Nature Neuroscience*, *21*(9), Article 9. https://doi.org/10.1038/s41593-018-0209-y
Nilsson, S. R., Goodwin, N. L., Choong, J. J., Hwang, S., Wright, H. R., Norville, Z. C., Tong, X., Lin, D., Bentzley, B. S., Eshel, N., McLaughlin, R. J., & Golden, S. A. (2020). Simple Behavioral Analysis (SimBA) – an open source toolkit for computer classification of complex social behaviors in experimental animals. *bioRxiv*, 2020.04.19.049452. https://doi.org/10.1101/2020.04.19.049452
Pereira, T. D., Shaevitz, J. W., & Murthy, M. (2020). Quantifying behavior to understand the brain. *Nature Neuroscience*, *23*(12), 1537–1549. https://doi.org/10.1038/s41593-020-00734-z
Pereira, T. D., Tabris, N., Matsliah, A., Turner, D. M., Li, J., Ravindranath, S., Papadoyannis, E. S., Normand, E., Deutsch, D. S., Wang, Z. Y., McKenzie-Smith, G. C., Mitelut, C. C., Castro, M. D., D'Uva, J., Kislin, M., Sanes, D. H., Kocher, S. D., Wang, S. S.-H., Falkner, A. L., … Murthy, M. (2022). SLEAP: A deep learning system for multi-animal pose tracking. *Nature Methods*, *19*(4), 486–495. https://doi.org/10.1038/s41592-022-01426-1
Sun, J. J., Marks, M., Ulmer, A., Chakraborty, D., Geuther, B., Hayes, E., Jia, H., Kumar, V.,

Oleszko, S., Partridge, Z., Peelman, M., Robie, A., Schretter, C. E., Sheppard, K., Sun, C., Uttarwar, P., Wagner, J. M., Werner, E., Parker, J., … Kennedy, A. (2023). *MABe22: A Multi-Species Multi-Task Benchmark for Learned Representations of Behavior* (arXiv:2207.10553). arXiv. https://doi.org/10.48550/arXiv.2207.10553

Tinbergen, N. (1965). *Social Behaviour in Animals*. Springer Netherlands. https://doi.org/10.1007/978-94-011-7686-6

Urai, A. E., Doiron, B., Leifer, A. M., & Churchland, A. K. (2022). Large-scale neural recordings call for new insights to link brain and behavior. *Nature Neuroscience*, *25*(1), Article 1. https://doi.org/10.1038/s41593-021-00980-9

Vaxenburg, R., Siwanowicz, I., Merel, J., Robie, A. A., Morrow, C., Novati, G., Stefanidi, Z., Both, G.-J., Card, G. M., Reiser, M. B., Botvinick, M. M., Branson, K. M., Tassa, Y., & Turaga, S. C. (2024). *Whole-body simulation of realistic fruit fly locomotion with deep reinforcement learning* (p. 2024.03.11.584515). bioRxiv. https://doi.org/10.1101/2024.03.11.584515

von Ziegler, L. M., Roessler, F. K., Sturman, O., Waag, R., Privitera, M., Duss, S. N., O'Connor, E. C., & Bohacek, J. (2024). Analysis of behavioral flow resolves latent phenotypes. *Nature Methods*, 1–12. https://doi.org/10.1038/s41592-024-02500-6

Weinreb, C., Pearl, J. E., Lin, S., Osman, M. A. M., Zhang, L., Annapragada, S., Conlin, E., Hoffmann, R., Makowska, S., Gillis, W. F., Jay, M., Ye, S., Mathis, A., Mathis, M. W., Pereira, T., Linderman, S. W., & Datta, S. R. (2024). Keypoint-MoSeq: Parsing behavior by linking point tracking to pose dynamics. *Nature Methods*, *21*(7), 1329–1339. https://doi.org/10.1038/s41592-024-02318-2

Wiltschko, A. B., Johnson, M. J., Iurilli, G., Peterson, R. E., Katon, J. M., Pashkovski, S. L., Abraira, V. E., Adams, R. P., & Datta, S. R. (2015). Mapping Sub-Second Structure in Mouse Behavior. *Neuron*, *88*(6), 1121–1135. https://doi.org/10.1016/j.neuron.2015.11.031

Wiltschko, A. B., Tsukahara, T., Zeine, A., Anyoha, R., Gillis, W. F., Markowitz, J. E., Peterson, R. E., Katon, J., Johnson, M. J., & Datta, S. R. (2020). Revealing the structure of pharmacobehavioral space through motion sequencing. *Nature Neuroscience*, 1–11. https://doi.org/10.1038/s41593-020-00706-3

Zhang, L. (2023). *From Behavioral Syllables to the Book of Life: A Dynamic Behavioral Topic Model*. Cosyne.

Chapter 5: Conclusions and Future Directions

Equipped with advanced tools for behavioral, neural, and theoretical experimentation, this thesis has advanced our understanding of the olfactory system as an adaptive, integrated part of a goal-directed organism. This approach finds that the olfactory system is not simply a sensory relay, but a participant in context-dependent perception. These experimental findings require us to reevaluate theoretical models of sensory processing to make sense of new data, a common trend across sensory neuroscience (Parker et al., 2020; Urai et al., 2022). How does the field move towards an understanding of the brain in all its naturalistic variability?

Overshooting ecological validity and the great divide for theory.
Experimental neuroscience has advanced to the point that experimenters are recording thousands of neurons across multiple brain regions while animals are able to explore environments with minimal restraint for hours on end. Environments can be virtual, small arenas, large arenas, or even acres of natural landscapes. What do we make of this data? While exploratory statistical analyses can begin to point the way towards theories, we have moved far beyond the realm of our understanding that making connections to existing theories can be quite difficult. In order to get to a theory of naturalistic cognition will require many paths (Cisek & Green, 2024; Fetsch, 2016; Potochnik & Oliveira, 2020).

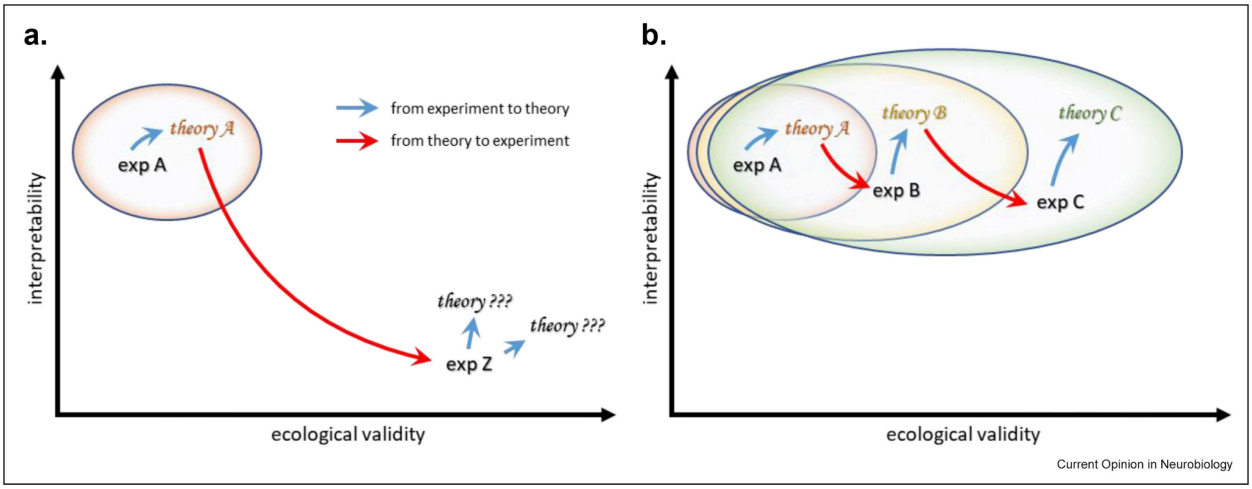

Figure 1: Alternative paths to a neuroscience of naturalistic behavior. Reproduced from (Cisek & Green, 2024)

One exciting avenue for an intermediate step towards ecologically valid experiments is virtual reality (Naik et al., 2020; Thurley, 2022; Thurley & Ayaz, 2017). These technically challenging experimental setups allow for investigators to use all of the advanced neural

recording technology available in head-fixed recordings, while still allowing animals to move through a virtual environment. While these do not reproduce the full repertoire of natural behaviors, they allow for active exploration. In olfaction, this offers the possibility of studying artificial turbulent stimuli through the use of optogenetics (Kadakia et al., 2022).

Simulating cognition through neural networks

In chapter 3, we show one example of how task-trained neural networks can be used to generate hypotheses about adaptive behaviors and neural dynamics. This growing literature offers exciting possibilities of using neural networks as a model organism to simulate behavior and neural data. Recurrent neural networks are universal dynamical systems approximators, which means that they can act like any arbitrary dynamical system (Doya, n.d.). In a way, this invert's Krough's principle that there is a model organism for every problem (Krogh, 1929); a RNN is the ultimate generalist. If neural networks are model organisms, can we apply Tinbergen's four questions to develop a pluralistic understanding of them? Table 1 lays out a possible sketch of these questions applied to recurrent neural networks.

	Dynamic	Static
How	*Ontogeny (development)*: How do dynamical motifs emerge during learning? (look at network structure and internal states across training)	*Mechanism (causation)*: How do dynamical motifs support foraging behaviors? (dynamical systems analyses of trained networks)
Why	*Phylogeny (evolution)*: What types of hyperparameter choices facilitate foraging behaviors? (comparative across regions of hyperparameter space)	*Function (adaptation)*: How do dynamical motifs support trained networks foraging behaviors? (ablation/perturbation experiments)

It is an exciting era for neuroscientists curious about the diverse behaviors abundant throughout the animal kingdom. The work increasingly requires interdisciplinary teams and open, reproducible methods working together to construct understanding from large and complex behavioral and neural datasets. We may never arrive at universal principles in biology, but the task of abstracting general principles from experimental techniques remains an essential task for computational neuroscience.

References

Cisek, P., & Green, A. M. (2024). Toward a neuroscience of natural behavior. *Current Opinion in Neurobiology*, *86*, 102859. https://doi.org/10.1016/j.conb.2024.102859

Doya, K. (n.d.). *Universality of Fully-Connected Recurrent Neural Networks 3*. 6.

Fetsch, C. R. (2016). The importance of task design and behavioral control for understanding the neural basis of cognitive functions. *Current Opinion in Neurobiology*, *37*, 16–22. https://doi.org/10.1016/j.conb.2015.12.002

Kadakia, N., Demir, M., Michaelis, B. T., DeAngelis, B. D., Reidenbach, M. A., Clark, D. A., & Emonet, T. (2022). Odour motion sensing enhances navigation of complex plumes. *Nature*, *611*(7937), 754–761. https://doi.org/10.1038/s41586-022-05423-4

Krogh, A. (1929). The progress of physiology. *American Journal of Physiology-Legacy Content*, *90*(2), 243–251. https://doi.org/10.1152/ajplegacy.1929.90.2.243

Naik, H., Bastien, R., Navab, N., & Couzin, I. D. (2020). Animals in Virtual Environments. *IEEE Transactions on Visualization and Computer Graphics*, *26*(5), 2073–2083. IEEE Transactions on Visualization and Computer Graphics. https://doi.org/10.1109/TVCG.2020.2973063

Parker, P. R. L., Brown, M. A., Smear, M. C., & Niell, C. M. (2020). Movement-Related Signals in Sensory Areas: Roles in Natural Behavior. *Trends in Neurosciences*, *43*(8), 581–595. https://doi.org/10.1016/j.tins.2020.05.005

Potochnik, A., & Oliveira, G. S. de. (2020). Patterns in Cognitive Phenomena and Pluralism of Explanatory Styles. *Topics in Cognitive Science*, *12*(4), 1306–1320. https://doi.org/10.1111/tops.12481

Thurley, K. (2022). Naturalistic neuroscience and virtual reality. *Frontiers in Systems Neuroscience*, *16*. https://doi.org/10.3389/fnsys.2022.896251

Thurley, K., & Ayaz, A. (2017). Virtual reality systems for rodents. *Current Zoology*, *63*(1), 109–119. https://doi.org/10.1093/cz/zow070

Urai, A. E., Doiron, B., Leifer, A. M., & Churchland, A. K. (2022). Large-scale neural recordings call for new insights to link brain and behavior. *Nature Neuroscience*, *25*(1), Article 1. https://doi.org/10.1038/s41593-021-00980-9